An updated climate change assessment for the Bay of Plenty

Prepared for Bay of Plenty Regional Council

13 December 2011

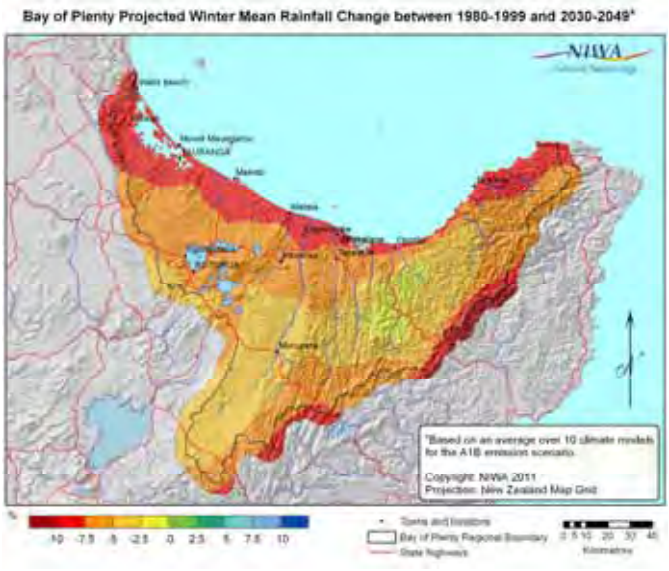

Authors/Contributors:
Georgina Griffiths, Brett Mullan, Duncan Ackerley, Abha Sood, Trevor Carey-Smith, Lara Wilcocks and James Sturman.

For any information regarding this report please contact:

Georgina Griffiths
Senior Climate Scientist - Auckland
Climate Applications
+64-9-375 4506
gm.griffiths@niwa.co.nz

National Institute of Water & Atmospheric Research Ltd
41 Market Place
Auckland Central 1010
Private Bag 99940
Newmarket
Auckland 1149

Phone +64-9-375-2050
Fax +64-9-375-2051

NIWA Client Report No: AKL-2011-019
Report date: 13 December 2011
NIWA Project: EBP11101

Disclaimer

As explained in this report, developing projections of future climate changes is still subject to significant uncertainty. The authors have used the best available information in preparing this report, and have interpreted this information exercising all reasonable skill and care. Nevertheless NIWA accepts no liability, whether direct, indirect or consequential, arising out of the provision of information in this report.

While every effort has been made to ensure that this report is as clear and accurate as possible, NIWA will not be held responsible for any action arising out of its use. This report should not be taken as providing a definitive statement for any particular user's circumstances. All users of this report should satisfy themselves concerning the application of this report to their situation; and in cases where there is uncertainty, seek expert advice.

Copyright

Contents

1. Executive summary 3

Modelling information 3

Key temperature projections 4

Key rainfall projections 5

Key circulation, storminess and extreme wind results 5

Extreme temperature projections 6

Extreme rainfall projections 6

Key drought results 6

Key pasture growth modelling results 6

Use of these results 7

2. Introduction 8

2.1 Options selected by the Council 9

2.2 Using this report 10

2.3 Report structure 10

3. Climate change science 12

3.1 About scenarios 12

3.2 Downscaling 14

3.3 About the GCMs used in this report 15

3.4 About the RCM used in this report 18

4. Regional and gridded results 19

4.1 Decadal variability 19

4.2 Downscaled GCM projections of Mean Temperature 22

4.3 Downscaled GCM projections of Precipitation 26

4.4 Projected changes in seasonal mean winds, storminess and extreme winds 30

4.4.1 Seasonal mean winds and storminess 30

4.4.2 Extreme winds (large scale) 31

4.4.3 Changes in small-scale convection 35

5. Site-Specific Results 36

5.1 Projected Temperature extremes 36

5.1.1 Frost Days 37

5.1.2 Cold Nights 37

5.1.3 Hot days and very hot days 38
5.1.4 Spread in global and regional model predictions 39
5.2 Projected Rainfall Extremes 40
5.3 Using HIRDS v3 with climate change scenarios 44
5.4 Drought and pasture growth projections 45
5.4.1 How is drought defined? 46
5.4.2 Present-day drought exposure 47
5.4.3 Modelled changes in drought under climate change 49
5.4.4 How is pasture growth calculated? 53
5.4.5 Current pasture growth in the Bay of Plenty 53
5.4.6 Modelled changes in pasture growth under climate change 55

6. A Synthesis of Results 59
6.1 Introduction 59
6.2 Modelling information 59
6.3 Key temperature projections 61
6.4 Key rainfall projections 61
6.5 Key circulation, storminess and extreme wind results 62
6.6 Extreme temperature projections 63
6.7 Extreme rainfall projections 63
6.8 Key drought results 63
6.9 Key pasture growth modelling results 64
6.10 Use of these results 64

7. Acknowledgements 66

8. References 66

Reviewed by

……

Andrew Tait, Principal Scientist

Approved for release by

……

David Wratt, Chief Scientist, Climate

1. Executive summary

Bay of Plenty Regional Council has requested an update of the climate change assessment that was undertaken for the region in 2003. This updated report draws on a significant body of climate change modelling and knowledge undertaken internationally and by NIWA over the intervening eight years.

Modelling information

The climate change modelling used in this report is based on (greenhouse gas) emission scenarios described in the Intergovernmental Panel on Climate Change Fourth Assessment Report (commonly abbreviated as IPCC AR4). These scenarios are divided into "storylines" that describe distinctly different future developments of economic growth, global population, and technological change. The three most comprehensively investigated storylines are known as: B1 (low emissions), A1B (mid-range emissions), and A2 (high emissions). The IPCC does not see any one scenario as being more likely than any other.

The projections for this Bay of Plenty Regional Council report focus on the A1B (mid-range) and A2 (high) scenarios, and two time slices: mid-century (2030-2049) and century-end (2080-2099), relative to present day (1980-1999). For convenience, these time periods are shortened to "1990" (equivalent to 1980-1999), "2040" (2030-2049) and "2090" (2080-2099).

The primary set of future projections described in this report are calculated from 10 Global Climate Models (GCMs) that have been empirically downscaled to a ~5km x 5km grid across New Zealand, which is known as the Virtual Climate Station (VCS) network. There are approximately 500 VCS grid-points covering the Bay of Plenty, of the 11,500 VCS grid-points over the New Zealand land mass.

Empirical downscaling is a technique for building in local scale detail that is consistent with the much larger-scale global climate model output. Statistical relationships that link large-scale atmospheric variables with local/regional climate variables are developed using several decades of past climatic data. These relationships are then applied to the large-scale projections from the GCMs. For example, large-scale pressure patterns might be related to local (station) observations of rainfall. In the past year, NIWA has developed a new, improved empirical downscaling approach, which is used here. In general, the new empirically downscaled climate change patterns are very similar to the earlier ones in the Bay of Plenty, and for the rest of New Zealand. In particular, the direction of rainfall change (wetter/drier) is the same, although the magnitude of the changes tends to be slightly smaller under the new downscaling.

In addition, NIWA runs a high-resolution climate model in the New Zealand region, known as a Regional Climate Model (RCM). To run the RCM, a GCM must be run first to provide the boundary conditions at the edges of the RCM domain, containing information on wind, pressure, temperature and moisture that allow weather systems to pass from the lower

resolution GCM into the higher resolution RCM. This approach is often called dynamical downscaling. For this report, one particular GCM (The United Kingdom Met Office HadAM3P model) is used to drive the RCM. Dynamical downscaling provides a more physics-based approach for developing future climate change scenarios at the meso-scale, compared with empirical/statistical downscaling. There are two RCM sets, one under the A1B scenario and the other under A2, of daily weather data at about 300 grid-points (~30km grid) over the New Zealand land mass, covering a 130-year period. Downscaling of the RCM datasets to the VCS grid enabled drought and pasture modelling in this report, as well as a comparison to the empirically downscaled GCM projections.

The primary results produced in this report (and presented as GIS layers of ~5km x 5km gridded data) are the '10-model averages' from the empirically downscaled GCM projections, since comparisons between observational data and multiple climate models have shown that the group average tends to have a lower error than most, if not all, of the individual models. In addition, to cater for an "envelope" approach, the lowest and highest response from the GCM empirical models, as well as the single result from the RCM (driven by one particular GCM), were also given for each scenario/time slice, for a selection of key sites.

Key temperature projections

Projections show an increase in temperature with time for the Bay of Plenty. The warming at 2040 is similar for A1B and A2, but is much higher at 2090 under A2 than A1B. There is very little spatial variation within the Bay of Plenty in the temperature projections (meaning that Tauranga warms about the same as Whakatane at 2090, for example). The projected RCM annual warming lies very close to the GCM 10-model average annual warming at all scenarios/time slices.

There is, however, a difference in the degree of warming from one season to another as well as a considerable difference between models. The *range* of warming seen across the models increases with time (i.e. the differences between the 10 models are larger by 2090 than at 2040). In terms of the GCM 10-model average, temperatures are projected to increase slightly faster for the autumn and winter seasons than for spring and summer. For the RCM, however, warming is faster in the summer and autumn seasons than for winter and spring.

The Bay of Plenty region (as a whole) is projected to:

- warm by about 1.2 °C (relative to 1990) by 2040 under the A1B scenario, in the annual mean, as an average across the 10 GCMs, with a range between 0.5 and 1.5 °C;
- warm by about 2.7 °C (range 1.7 to 3.2 °C) by 2090 under A1B (annual mean);
- warm by about 3.2 °C (range 2.5 to 3.6 °C) by 2090 under the higher A2 emission scenario (annual mean); and
- warm slightly more in winter than the annual mean.

Key rainfall projections

In contrast to projected temperature changes, the projected rainfall changes show marked spatial variation across the Bay of Plenty. In summer by century-end, the GCM 10-model average rainfall increases over almost the entire Bay of Plenty, being largest (~10%) in the far east and northeast of the district, and inland between Rotorua and Edgecumbe. The 10-model average shows almost no rainfall change relative to 1990 along the south-western boundary. The projected autumn rainfall changes are similar to those in summer.

Seasonally, projected changes to summer-autumn rainfall are primarily a reflection of increased variability; in the projected future climate, very dry summer-autumn seasons become more common as do extremely wet ones, with the net effect of increased rainfall in a long-term average sense.

There is a complete contrast in winter, when the 10-model average projected rainfall decreases by century-end about 10% relative to 1990 levels along the coast and the south-eastern boundary of the Bay of Plenty region. The spring rainfall changes are similar to those in winter.

Averaged over the region, there is little change projected in the annual rainfall, owing to the opposing rainfall trends in summer/autumn and winter/spring. Rainfall projections for the Bay of Plenty (as a whole) indicate virtually no change relative to 1990 in the 10-model average annual precipitation by century-end, but there is a range across the models from a 10% decrease to a 15-20% increase (A1B and A2 combined). Along the coast, there is a weak tendency for decreased precipitation by century-end (about 5%).

Key circulation, storminess and extreme wind results

A southward shift in the low pressure/storm track near New Zealand in a future, warmer climate is projected, meaning a reduction in the number of lows over the North Island and to the east of the country in winter. In summer, however, an opposite pattern is likely, with increased low pressure activity over the Tasman Sea. This pressure pattern is meteorologically consistent with the projection of drier winters but wetter (more variable rainfall) summers, and relates to an increase in easterly days in the Bay of Plenty in summer and autumn, and an increase in westerly days in winter and spring.

Daily extreme winds generated by large-scale weather systems (such as fronts and lows) are projected to decrease in summer but increase in winter, based on an analysis of weather map "types" which have historically produced extreme winds. Atmospheric stability indices project an increase in small-scale convection under climate change (all year round, but particularly important in the warmer part of the year), which is likely to affect small-scale extreme winds associated with thunderstorms and gust fronts.

Extreme temperature projections

The projected frequency of an air frost[1] (air temperature below 0°C) becomes vanishing small by century-end at the selected Bay of Plenty sites, under GCM projections. At present, the frequency of air frosts ranges from about 5 per year in Opotiki to 20 per year in Rotorua. By the end of the century, Rotorua is projected to experience an air frost only 1 to 2 days a year under the A1B scenario, and is projected to go some years without seeing a frost at all under A2. The frequency of cold nights is also projected to become significantly smaller in all the future scenarios.

Hot days (recording 25°C or more) are projected to become the norm during the summer months by the end of the century. For example, at Whakatane, on average about 22 hot days currently occur per year, but by 2090 between 80 and 100 hot days per year are projected. It should be noted that the RCM estimates a larger number of both air frosts and hot days, both under current climate and into the future.

Extreme rainfall projections

Since the water-holding capacity of the atmosphere increases with the temperature (by about 7-8% more for every 1°C rise in temperature), it is widely accepted that extreme rainfalls will also increase in a future warmer climate. A recent New Zealand study suggests that increases in extreme precipitation events are likely to be seen in nearly all regions of the country under a warmer climate, and may well show increases larger than 7 - 8% for every 1°C rise in temperature. GCM and RCM projections of extreme 24-hour rainfall at selected sites within the Bay of Plenty show a general increase in the magnitude of extreme events in the future, although there are differences between the model projections.

Key drought results

On average, under current climate, droughts lasting more than a month are infrequent in the Bay of Plenty. Low intensity droughts lasting more than 14 days are currently experienced in summer (on average) around 30% of the time at Katikati and Te Puke, and about 20% of the time at Whakamarama, and the eastern sites Te Teko and Opotiki.

Projections under both A1B and A2 by century-end show the largest changes are likely to occur in droughts lasting longer than a month. At the five sites analysed, increases of between 9% and 17% in time spent in low intensity summer drought, lasting 1 month or more, are likely at 2090 under A1B (compared to 20-26% under A2, with the exception of Opotiki). Notably, under A2 at 2090, the time spent in moderate intensity and high intensity droughts lasting a month or more is also generally increased (by between 0-8% across all five sites), which is consistent with the predictions in previous national drought analyses.

Key pasture growth modelling results

The relatively warm, dry summers and cool, wet winters in the Bay of Plenty currently yield an annual pasture growth curve with a distinct, reliable, spring growth peak, variable autumn

[1] Measured at ~ 1.5m above the ground.

growth peak, and low winter growth (due to cool temperatures limiting growth rates). Near the ranges, winter growth is lower and summer growth is higher than that seen along the coast, due to the lower temperatures and higher summer rainfall observed.

A coupled soil-water balance and pasture production model of stock-grazed ryegrass pasture was used to model future pasture growth (with no adaptation). Projections at 2090 show little change in *annual* pasture biomass but significant changes in the *seasonality* of pasture growth in the Bay of Plenty. Projected higher summer temperatures reduce summer pasture growth significantly at 2090 under both A1B and A2. Milder winter temperatures result in large increases in winter growth (double current levels along the coast, and treble inland by 2090). Total spring growth and reliability of spring growth are unchanged.

In contrast, at mid-century under A1B, there is a projected reduction of low growth years, giving a slightly higher median summer pasture growth, which reflects the RCM and GCM 10-model average projection of increased summer rainfall under A1B at 2040. This is most likely to be due to inter-decadal climate variability (i.e. wet decades, dry decades), based on natural climate cycles.

Use of these results

Climate change science is complex, as is interpreting and using the results found. The science answers "what might" questions (such as "what might winter rainfall in the Bay of Plenty do in a warmer future?"), and there is often a large spread in results from model to model, even under the same climate change scenario. This report should initially be used in a qualitative sense, such as understanding, for example, that drier winters are more likely in the future, overall. In addition, there are a large number of quantitative results available within this report and the associated Appendices. To cater for an "envelope" approach, the lowest and highest responses from the GCM models, as well as the single result from the RCM, are given for a selection of sites.

In addition to this report, the present-day climatological fields (seasonal mean temperature, seasonal mean rainfall) and the GCM 10-model average projected changes, have been provided to the Council in GIS format, on a ~5km x 5km grid. These 32 data layers will prove useful over time when investigating possible opportunities, or risks, in the Bay of Plenty under climate change.

2. Introduction

Bay of Plenty Regional Council has requested an update of the climate change assessment that was undertaken for the region in 2003 (Griffiths *et al.*, 2003). This updated report draws on a significant body of climate change modelling and knowledge undertaken by NIWA over the intervening eight years. NIWA's regional climate modelling programme[2] has provided the underlying climate change modelling advances, and enabled the production of several key documents (sometimes in conjunction with other funding partners) which form 'building blocks' of recent climate change knowledge for New Zealand.

Results from four of these documents are used in this report (Figure 1), to underpin key results specific to the Bay of Plenty region. They are loosely known as the 'Guidance Manual' (MfE, 2008), the 'Wind Report' (Mullan *et al.*, 2011), the 'Drought Report' (Clark *et al.*, 2011) and the 'Extreme Rainfall Paper' (Carey-Smith *et al.*, 2010).

In addition, the regional climate modelling programme has kept abreast of international modelling practices and knowledge, and utilises the available global climate change modelling dataset[3].

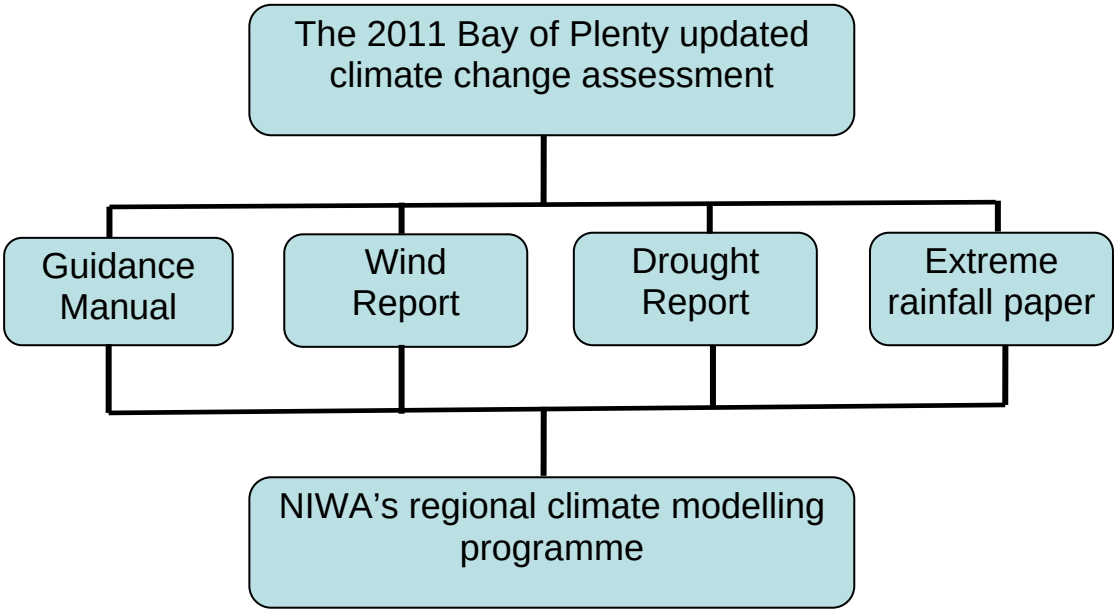

Figure 1: A conceptual diagram of knowledge transfer underlying the results presented in this report.

[2] Funded by the New Zealand Government previously through the Foundation for Research, Science and Technology (FRST) and now through the Ministry for Science and Innovation (MSI).
[3] The Intergovernmental Panel on Climate Change (IPCC) 4th Assessment Report CMIP3 simulations.

2.1 Options selected by the Council

The Bay of Plenty Regional Council has selected three "what might" scenarios[4] to investigate in this updated climate change assessment:

- If the middle-of-the-road greenhouse gas emission scenario (known as A1B) occurred, what might the climate of the Bay of Plenty likely look like at mid-century (2030-2049)?

- If the middle-of-the-road greenhouse gas emission scenario (known as A1B) occurred, what might the climate of the Bay of Plenty likely look like at century-end (2080-2099)?

- If the high greenhouse gas emission scenario (known as A2) occurred, what might the climate of the Bay of Plenty likely look like at century-end (2080-2099)?

For convenience, these time periods are shortened to "2040" (equivalent to 2030-2049) and "2090" (2080-2099).

Three spatial scales were used to inform these "what might" questions:

- The Bay of Plenty average (i.e. the region as a whole), for seasonal and annual mean rainfall and mean temperature.

- The within Bay of Plenty response; namely gridded data provided as GIS layers, with data on a ~5km x 5km grid across the entire Bay of Plenty Regional Council area of responsibility, for seasonal mean rainfall and seasonal mean temperature.

- Site specific information (for example, assessing air frosts at Rotorua), for a range of extremes, such as air frosts, hot days, cold nights, drought and pasture modelling, at sites selected by Council.

Lastly, two modelling approaches were used to inform the "what might" questions:

- The average (mean) of 10 Global Climate Models (GCMs) empirically downscaled to the Bay of Plenty region is the primary output given in this report, for both tabular data and all of the GIS layers containing gridded ~5km x 5km data. Since comparisons between observational data and multiple climate models (Lambert and Boer, 2001) show that the group mean tends to have a lower error[5] than most, if not all, of the individual models, the 10-model average is the recommended "result" for Councils to use, if not using an "envelope" approach. To cater for an "envelope" approach, the lowest and highest response from the empirically downscaled GCM models, as well as the single result from the Regional Climate Model (see below) are given, for a selection of sites and variables.

[4] Section 3.1 contains detailed information about climate change scenarios.
[5] RMSE – Root mean square error.

- NIWA's Regional Climate Model (RCM) was run, nested under one GCM, and the single RCM result was incorporated into the report where relevant in Tables and Figures. In particular, the RCM outputs were downscaled to the same ~ 5km x 5km grid as the GCM data, and to selected station observations, and used to model drought and pasture growth at selected sites, since there are more daily climate variables available under the RCM projection than just temperature and rainfall. Key differences between the GCM and RCM results were noted, and contributed to the overall synthesis of likely future climate in the Bay of Plenty.

2.2 Using this report

Climate change science is complex, as is interpreting and using the results found. This report can initially be used in a qualitative sense i.e. for "big-picture" understanding of the likely climate of a future, warmer Bay of Plenty - such as understanding, for example, that drier winters are likely, overall. The Executive Summary and Section 6 (the synthesis section) are good places to get an overview of the major results, whilst this section (Section 2) and Section 3 (which contains key climate change science concepts) are recommended to understand the process behind the modelling undertaken.

In addition, there a large number of quantitative results available within this report, both for the Bay of Plenty (as a whole), or for selected sites, using both GCM and RCM results, contained in Tables and Figures in the main body of the report, as well as in the Appendices.

Selected quantitative results are also provided as GIS layers, with data on a ~5km x 5km grid across the Bay of Plenty region. There are 32 GIS layers provided to Bay of Plenty Regional Council which accompany this report. Eight of these are climatological layers (i.e. reflect the present climate), quantifying present seasonal mean rainfall and seasonal mean temperature, and 24 layers are future (seasonal) projections of likely change in mean rainfall and temperature, based on the three "what might" situations outlined previously. All the future layers are based on the (GCM) 10-model average (see Section 3.3 for more detail on this).

To help users cope with the large number of results available, Figure 2 has been provided as a conceptual schematic, showing a directory of useful Sections, Tables and Figures to access.

2.3 Report structure

Section 3 contains information about climate change scenarios, the international context, and the climate change modelling and downscaling used in this report. Section 4 contains modelling results for the Bay of Plenty region (both for the region as a whole and within-region results), whilst Section 5 contains the site-specific results, focussing on the extremes in temperature and rainfall at selected locations, as well as drought and pasture-growth modelling. Section 6 draws together the key results from the GCM and RCM modelling into an overall synthesis of likely future climate in the Bay of Plenty.

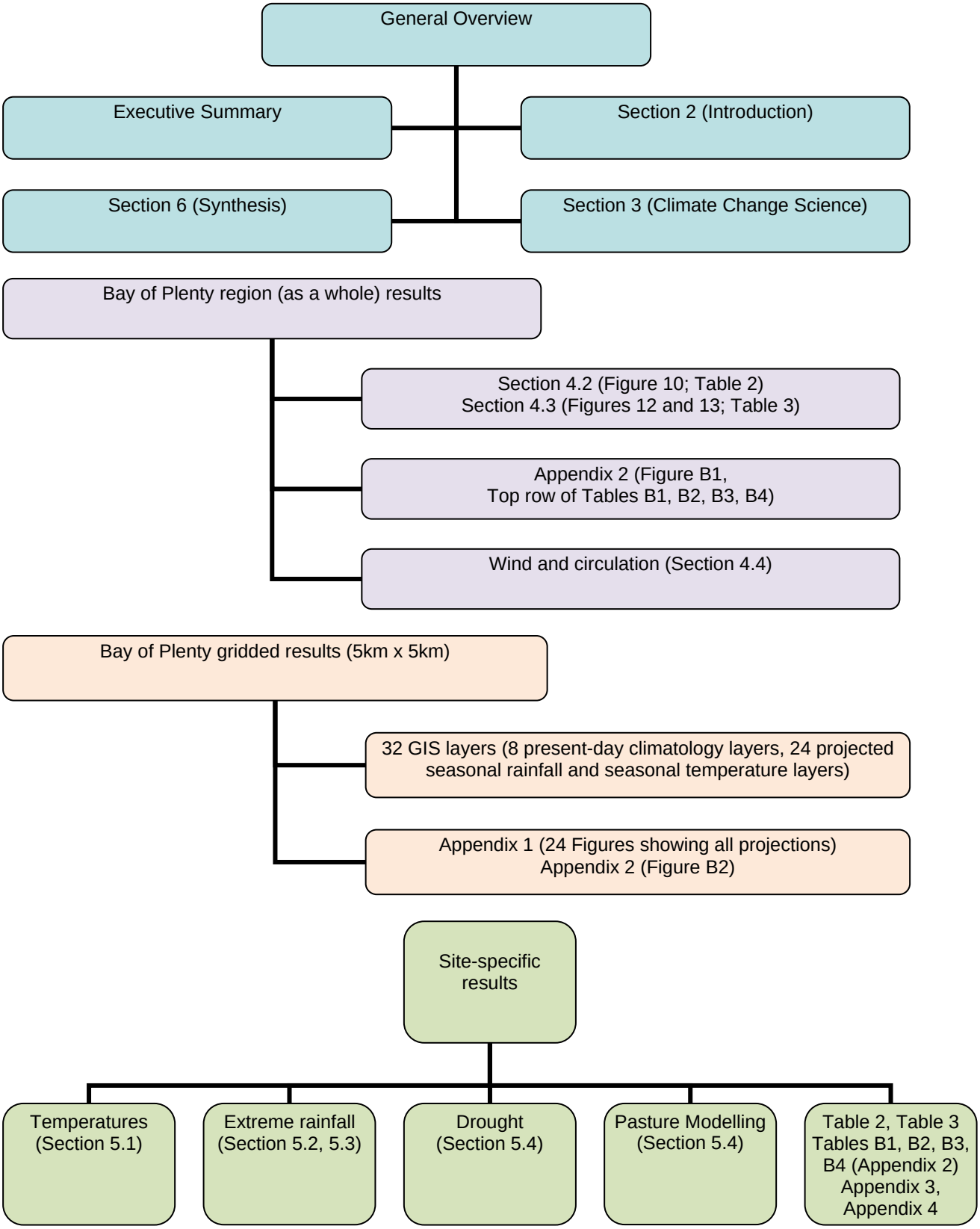

Figure 2: A conceptual diagram for users regarding key tables and figures within this report.

3. Climate change science

NIWA has previously used climate model data from the IPCC Fourth Assessment (IPCC, 2007) to update the climate change projections for New Zealand. These are described in a guidance manual prepared for the Ministry for the Environment (MfE, 2008). This report provides an update on that information for the Bay of Plenty region.

3.1 About scenarios

Climate scenarios are self-consistent and plausible storylines of possible future climates. They are intended for use in studies exploring the impacts of climate change, and to formulate possible adaptation strategies. The term 'scenario' can be applied to any aspect of the future being considered: from emissions to atmospheric concentrations of greenhouse gases, to changes in temperature and sea level, or to associated impacts.

The scenarios presented in this report are based on the IPCC emission scenarios (Nakicenovic and Swart, 2000) used to drive global climate models described in the IPCC Fourth Assessment Report (commonly abbreviated as AR4). These emission scenarios cover a wide range of possible future economic, political and social developments during the 21st century. These scenarios are divided into "storylines" that describe distinctly different future developments of economic growth, global population, and technological change[6]. The three most comprehensively investigated storylines are known as: B1 (low emissions), A1B (mid-range emissions), and A2 (high emissions[7]). The IPCC does not attach any probabilities to these emission scenarios; in other words, they do not see any one scenario as being more likely than any other.

Recent studies (Manning *et al.*, 2010) show the observed global carbon dioxide emissions (Figure 3) are tracking within the scenario bands during the 10 years where the scenarios overlap observations, and are also tracking within the band of the 6 illustration scenarios most commonly assessed (including A1B, the mid-range emission scenario, and A2, the high scenario, both assessed in this report).

[6] See Appendix 1 of MfE (2008) for more discussion of the storylines associated with each emission scenario.

[7] Although the cumulative A2 emissions are much higher than A1B by century-end, the A1B emissions are actually higher than A2 for the first three decades of the 21st century.

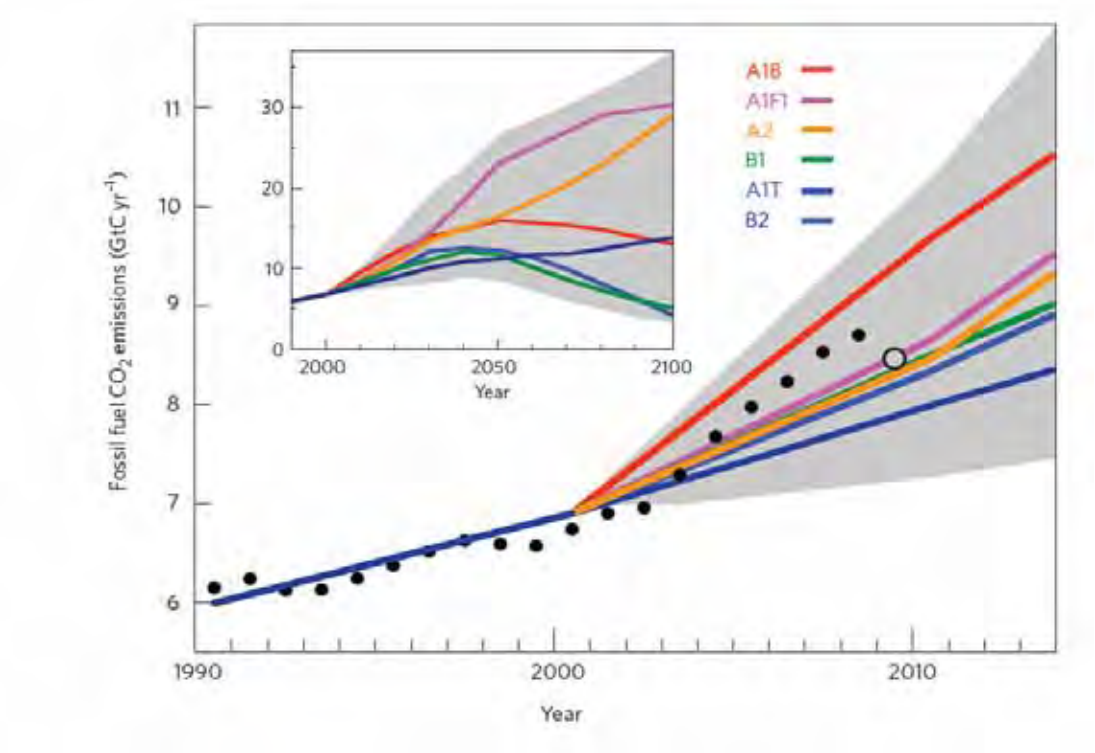

Figure 3: Fossil fuel CO_2 emissions. The graph shows that estimates of annual industrial CO_2 emissions in gigatons of carbon per year ($GtC\ yr^{-1}$) for 1990-2008 (black circles) and for 2009 (open circle) fall within the range of all 40 scenarios (grey shaded area) and of the six illustrative marker scenarios (coloured lines). The inset in the upper left corner shows these scenarios to the year 2100. (Directly from Manning *et al.,* 2010).

Figure 4 (from IPCC, 2007) indicates the range of global temperature increases that are likely out to 2100. This range encompasses not only the range of plausible emissions scenarios, but also the uncertainty in the climate response as represented by a number of different global climate models. The coloured lines in Figure 4 show the temperature increase over the century in the three most widely studied emission scenarios: the low emission scenario B1, the mid-range scenario A1B, and the high scenario A2.

This report for Bay of Plenty Regional Council focuses on the A1B and A2 scenarios. As an example, for the A2 scenario, the IPCC[8] "average" projected global warming by 2090-2099 is +3.4 °C relative to the 1980-1999 period. (The "average" warming is +3.6 °C by the year 2100 itself). This "average" is taken over about 20 global climate models, which cover a wide range of sensitivity. The variation across models, for the same emission scenario, is highlighted by the grey bars in Figure 4. For the A2 scenario the 2090-2099 range in global temperature increase is from +2.0 to +5.4 °C (with a multi-model average of +3.4 °C); for A1B, this range is from +1.7 to +4.4 °C (with an average of +2.8 °C).

[8] The temperature projections quoted here are taken directly from the IPCC Fourth Assessment Summary for Policymakers, where the changes are specified for the decade 2090-2099 relative to the 20-year period 1980-1999. Note that this differs from the NIWA projections quoted in this report, which uses the 20-year period 2080-2099.

If the other emission scenarios of Figure 4 are considered, then the global-average temperature increase at 2090-2099, relative to the average over 1980-1999, varies from +1.1°C (least sensitive model combined with the lowest emission scenario B1) to +6.4°C (most sensitive model with the highest emission scenario A1FI). On average, the temperature increase for New Zealand tends to be around two-thirds of the global increase (see, for example, Figure 2 in Reisinger *et al.*, 2010), but this ratio will vary from model to model.

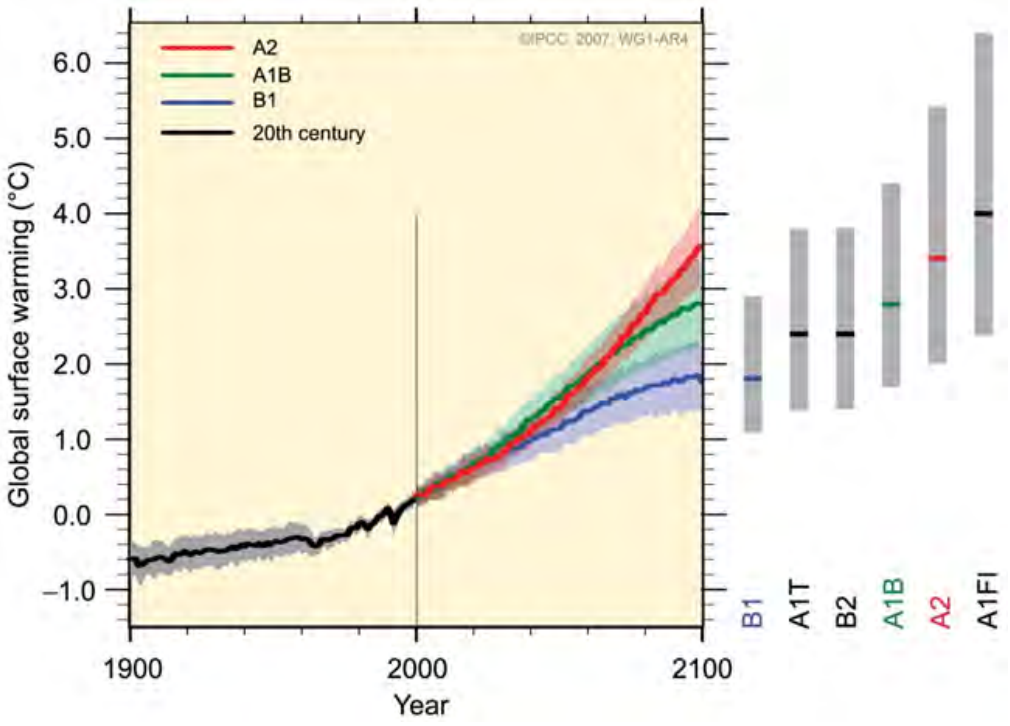

Figure 4: IPCC projections of global temperature increase. Solid coloured lines are multi-model global averages of surface warming (relative to 1980-1999) for emission scenarios B1, A1B and A2, shown as continuations of the 20th century simulations (black line). The coloured shading denotes the ±1 standard deviation range of individual model annual averages. The grey bars at right indicate the 'likely range' of temperature increase at 2090-2099 relative to 1980-1999, along with the best estimate (coloured horizontal line within each grey bar), for 6 scenarios that span the full range of all IPCC emission scenarios. (Adapted from Figure SPM-5, IPCC 2007).

3.2 Downscaling

Downscaling is a technique for building in local scale detail that is consistent with the global climate model (GCM) output at a much larger spatial scale. Two approaches are commonly used for downscaling, known as regional climate modelling (RCM), and empirical-statistical downscaling (ESD). In the RCM approach, the GCM provides boundary conditions for a limited area physical model. In the ESD approach, broad-scale climate predictors are related to local-scale predictands (both observations) by empirical transfer functions. For example, large-scale pressure patterns might be related to station observations of precipitation. Future precipitation changes could then be derived by applying the transfer equations to the GCM-projected change in pressure patterns.

The RCM method (dynamical downscaling) provides a more physics-based approach for developing future climate change scenarios at the meso-scale, but requires considerably more computational resources than ESD. As a result it is usually only applied to a small number of GCMs. By comparison, ESD is computationally efficient, can be readily applied to a large number of GCMs and has been shown to exhibit similar local level precision compared to RCM (Benestad *et al.,* 2008). The application of the RCM methodology for this Bay of Plenty Regional Council report is described in Section 3.4.

In the past year, NIWA has developed a whole new empirical/statistical downscaling approach, as described in Clark *et al.* (2011). Predictors and predictands are related through what is known as "partial least squares" (PLS) regression (Stone and Brooks, 1990). PLS regression operates by identifying an optimum linear combination of multiple predictors, and has been shown to be particularly useful where there is a high degree of spatial and temporal correlation in the predictor fields (which is often the case in climatology). The new PLS approach of Clark *et al.* (2011) achieves a higher explained variance on the training data sets than does the multiple linear regression of Mullan *et al.* (2001), although the new downscaled climate change patterns are mostly very similar to the earlier patterns of change in the Bay of Plenty, and for the rest of New Zealand. In particular, the direction of rainfall change (wetter/drier) is the same, although the magnitude of the changes tends to be slightly smaller under the new downscaling.

The Clark *et al.* (2011) downscaling has been applied to the climate variables of mean temperature, precipitation, solar radiation and potential evapotranspiration, compared to the earlier Mullan *et al.* (2001) ESD which considered only temperature and precipitation. The Clark *et al.* (2011) PLS regression functions use global model mean sea-level pressure and surface temperature as the predictors of local surface temperature, and model mean sea-level pressure and precipitation as the predictors of local precipitation.

The future projections are applied to a NIWA gridded data set that covers all of New Zealand with 0.05° latitude-longitude grid points (approximately 5km by 5km grid squares), which is known as the Virtual Climate Station (VCS) network (Tait *et al.,* 2006). There are approximately 11,500 grid-points over the New Zealand land mass, and 500 points covering the Bay of Plenty Regional Council area.

3.3 About the GCMs used in this report

MfE (2008) applied an ESD approach derived by Mullan *et al.* (2001), and calculated projected changes in temperature and precipitation. The projections were taken from GCM output under the A1B emission scenario. Thus, all the climate change maps in MfE (2008) apply only to the A1B scenario. The other IPCC emission scenarios were taken account of in

the various Tables by scaling the A1B changes[9], under the assumption that the spatial patterns are the same.

In this report for Bay of Plenty Regional Council, the climate change patterns from other emission scenarios are downscaled individually. This means that the A2 rainfall change at 2090, say, may not only be a different magnitude to A1B but have a different spatial pattern.

A further difference is the number of GCMs considered. MfE (2008) initially examined 17 GCMs and discarded 5 as having poor current climate simulations; thus, the downscaling was applied to a group of 12 models which had been forced by the A1B scenario. Not all these models were run for the A2 scenario, and so a different model selection was required here. Table 1 lists the GCMs that NIWA has statistically downscaled. The top group of 10 models are the ones used in this Bay of Plenty Regional Council (BOPRC) study; it does not include any of the previously discarded 5 poorly performing models. Also shown in Table 1 are the 12 models used in MfE (2008).

Table 1: Information on IPCC Fourth Assessment GCMs that NIWA has statistically downscaled to produce climate change projections for New Zealand. The top group are the 10 models used in this report. The column headed MfE shows what models were used (tick) in the MfE 2008 Guidance Manual.

Model Name	Country	Resolution	Used in MfE (2008)
USED in BOPRC update		**Lat x Long**	
bccr_bcm20	Norway	1.9° x 1.9°	
cccma_cgcm31_t47	Canada	3.75° x 3.75°	
cnrm_cm3	France	1.9° x 1.9°	✓
csiro_mk30	Australia	1.9° x 1.9°	✓
gfdl_cm20	USA	2.0° x 2.5°	✓
gfdl_cm21	USA	2.0° x 2.5°	✓
miroc32_medres	Japan	2.8° x 2.8°	
miub_echog	Korea/ Germany	3.75° x 3.75°	✓
mpi_echam5	Germany	1.9° x 1.9°	✓
mri_cgcm232a	Japan	2.8° x 2.8°	✓
NOT USED in BOPRC update			
cccma_cgcm31_t63	Canada	1.9° x 1.9°	✓
miroc32_hires	Japan	1.1° x 1.1°	✓
ncar_ccsm30	USA	1.4° x 1.4°	✓
ukmo_hadcm3	UK	2.5° x 3.75°	✓
ukmo_hadgem1	UK	1.25°x1.875°	✓

[9] The scaling factor is the ratio of the global temperature increases between the selected scenario and A1B.

In summary, the key differences between the downscaled GCM climate change patterns in this report, compared to those in MfE (2008) are as follows:

- A new ESD technique has been applied (Clark *et al.*, 2011), instead of Mullan *et al.*, 2001);
- Downscaling has been applied directly to A2 GCM output, instead of estimating A2 changes by a simple scaling of the A1B results; and
- A slightly different set of GCMs has been used (10 GCMs of which only 7 are common to the 12 used in MfE (2008)).

There is one important consequence of the different sub-set of GCMs used here. One of the A1B GCMs (labelled miroc32_hires in Table 1) has a much higher sensitivity to CO_2 increase than the other models; this has a major effect on the top end of the model warming range. This effect is illustrated in Figure 5 which compares the global temperature projections from 17 A2 models and 21 A1B models. Note that there is one outlier in the A1B set (miroc32_hires) that has a much larger warming than all the other A1B models, and is also warmer than any of the A2 models. This particular model did not produce an A2 simulation so is missing from the top panel of Figure 5. The consequence for this report is that the extreme top end of the temperature range will be smaller than in MfE (2008) and the model spread will be tighter.

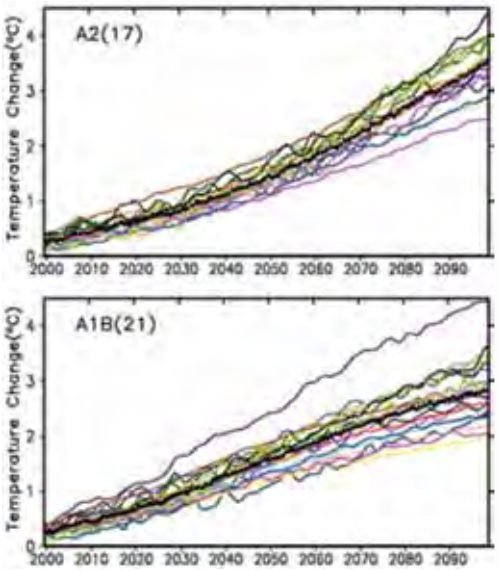

Figure 5: Time series of globally averaged surface air temperature change (°C) over the period 2000-2100, from the various global coupled models for the scenarios A2 (top) and A1B (bottom). Numbers in parentheses following the scenario name represent the number of simulations shown. Values are annual means, relative to the 1980 to 1999 average from the corresponding 20th-century simulations. Multi-model mean series are marked with black dots. [Adapted from Figure 10.5 in Meehl *et al*. (2007). Refer to that figure for colour coding of the various models].

3.4 About the RCM used in this report

In addition to analyzing global climate simulations from overseas research institutions, NIWA also operates its own climate modelling programme. The models NIWA used to undertake the simulations for the Bay of Plenty study were the Hadley Centre Atmospheric Model version 3 (HadAM3P) and the Hadley Centre Regional Model version 3 (HadRM3P). HadAM3P is a global General Circulation Model (GCM) (Pope *et al.*, 2000, Gordon *et al.*, 2000) with a grid spacing of 1.875^{o} longitude and 1.25^{o} latitude (~150km) and 19 vertical levels. The model represents many processes, which include radiation and radiative transfer, cloud cover, precipitation, convection, gravity-wave drag, the surface energy budget, diffusion and atmospheric aerosols. This is an 'atmosphere-only' model, but in the IPCC climate change experiments is coupled to a similarly complex ocean model, where the combined atmosphere-ocean model is known as HadCM3.

HadRM3P is a climate model that represents all of the processes given above for HadAM3P, but has a much higher horizontal resolution (0.27^{o} longitude and latitude grid spacing, or ~30km), and is run only over a specified region of the globe. It is therefore known as a Regional Climate Model (RCM), with the geographic domain as shown in Figure 6. The RCM was developed for use in the New Zealand region by Bhaskaran *et al.* (1999, 2002) and applied further in Drost *et al.* (2007).

To run the RCM, the GCM must be run first to provide the Lateral Boundary Conditions (LBCs) at the edges of the RCM domain. These LBCs contain information on wind, pressure, temperature and moisture that allow weather systems to pass from the lower resolution GCM into the higher resolution RCM. Therefore two model simulations must be run (one GCM and one RCM) in order to get high-resolution model data for New Zealand. Both the RCM and GCM require other boundary conditions too, and both include representations of surface topography, vegetation, soils, greenhouse gas concentrations (carbon-dioxide, nitrous-oxide, methane and chlorofluorocarbons), sea ice and sea surface temperature (SST), which allow the model to represent the current climate and attempt to forecast future climate.

In this case, SST data were taken from the coupled model HadCM3 simulation forced under the A1B and A2 IPCC scenarios. The SSTs were bias corrected (Abha Sood, personal communication) for the period 1969 – 2000 (in a similar manner to Rowell, 2005) to remove biases in the HadCM3 data. The same correction was then applied to all of the years from 2000 to 2100. The RCM SSTs were derived from the bias corrected GCM SST data. The GCM simulation was then run to represent the period 1969 – 2100 with the LBCs generated by the GCM used to force the RCM. The result is a huge archive of daily weather data at about 300 grid-points over the New Zealand land mass, covering a 130-year period. Two such data sets, one under the A1B forcing and the other under A2, were analysed for this report.

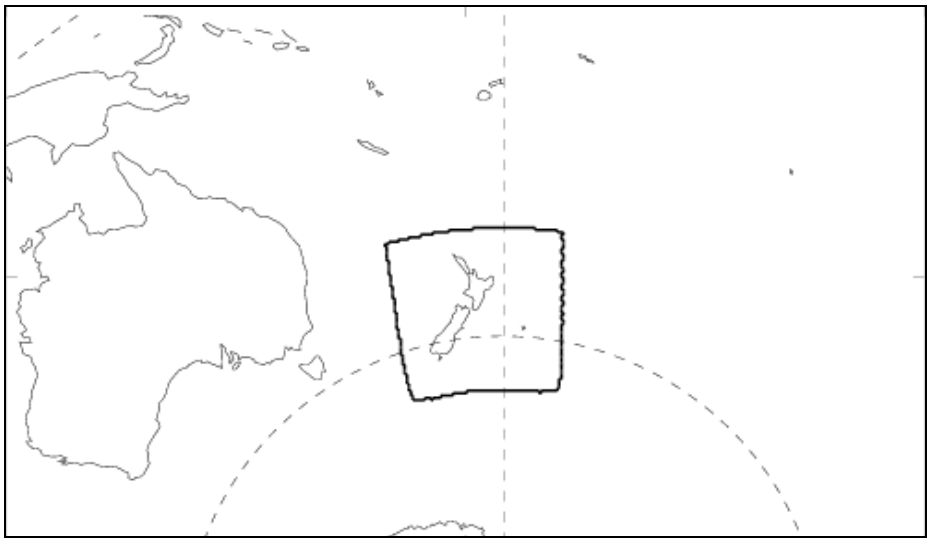

Figure 6: The domain of HadRM3P used in this work (solid, black line) in relation to the southwest Pacific region. The vertical dashed line is 180°E and the curved, dashed line is 45°S.

4. Regional and gridded results

This section describes projected climate changes for the Bay of Plenty region from a group of 10 GCMs, as described in Section 3.3 and summarized in Table 1.

4.1 Decadal variability

The GCM projections for temperature and precipitation (but not for wind) have been downscaled to a ~5km grid covering New Zealand. However, before considering the downscaled results, we start with a broader perspective at the GCM scale to highlight inter-model differences and natural decadal variability.

Figure 7 shows normalized time series of annual temperature and precipitation from the 10 GCMs used in this study. The model data have been directly interpolated to the latitude/longitude of Tauranga, with no attempt to downscale statistically. Temperatures in the Bay of Plenty Regional Council region increase through the century as is expected under the increasing greenhouse gas concentration in the atmosphere (A1B scenario). The csiro_mk30 model (solid red line) has the least warming by the end of the century, and the miroc32_medres model (dotted red line) the most. There is also substantial multi-decadal variability in the warming patterns. For example, the German mpi-echam5 model (dotted purple line) projects a Tauranga warming of close to the model-average by century end, but has the least warming of all models at 2040.

The warming is also not monotonic (each subsequent year warmer than the last) even with the smoothing that has been applied in Figure 7; that is, there are warm and cold decades which represent the local consequences of natural variability (to the extent that the model simulates it). Annual rainfall (Figure 7, lower panel) is much more variable than annual mean temperature. The 10-model average annual rainfall shows a small decline through the century,

but this is small compared to the variability[10]. The two driest models are mpi-echam5 (dotted purple line) and gfdl_cm20 (solid green line), with the Japanese miroc32_medres model (dotted red line) the wettest.

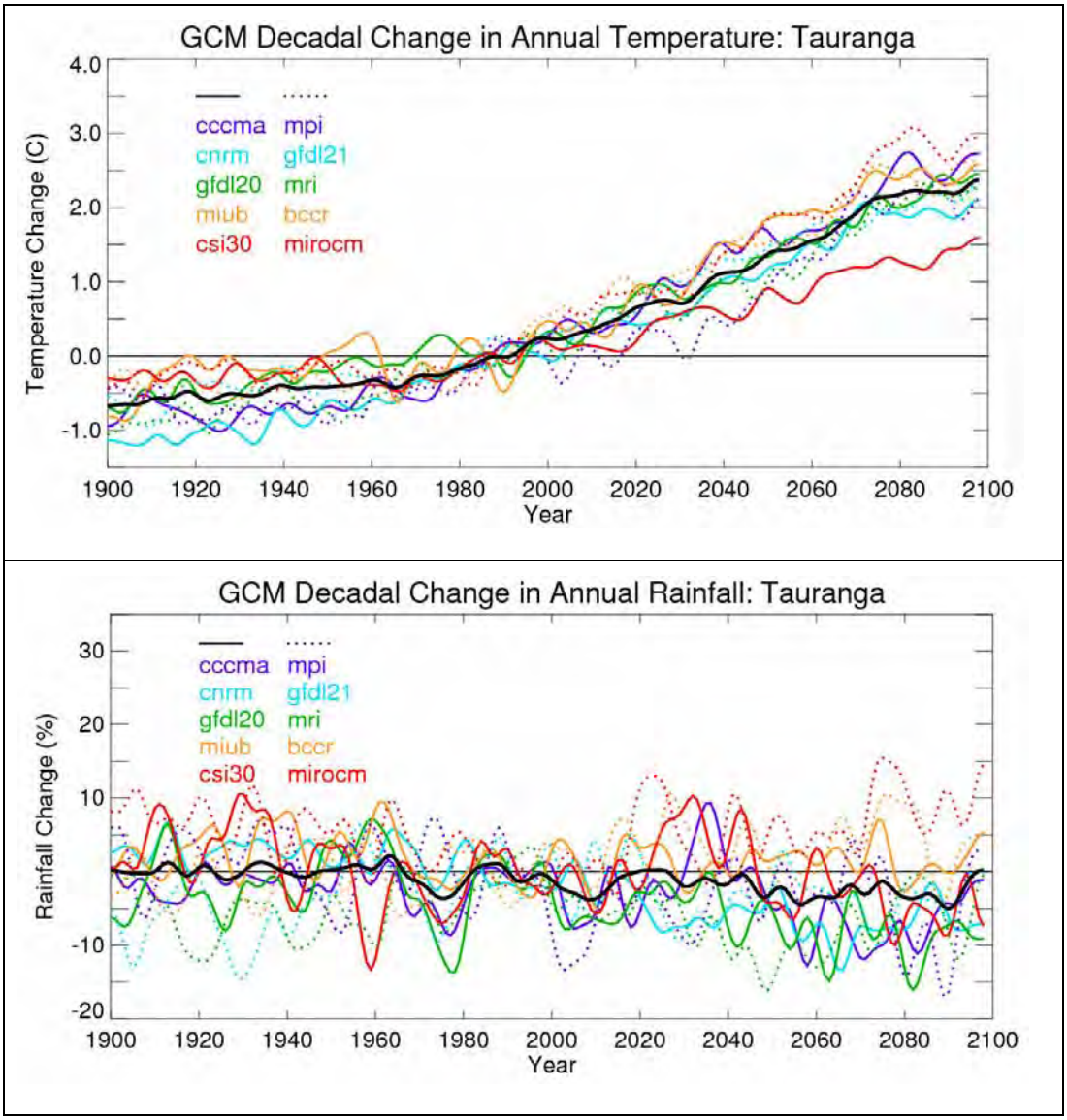

Figure 7: (Upper panel): Annual average temperature, expressed as a deviation in °C from the 1980-1999 average. (Lower panel): Annual total rainfall, as a % deviation from the 1980-1999 average. Time series are shown for the 10 global climate models used in the study, under the A1B emission scenario. The annual deviations are smoothed with a low-pass filter to remove sub-decadal fluctuations. Five of the models are shown as solid coloured lines, and five as dotted lines (using the colours according to the inset legend). The 10-model average is given by the heavy black line.

[10] Note that variability is artificially constrained over the 1980-1999 period, since all data are normalized relative to this period.

Figure 8 shows model rainfall time series interpolated to Tauranga, similar to the lower panel of Figure 7, except the results are presented separately for the summer-autumn and winter-spring half-years. The decrease in the winter-spring half-year rainfalls for the Bay of Plenty is more evident than with the annual case, although there are a couple of exceptions. The upper panel of Figure 8 suggests a long-term *increase in rainfall variability* in the warmer half of the year, although again this is not universal across all the climate models, implying an increase in both very dry summer-autumn seasons, as well as extremely wet ones.

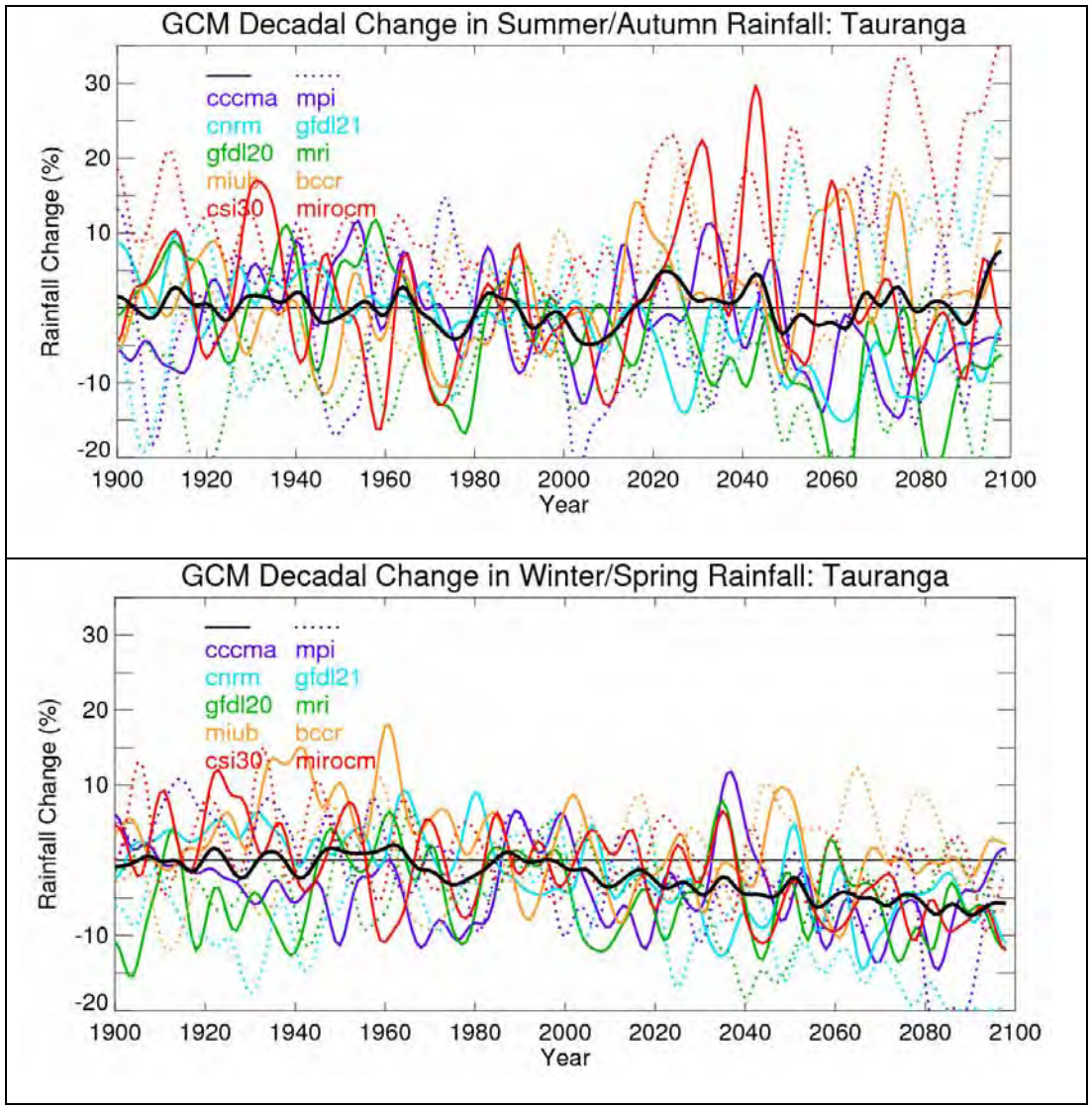

Figure 8: As for Figure 7 (lower panel), except for summer-autumn (upper panel) and winter-spring (lower panel) half-years.

4.2 Downscaled GCM projections of Mean Temperature

Projected temperature changes have been downscaled on to the ~5km grid for 10 global climate models (GCMs) under two emission scenarios: A1B, for mid-century (2030-2049 average relative to 1980-1999) and end-of-century (2080-2099 average relative to 1980-1999), and for A2 at end-of-century. This section presents the results in both tabular and map formats. Projections from the Regional Climate Model (RCM), used elsewhere in this report, are placed in context with respect to the range across the GCMs.

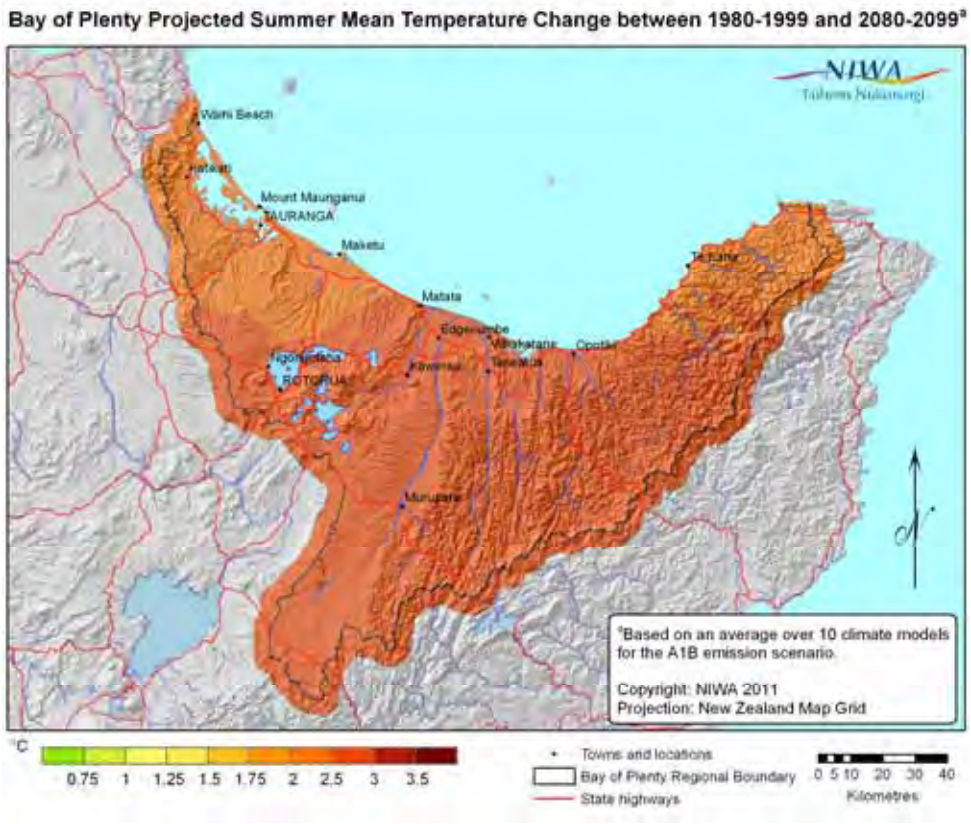

Figure 9: **The 10-model average projected summer temperature change between 1980-1999 and 2080-2099, under an A1B emission scenario.**

Figure 9 shows one example from a set of GIS layers provided to Bay of Plenty Regional Council (Appendix 1 contains maps of all 24 projection (change) layers provided). This particular map shows the summer temperature change at 2090 under the A1B scenario. As is typically found in statistical downscaling of temperature projections, there is very little spatial variation in Figure 9. This is true of each model and season individually. There is, however, a difference in the degree of warming from one season to another (see Appendix 1) as well as a considerable difference between models (as suggested in Figure 7).

Figure 10 shows the projected changes in annual temperature, averaged across all ~500 VCS grid-points that lie within the Bay of Plenty Regional Council Boundary. Results are presented for the two time periods, labelled 2040 and 2090 in short, and for the A1B and A2

scenarios[11]. The presentation in Figure 10 is known as a "box and whisker" plot, which allows for various statistics of the distribution to be shown graphically. The caption under Figure 10 describes how to interpret the box and whisker plot.

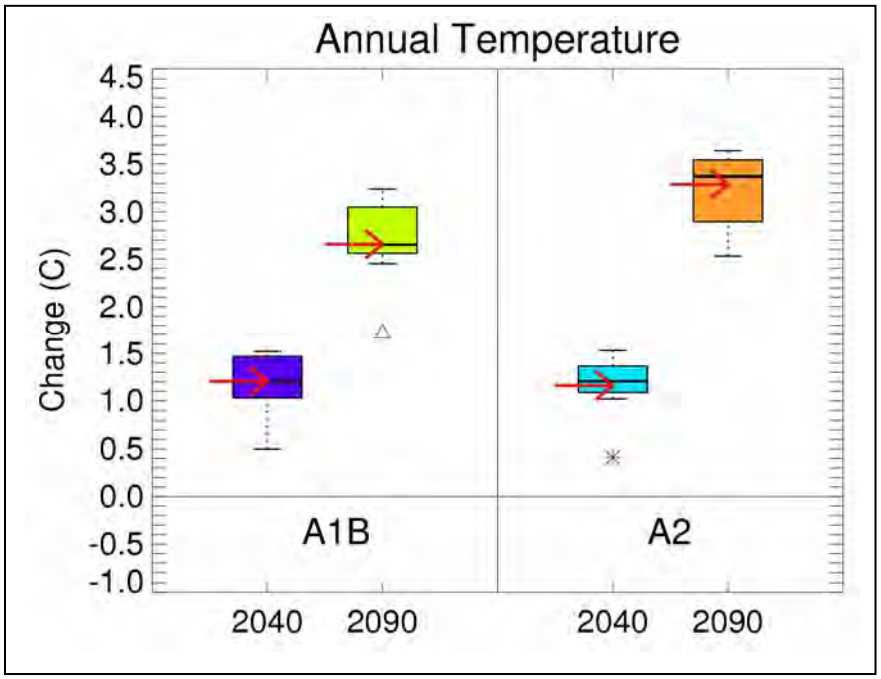

Figure 10: **Box and whisker plots of downscaled annual temperature change projections (°Celsius) for Bay of Plenty from 10 climate models, averaged over all VCS grid-points within the Bay of Plenty Regional Council Boundary. Plots show the range of warming projected by the 10 models for the 2030-2049 ('2040') and 2080-2099 ('2090') periods, for the two emission scenarios A1B and A2. The RCM result is shown with a red arrow.**

In each column of the plot, the median change is indicated by the heavy black line, with the surrounding "box" extending from the estimated 25th percentile to 75th percentile of the data known as the inter-quartile range (IQR). The "whiskers" are indicated by the short horizontal lines, and are positioned at the last data points that lie within 1.5 times the inter-quartile range of the 25th and 75th percentiles. Outliers are plotted as triangles (if they lie between 1.5 and 3 times the IQR outside the 25 and 75 percentiles) or asterisks (if more than 3 times the IQR outside the box).

The main features of the temperature projections displayed in Figure 10 are:

- There is an increase in temperature with time. The warming at 2040 is similar for A1B and A2, but A2 has clearly promoted more warming by 2090 than A1B;
- The RCM annual warming is represented by the red arrows in Figure 10. For the annual mean changes, the RCM warming lies very close to the median warming from the 10 GCMs;

[11] Scenario A2 at 2040 is considered in less detail in this report (following NIWA's recommendation in its proposal) because at mid-century the global and local warming for A2 is very similar to that from A1B. However, in these box and whisker plots, A2 at 2040 is shown for completeness.

- The range across the models, as represented by the inter-quartile range (the coloured box) increases with time[12] due to differences in sensitivity of the models (and differing magnitudes of cloud feedbacks and other factors).

Appendix 2 reproduces box and whisker plots of projected temperatures for each of the four seasons. The key findings in Appendix 2 are:

- In terms of the median model warming, temperatures are projected to increase slightly faster for the autumn and winter seasons than for spring and summer;
- For the RCM, however, warming is faster in the summer and autumn seasons than for winter and spring. Thus, the RCM warming lies above the 10-model inter-quartile range of warming in summer, and below the 10-model inter-quartile range of warming in winter.

Further detail on temperature projections for Bay of Plenty is provided in Table 2, for A1B at 2090, and in Tables B1-B4 in Appendix 2 (for other time periods and scenarios). Projections are shown for each of the four seasons and also for the annual mean. The first row in Table 2 (and in Tables B1-B4) is the average temperature change across all the VCS grid-points in the Bay of Plenty region, with similar information then provided for 5 coastal locations (Katikati, Tauranga, Te Puke, Whakatane and Opotiki), and two inland locations (Rotorua and Kawerau) in the subsequent rows. This provides "envelope" information for Council staff. The projection information includes the following:

- The average of the downscaled temperatures over the 10 GCMs;
- The extreme GCM values (i.e., the GCM with the least warming and the one with the most warming); and
- For comparison, the Regional Climate Model (RCM) change.

As already noted, the warming for a particular scenario and time has little spatial variation, but can be very different across the models used.

[12] The 2040 inter-quartile range is larger for A1B than for A2. This probably occurs because the A1B emissions increase faster in the first 2-3 decades, and A2 emissions are increasing faster by mid-century. Thus, the more sensitive GCMs have more time to respond to the early-century higher A1B CO_2 concentrations than to the A2 concentrations.

Table 2: Projected temperature changes (°Celsius) for Bay of Plenty at 2090 under the A1B emission scenario, as represented by 10 downscaled GCMs. For the region as a whole (i.e., average across all VCS grid-points with the region), and for selected grid-points co-located with named towns, the following information is given: the 10-model average, the extreme low and high values from the model distribution, and the single projected value for the RCM. Changes are shown for the four seasons and for the annual average[13].

Region or Site	Summer	Autumn	Winter	Spring	Annual
Region average:					
10-model average	2.6	2.7	2.9	2.5	2.7
Lowest, Highest	1.9, 3.2	1.8, 3.6	1.9, 3.4	1.4, 3.0	1.7, 3.2
RCM	3.1	2.9	2.4	2.2	2.7
Katikati:					
10-model average	2.3	2.5	2.7	2.3	2.5
Lowest, Highest	1.7, 2.9	1.6, 3.3	1.8, 3.2	1.3, 2.7	1.6, 3.0
RCM	3.1	2.8	2.4	2.1	2.6
Tauranga:					
10-model average	2.4	2.5	2.7	2.3	2.5
Lowest, Highest	1.7, 2.9	1.6,3.3	1.7, 3.1	1.3, 2.7	1.6, 3.0
RCM	3.0	2.8	2.3	2.1	2.5
Te Puke:					
10-model average	2.4	2.5	2.7	2.3	2.5
Lowest, Highest	1.7, 3.0	1.6, 3.3	1.8, 3.1	1.3, 2.7	1.6, 3.0
RCM	3.0	2.8	2.3	2.2	2.6
Whakatane:					
10-model average	2.6	2.7	3.0	2.5	2.7
Lowest, Highest	1.9, 3.2	1.8, 3.6	2.0, 3.5	1.4, 2.9	1.8, 3.3
RCM	3.0	2.9	2.4	2.1	2.6
Opotiki:					
10-model average	2.5	2.6	2.8	2.4	2.6
Lowest, Highest	1.9, 3.2	1.7, 3.6	1.7, 3.2	1.3, 2.9	1.7, 3.2
RCM	2.9	2.8	2.3	2.0	2.5
Rotorua:					
10-model average	2.5	2.7	2.9	2.5	2.6
Lowest, Highest	1.9, 3.2	1.8, 3.6	1.9, 3.3	1.3, 2.9	1.7, 3.2
RCM	3.3	2.9	2.4	2.2	2.7
Kawerau:					
10-model average	2.6	2.7	3.0	2.5	2.7
Lowest, Highest	1.9, 3.3	1.8, 3.7	2.0, 3.5	1.4, 3.0	1.8, 3.3
RCM	3.1	2.9	2.4	2.3	2.7

[13] Note that the annual extremes are not the averages of the seasonal extremes (because in some cases different models are involved).

In summary, the Bay of Plenty region is projected to:

- warm[#] by about 1.2 °C by 2040 under the A1B scenario[*], in the annual mean, as an average across the 10 GCMs, with a range between 0.5 and 1.5 °C;
- warm by about 2.7 °C (range 1.7 to 3.2 °C) by 2090 under A1B (annual mean);
- warm by about 3.2 °C (range 2.5 to 3.6 °C) by 2090 under the higher A2 emission scenario (annual mean).
- warm slightly more in winter than the annual mean[α].

All temperature changes relative to the baseline period (1980-1999).
* And also by the same amount, 1.2 °C, under the A2 scenario (not shown in the Tables).
α This applies to 7 of the 10 GCMs individually for A1B at 2090; one GCM warms most in summer, and two warm most in autumn. The RCM warms most in summer.

4.3 Downscaled GCM projections of Precipitation

Projected changes in precipitation have been downscaled on to the ~5km grid for 10 global models under two emission scenarios: A1B, for mid-century (2030-2049 average relative to 1980-1999) and end-of-century (2080-2099 average relative to 1980-1999), and for A2 at end-of-century. This section presents the results in both tabular and map formats. Figure 11 shows projected precipitation changes for the summer (December – February) and winter (June – August) seasons at 2090 under A1B. Maps of other seasons, times and scenarios can be found in Appendix 1, and all have been provided to the Regional Council as GIS layers (as well as 8 layers which contain climatological mean seasonal rainfall and mean seasonal temperature). In contrast to temperature changes, the rainfall changes can show marked spatial variation (especially at the national scale, see Figure B2, Appendix 2).

In summer, the 10-GCM average rainfall increases over almost the entire Bay of Plenty relative to 1990 levels, being largest (~10%) in the far east and northeast of the district. The model-average shows almost no rainfall change along the south-western boundary with Environment Waikato. The autumn rainfall changes are similar to those in summer. There is a complete contrast in winter, when rainfall decreases by about 10% along the coast and the south-eastern boundary. The spring rainfall changes are similar to those in winter.

Figure 12 shows the box and whisker plot for annual rainfalls, whilst Figure 13 shows seasonal rainfalls. There is little change in the annual rainfall (Figure 12), owing to the previously discussed opposing trends in summer/autumn and winter/spring. The most marked seasonal trends in Figure 13 are for an increase in autumn and a decrease in winter rainfall. Note, too, that the projected range increases with time. For the summer season in particular, the range includes both drier and wetter summers relative to the current climate. Table 3 provides more ("envelope") detail on the seasonal rainfall changes, for the average across all VCS points within the Bay of Plenty region, and for individual locations.

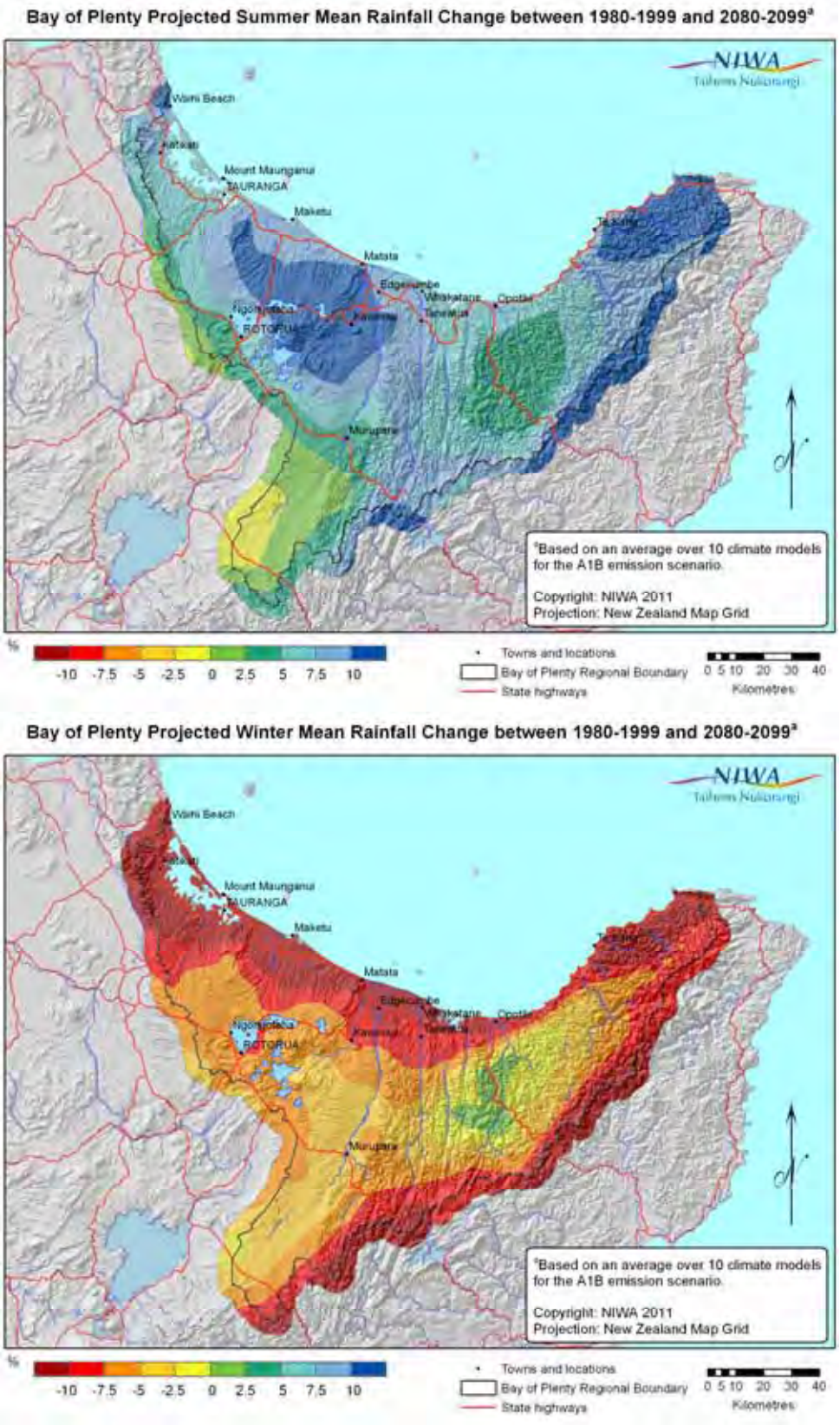

Figure 11: The 10-model average projected rainfall change (%) between 1980-1999 and 2080-2099, for the summer (upper) & winter (lower) seasons, under A1B emission scenario.

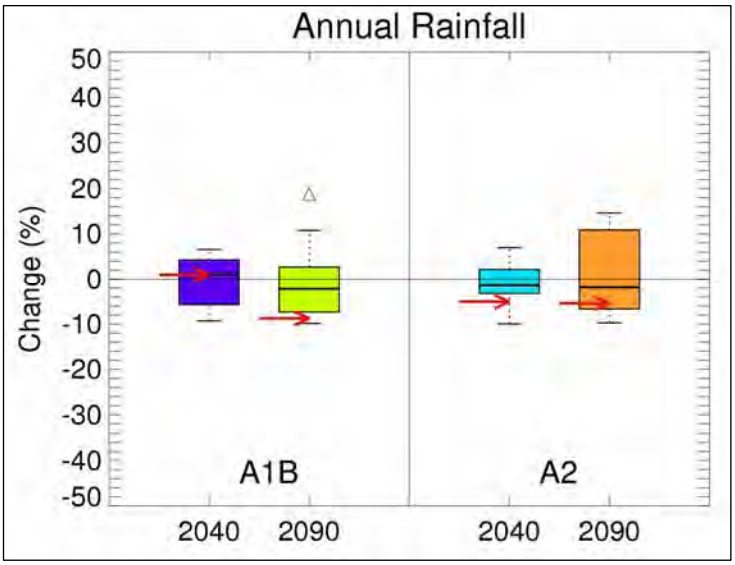

Figure 12: Box and whisker plots of downscaled annual rainfall change projections (%) for Bay of Plenty from 10 climate models, averaged over all VCS grid-points within the Bay of Plenty Regional Council Boundary, as per Figure 10. The RCM result is shown by a red arrow.

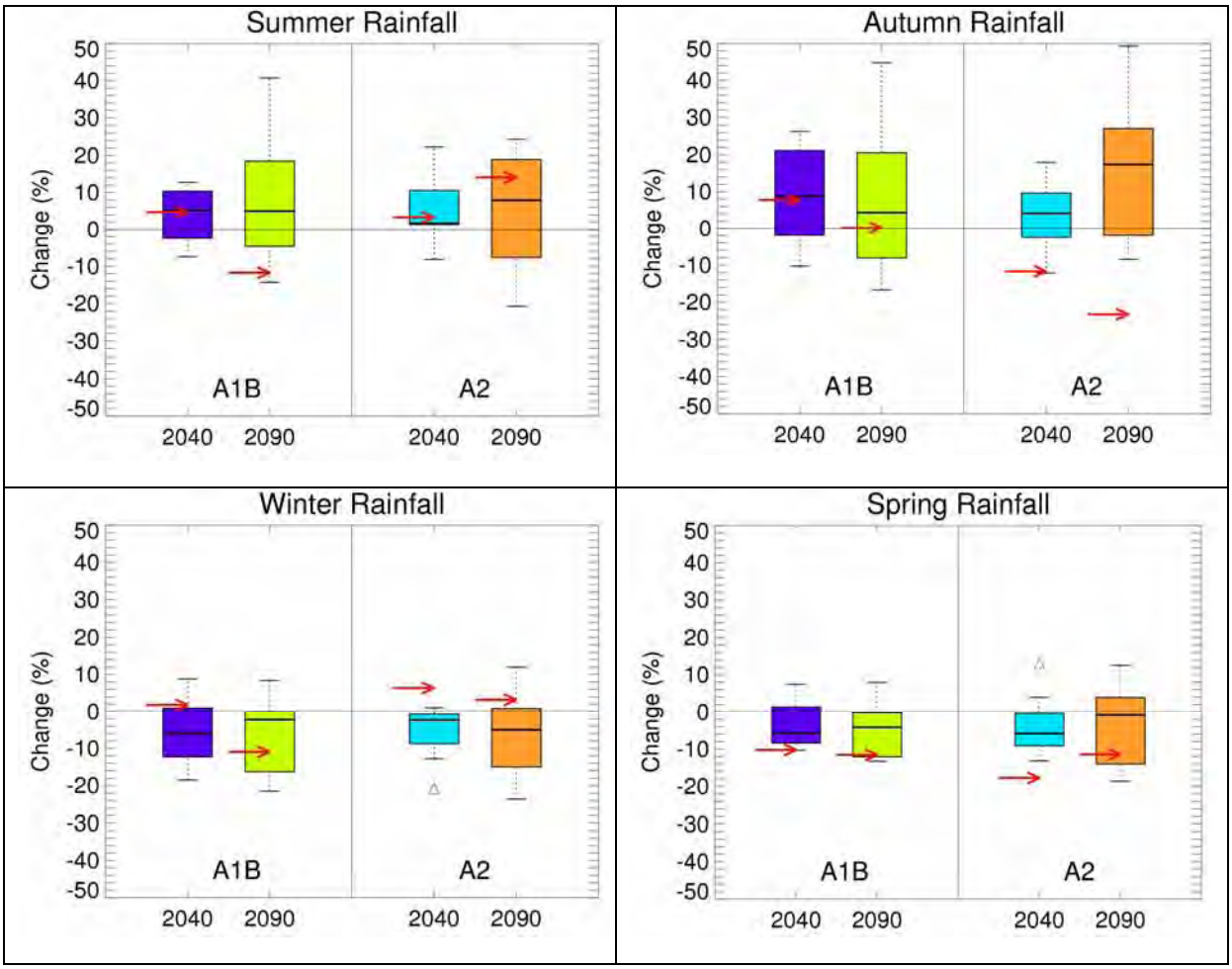

Figure 13: As for Figure 12, but for four seasons separately for projected rainfall changes (%).

Table 3: As for Table 2, but for projected rainfall changes (%) under A1B at 2090[14].

Region or Site	Summer	Autumn	Winter	Spring	Annual
Region average:					
10-model average	7	7	-7	-5	-1
Lowest, Highest	-14, 41	-17, 45	-22, 8	-13, 8	-10, 19
RCM	-12	0	-11	-12	-9
Katikati:					
10-model average	7	5	-14	-11	-5
Lowest, Highest	-12, 37	-17, 46	-27, 9	-24, 4	-15, 14
RCM	-9	2	-14	-12	-9
Tauranga:					
10-model average	6	5	-14	-11	-5
Lowest, Highest	-14, 34	-18, 45	-27, 10	-24, 3	-16, 13
RCM	-5	3	-14	-11	-8
Te Puke:					
10-model average	8	6	-12	-9	-3
Lowest, Highest	-13, 41	-18, 51	-26, 10	-21, 5	-14, 17
RCM	-8	5	-14	-7	-7
Whakatane:					
10-model average	6	5	-14	-11	-5
Lowest, Highest	-16, 38	-18, 45	-29, 8	-23, 4	-16, 10
RCM	-6	1	-11	-13	-8
Opotiki:					
10-model average	6,	6	-11	-8	-4
Lowest, Highest	-16, 39	-17, 44	-25, 8	-19, 5	-13, 15
RCM	-8	0	-11	-14	-8
Rotorua:					
10-model average	6	6	-9	-6	-2
Lowest, Highest	-17, 40	-18, 45	-25, 8	-15, 8	-11, 17
RCM	-9	4	-12	-8	-7
Kawerau:					
10-model average	13	11	-8	-5	1
Lowest, Highest	-11, 56	-16, 58	-25, 10	-17, 10	-11, 25
RCM	-8	4	-11	-8	-6

[14] Note that the annual extremes are not the averages of the seasonal extremes; different models are involved and there is often compensation across seasons.

In summary, rainfall projections for the Bay of Plenty include:

- for the region as a whole, virtually no change[#] in the 10-model average annual precipitation by century-end, but a range across the models from a 10% decrease to a 15-20% increase (A1B and A2 combined);
- a weak tendency for decreased precipitation by 2090 along the coast (about 5%);
- a marked trend to winter rainfall decreases[*], especially for coastal locations;
- a similar rainfall trend in spring to that in winter (i.e., a decrease);
- a trend to increasing rainfall in the summer season[α], which is more marked for inland locations than at the coast;
- a similar rainfall trend in autumn to that in summer (i.e., an increase).

All rainfall changes relative to the baseline period (1980-1999).
*For example, at 2090, 8 of the 10 GCMs are projecting a winter rainfall decrease under A1B, and 7 under A2.
[α] At 2090, 7 of the 10 GCMs are projecting a summer rainfall increase under A1B, and 7 under A2.

4.4 Projected changes in seasonal mean winds, storminess and extreme winds

The 'Wind Report' (Mullan et al., 2011) recently assessed projections of wind changes over New Zealand, including changes in mean and extreme winds, as well as changes in storminess (i.e. whether low pressure systems would become more frequent in the New Zealand region). This section extracts results for the Bay of Plenty from that report.

The 'Wind Report' did not apply any statistical downscaling to the global model wind fields. Monthly and daily winds were extracted for 19 GCMs for the 20th century simulation and the A1B scenario to 2100, and 15 models under the A2 scenario. Thus, a larger sample of models was considered than has been downscaled in other sections of this Bay of Plenty study. For changes in mean seasonal winds, direct model output was used. Changes in daily extreme winds were inferred by examining daily pressure data from the models and identifying weather patterns associated with strong winds.

4.4.1 Seasonal mean winds and storminess

The 'Wind Report' indicated that there is likely to be southward shift in the low pressure/storm track near New Zealand in a future, warmer climate, meaning a reduction in the number of lows over the North Island and to the east of the country in winter, with the chance of slightly increased low pressure frequency to the south of the country. In summer, however, an opposite pattern is seen - it is likely that there will be increased low pressure activity over the Tasman Sea and a decrease in activity south of New Zealand.

A key result for seasonality changes is shown in Figure 14. For the Bay of Plenty region it indicates increasing easterly circulation in summer and increasing westerly winds in winter (top panel), consistent with the altered storm tracks as discussed above.

The lower panel of Figure 14 gives an example from one of the 19 models of the daily distribution of west-east wind speeds - here for GCM data interpolated to the latitude/longitude of East Cape - which shows a projected decrease in the summer percentage of westerly winds at East Cape.

4.4.2 Extreme winds (large scale)

Kidson (2000) analysed 40 years of daily weather maps from the NCEP reanalysis dataset, and diagnosed 12 weather 'types' that affect New Zealand (these are described in detail in Figure 15). The 'Wind Report' analysed historical archives of extreme winds and grouped extreme wind occurrence in terms of the Kidson circulation types, for each Regional Council region of the country. The results were in close agreement with a direct correlation between VCS extreme daily winds and Kidson types. There are two Kidson weather types (T=trough, and SW=south-westerly flow) which have a strong association with daily extreme winds in the Bay of Plenty region. These two weather patterns are shown in the upper panels of Figure 16, and are associated with winds from the west and southwest.

Figure 16 also shows the historical association of Kidson types with extreme wind occurrence in the Bay of Plenty region. The 'trough' (T) weather type produces the largest number of days when daily wind speeds were in the top 1% of the distribution. If the 'south-westerly' (SW) type is included as well, then almost half the windiest days in Bay of Plenty are accounted for.

Mullan *et al.* (2011) then went on to analyse daily weather patterns in all the GCMs under the A1B and A2 emission scenarios. Figure 17 shows the projected average change in Kidson type frequency for the summer and winter seasons. The T and SW Kidson types most relevant to Bay of Plenty extreme winds are components of the "Trough" regime under the Kidson classification, and occur on the left-hand side of each of the panels in Figure 17. The analysis shows that by the end of the century, the frequency of occurrence of the T and SW weather patterns decreases in summer but increases in winter. In both of these seasons, the T and SW types occur around 10-12% of the time under the present climate, and the models project a change of 2-3% under either A1B or A2 by 2100: i.e., down to about 7-8% of the time in summer and up to about 14% of the time in winter.

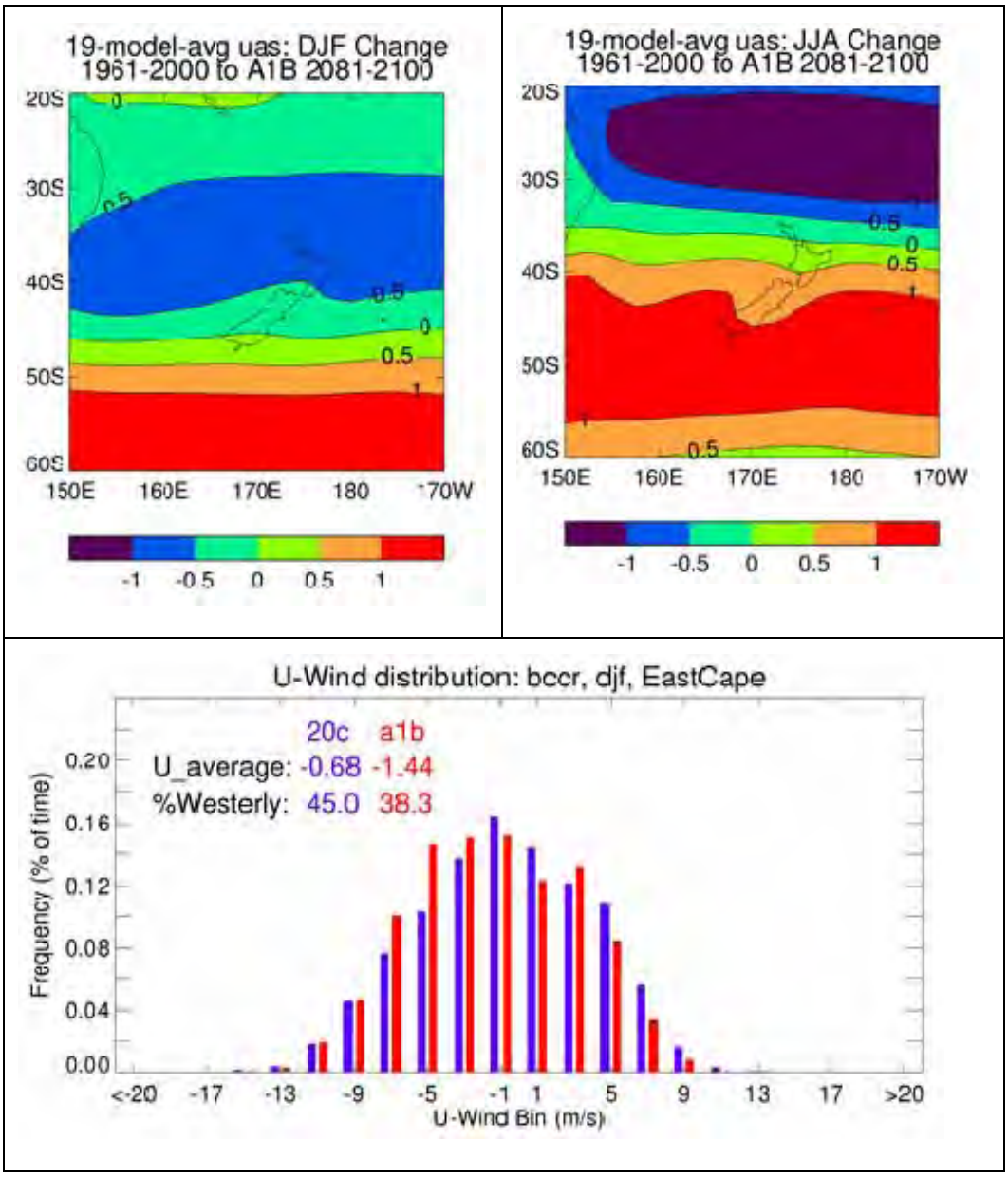

Figure 14: (Top panels) Projected change (in m/s) in the west-east component of the 10-m wind between 1961-2000 and 2081-2100, averaged over 19 GCMs run under the A1B scenario: for summer (top left) and winter (top right) seasons.

(Bottom panel) Histogram of daily west-east wind distribution in summer from the bccr GCM. Daily wind speeds have been interpolated to East Cape and are grouped into 4 m/s bins, and shown as blue bars for the 20th century (1961-2000) and red bars for A1B in 2081-2100. The inset numbers show the average westerly (negative if easterly), and the percentage of westerly days. (From Mullan *et al.,* 2011.)

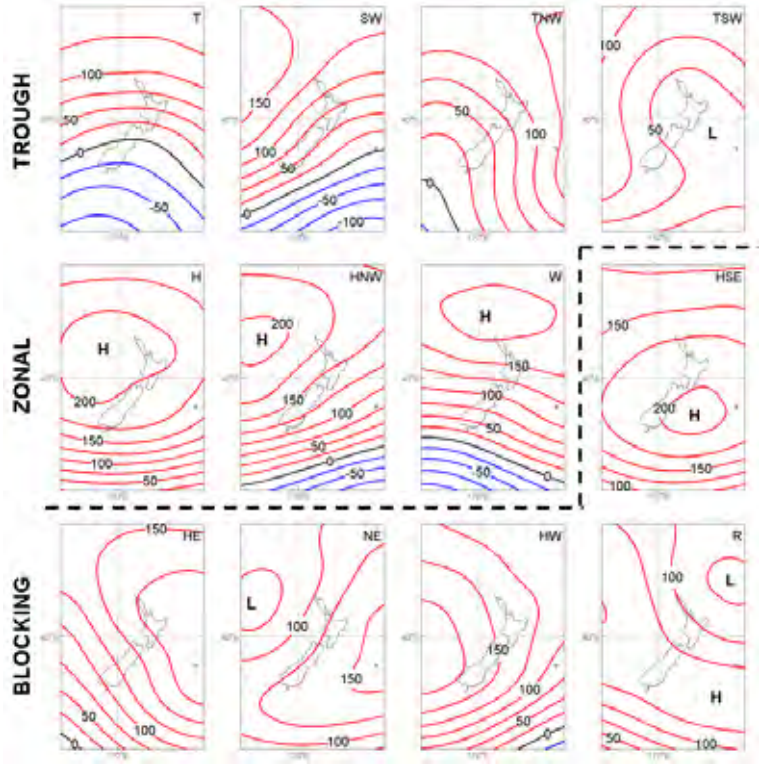

Index	Weather Type	Description
T	Trough	Trough in westerly flow crossing New Zealand
SW	Southwesterly	Southwesterly flows
TNW	Trough/northwesterly	Trough to the west preceded by northwesterly flow
TSW	Trough/southwesterly	Trough in southwest flow crossing New Zealand
H	High	Light winds – North Island; Westerly flow – far south
HNW	High to northwest	High west of the North Island with southwesterly flow
W	Westerly	Westerly flow
HSE	High to southeast	High east of South Island; easterly flow for North Island
HE	High to east	High to the east with developing northwesterly flow
NE	Northeasterly	Northeasterly flows
HW	High to west	High to west of South Island with light south or southwest flows
R	Ridge	Ridge – light winds over the south, easterlies over the north

Figure 15: The 12 Kidson weather types, shown as average patterns of 1000 hPa geopotential height (m), with associated description. These are analogous to mean sea level pressure maps (i.e. the daily weather map). For example, the NE type (bottom row, second from left) shows low pressures over the Tasman Sea, and northeasterly air flows over the North Island. Names are shown at top right of each panel i.e. "T" stands for Trough, "SW" for southwesterly, etc. The three regimes are indicated at left: the top row is the trough regime, the first three in the middle row are the zonal regime, and the remainder are in the blocking regime.

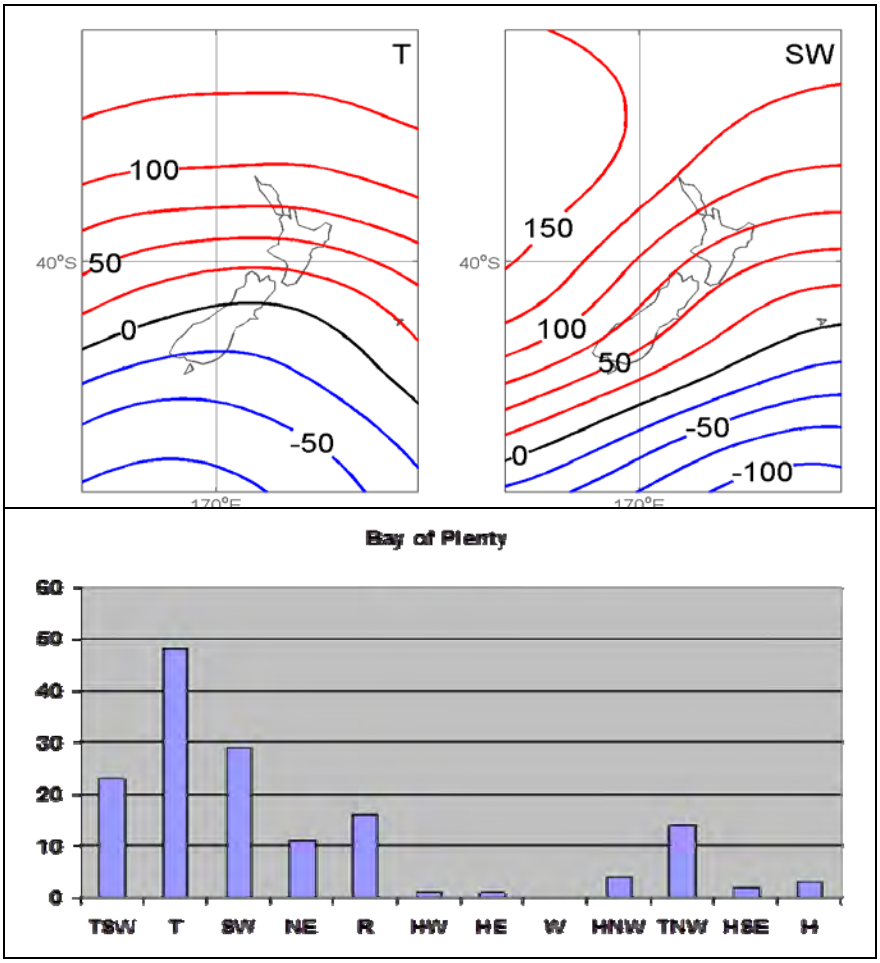

Figure 16: (Upper panel) The Kidson circulation types T and SW (see acronym in top right-hand corner), represented in terms of 1000hPa geopotential heights (m). (Lower panel) Occurrence (in days) of extreme winds (approximately top 1 percent), subdivided by Kidson weather type, over the period 1957-2008, for the Bay of Plenty region, as determined from historical archives. (From Mullan *et al*., 2011.)

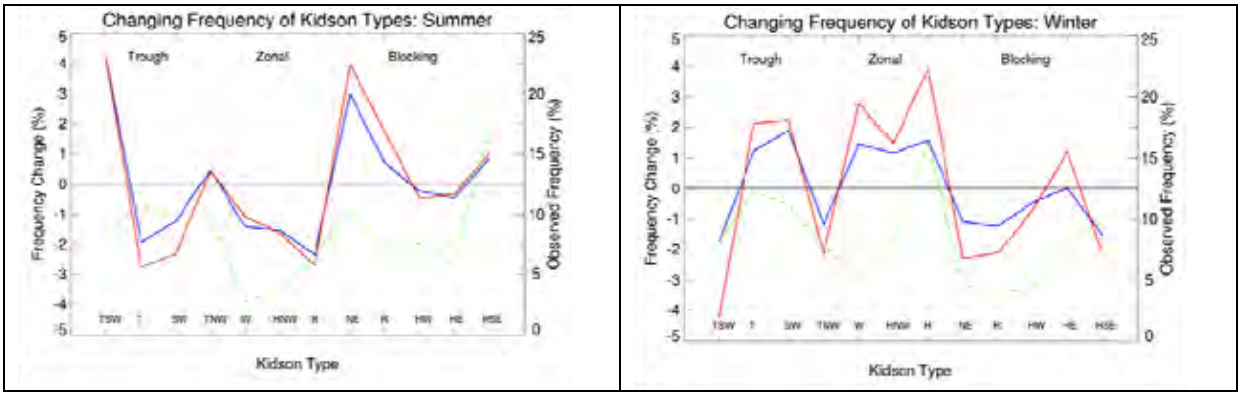

Figure 17: Observed frequency 1961-2000 (dotted green line, right-hand ordinate scale), and projected frequency change 1961-2000 to 2081-2100 (blue, A1B scenario; red, A2 scenario, left-hand ordinate scale) of the 12 Kidson weather types for summer (left) and winter (right) seasons. The types are identified along the bottom of each graph, and are grouped by regime, as labelled. (From Mullan *et al*., 2011.)

4.4.3 Changes in small-scale convection

Strong winds often occur at very small scales, well below the resolution of climate models (both global and regional). Meteorologists have developed "Stability Indices" which represent the vertical variation in moisture content and buoyancy of air parcels in the lower atmosphere, and thus relate to the likelihood for vertical convection to occur. An index which has been found most useful for forecasting thunderstorms in the absence of strong, larger-scale forcing is known as the "K-index" (see the 'Wind Report' for a full definition).

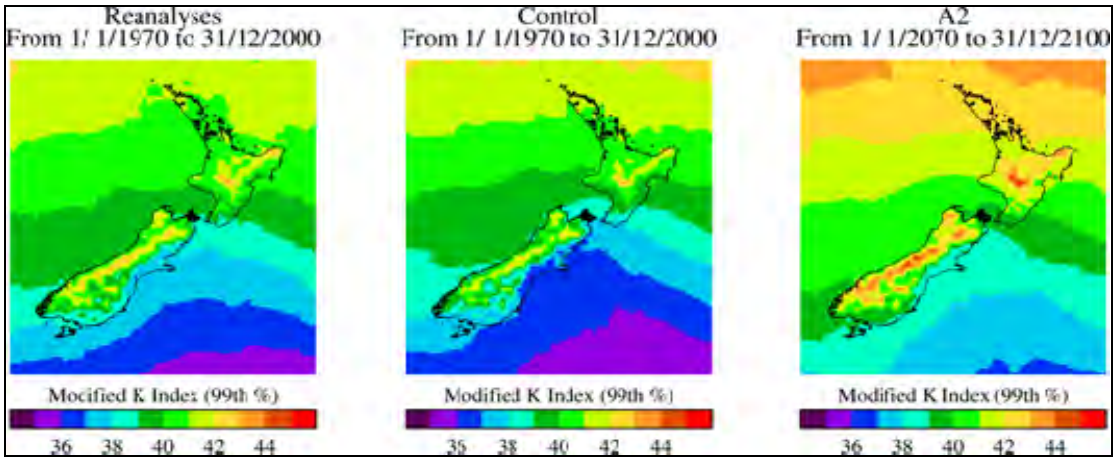

Figure 18: The 99th percentile of the modified K-index over 30 years for the RCM driven by ERA40 reanalyses (left), the RCM 20th century control (centre) and the RCM driven by the A2 emissions scenario (right). (From Mullan *et al*., 2011).

The K index (Figure 18) shows increases in the frequency of severe weather events over much of the New Zealand domain in a future climate that is approximately 2°C warmer than present (compare the map on the right with the other two maps in Figure 18). Thus, we would expect vigorous small-scale convective events to be more common and more intense in a future warmer climate. However, further work would be required to relate these severe weather indices to quantitative changes in extreme surface winds.

In summary, the 'Wind Report' came to the following conclusions for the Bay of Plenty region:

- Seasonal mean winds projections show an increase in easterly days in summer and autumn, and an increase in westerly days in winter and spring, by century-end.
- Daily extreme winds, based on analysis of Kidson weather types for present and future climate, are projected to decrease in summer (associated with T and SW types) and increase in winter. This applies to extreme winds generated by large-scale synoptic* weather patterns.
- Stability indices suggest an increase by 2090 in small-scale convection (all year, but particularly important in the warmer part of the year) and thus likely also to affect small-scale extreme winds that are associated with thunderstorms and gust fronts.

*Synoptic-scale charts (such as the common weather map) capture large-scale atmospheric features such as highs, lows, and fronts.

5. Site-Specific Results

Whilst the previous section primarily concentrated on results for the Bay of Plenty region (as a whole) and across the region (based on gridded data), this section presents results at selected sites within the Bay of Plenty. Variables assessed here include air frosts, hot days and very hot days, extreme 24-hour rainfall, how to handle projected annual temperature changes within the HIRDS v3 (High Intensity Rainfall Design System) interface, drought projections, and pasture growth modelling.

5.1 Projected Temperature extremes

One of the ways the changing climate will be most noticeable will be through the changing occurrence of temperature extremes (defined below). An increase in mean temperature of 2°C may not seem very large, but if the temperature distribution at a specific location is shifted by this amount, what is a very rare event now may become commonplace and conversely, some common events may become increasingly rare.

To assess how the changing climate may affect a selection of sites in the Bay of Plenty region, monthly mean temperature changes simulated by a group of 10 global climate models have been combined with climatological observations to produce projections of daily minimum and maximum temperatures.

The monthly mean temperature changes were taken from the 10 GCMs (see Section 3.3) using outputs that have been empirically downscaled and bias corrected using a gridded observational dataset. Data from the grid point nearest to each site of interest has been used to generate the future daily time-series. At each site a set of 10 simulated maximum temperature time-series has been generated at 2040 for the A1B scenario and at 2090 for the A1B and A2 scenarios (i.e. 30 time-series per site). The same set of simulated time-series has also been generated for daily minimum temperature. By using the scaling method, the day-to-day variability present in the historical data is retained in the simulated future data. In all cases, observed data was taken from 1980 - 1999, 2040 refers to the period 2030 - 2049 and 2090 includes the years 2080 - 2099.

A frost day occurs when the air temperature at ~1.5m above the ground falls below 0°C.
(At some locations, frost days are rare, but at other locations, they occur more often).

A hot day occurs when the air temperature at ~1.5m above the ground exceeds 25°C.
(At some locations, hot days are unusual, but at other locations, they occur more often).

A very hot day occurs when the air temperature at ~1.5m above the ground exceeds 30°C.
(At some locations, very hot days are rare, but at other locations, they do occur from time to time).

The cold night definition is different. There is no single temperature of interest – instead it depends on the location. The cold night index is designed to identify *unusually cold nights at a given location*, by finding the threshold temperature at each location below which the minimum temperature falls only 5% of the time. **A cold night occurs if the temperature at ~1.5m falls below this threshold**.

5.1.1 Frost Days

The frequency of occurrence of frost days and how that frequency may change in a future warmer climate is shown in Table 4. The table shows the mean number of days per year, over a twenty year period, where the air temperature[15] dropped below 0°C. For the future scenarios, the figure given is the 10-model median occurrence frequency.

In the current climate, the frequency of frost days ranges from approximately 5 per year in Opotiki to 20 per year in Rotorua (Table 4). However, by the end of the century under the A1B scenario, Rotorua is projected to experience an air frost only 1 to 2 times a year and under the A2 scenario, is projected to go some years without seeing a frost at all. At all the other sites shown, the end of the century may see the occurrence of air frosts ranging from once every three years to almost never.

Table 4: Number of frost days per year

	Observed	A1B 2040	A1B 2090	A2 2090
Katikati	10.7	3.5	0.3	0.1
Kawerau	8.0	1.5	0.2	0.1
Opotiki	4.9	1.2	0.1	0.0
Rotorua (Airport)	20.0	8.5	1.7	0.8
Te Puke	6.7	1.5	0.2	0.2

5.1.2 Cold Nights

For this report, the temperature of a cold night is defined, on a per site basis, as the 5th percentile of the daily minimum air temperature recorded over the observational period. That is, it is the threshold that the daily minimum temperature goes below only five percent of the time. The number of observed cold nights is the same for each site (on average, ~18 days per year) - unlike the number of frost days, for example - so Table 5 instead shows the cold night temperature *threshold* at each site instead, calculated from observed daily minimum temperatures recorded from 1980 - 1999. This threshold ranges from -0.2°C at Rotorua to 2.6°C at Tauranga. The cold night threshold for Whakatane is equivalent to an air frost.

As was seen for the frost occurrence, the frequency of cold nights is projected to become significantly smaller in all the future scenarios. Even by mid-century under A1B conditions, the frequency has already more than halved from around 18 to approximately 7 cold nights per year for all sites shown. By the end of the century, this is projected to reduce even further to around 1 night per year for A1B and 1 night every two years for A2.

[15] Ground frosts will be more frequent than air frosts, which are measured at 1.5m above the ground.

Table 5: Number of cold nights per year (T < 5th percentile)

	Observed	A1B 2040	A1B 2090	A2 2090
	Threshold	Number of events per year		
Opotiki	1.6°C	7.3	1.2	0.6
Rotorua (Airport)	-0.2°C	7.2	1.3	0.6
Tauranga (Airport)	2.6°C	7.4	1.2	0.6
Te Puke	1.3°C	7.6	0.9	0.4
Whakatane (Airport)	0.0°C	6.3	0.5	0.2

5.1.3 Hot days and very hot days

For this report, a hot day is defined as when the maximum temperature exceeds 25°C (Table 6) and a very hot day is when it exceeds 30°C (Table 7). For both events, significant change is expected in the future.

For many locations in the Bay of Plenty, 25°C days are projected to become the norm during the summer months by the end of the century. For example, in the observations from Whakatane this threshold is exceeded about 22 times a year, but by 2090 the temperature is projected to reach 25°C between 80 and 100 times a year. In Opotiki, the end of century A2 scenario projects a more than 8 fold increase in the number of 25°C days.

Thirty degree days, which are now relatively rare, are likely to occur multiple times per year in the future. For example, Rotorua, which reaches 30°C once every 5 years in the current climate may see that temperature once every 2 years by 2040 and twice a year by 2090 under the A1B scenario. Under the A2 scenario, warmer locations such as Tauranga and Whakatane may reach 30°C five or six times a year by 2090.

Table 6: Number of hot days per year (T > 25°C)

	Observed	A1B 2040	A1B 2090	A2 2090
Opotiki	9.6	25.6	61.1	80.6
Rotorua (Airport)	12.0	25.3	49.6	62.6
Tauranga (Airport)	21.7	41.6	73.8	89.4
Te Puke	21.3	38.2	68.4	84.9
Whakatane (Airport)	22.2	47.4	82.7	102.3

Table 7: Number of very hot days per year (T > 30°C)

	Observed	A1B 2040	A1B 2090	A2 2090
Opotiki	0.0	0.1	0.5	0.9
Rotorua(Airport)	0.2	0.6	2.2	3.2
Tauranga (Airport)	0.3	0.7	2.9	5.4
Te Puke	0.4	1.0	3.6	5.0
Whakatane (Airport)	0.9	1.4	3.9	6.2

5.1.4 Spread in global and regional model predictions

The predicted occurrences of temperature extremes in Table 4 to Table 7 are the median of the occurrence frequencies derived from 10 global climate models. In some cases there are significant differences between the models and it is of interest to examine the spread in the model results.

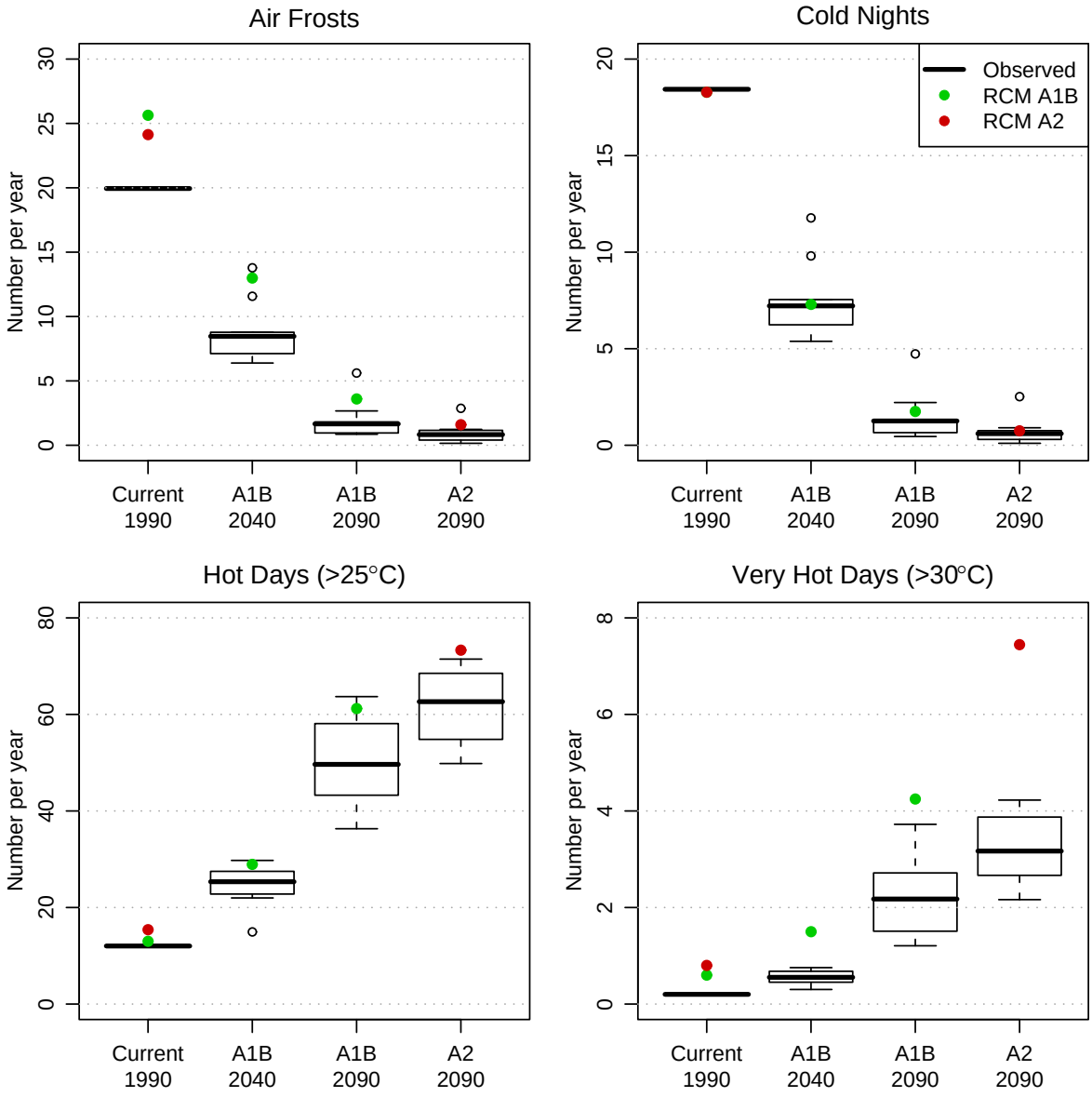

Figure 19: Projected changes in the occurrence of extreme temperatures at Rotorua Airport. The box and whisker plots show the spread in the projections from the 10 GCM members. The red and green dots are the projections from the RCM.

Figure 19 shows the occurrence frequency of the four different temperature extremes for Rotorua. For the future periods, the box and whisker plots show the spread in global climate

model results. For frosts and cold nights, the spread between models is quite small except for one or two outlier models (mainly a model called csiro_mk30). For hot days at the end of the century the spread is much wider and there is significant overlap between the A1B and A2 scenarios. However, even taking this spread into account there are still marked differences between the observations, the mid century and the end of century occurrences.

Also shown on Figure 19 are the RCM projections from two regional climate model (RCM) simulations (under A1B and A2). These RCM simulations are described in Section 3.4. The time-series used to calculate the occurrence frequencies were created from daily minimum and maximum temperatures output by the RCM that had been downscaled and bias corrected. This is different from the GCM projections which applied a temperature offset, calculated from the model, to the observed time-series. Similar figures for the 4 other selected sites discussed in this section are shown in Appendix 3.

The RCM extreme temperature results are broadly consistent with the downscaled GCM projections. Differences between the RCM and GCM projections are mainly seen in the frost days and very hot days, where the RCM has a larger number of both of these extreme events (under current climate and into the future). One reason for this difference may be due to the procedure used to downscale the RCM which is tailored to produce the best results for the centre of the temperature distribution, but not necessarily the extremes. An additional reason for the RCM showing larger increases in the occurrence of very hot days toward the end of the century is that these extreme temperatures may increase by a larger amount than the mean temperature increase. That is, adding a fixed temperature offset to observed daily temperatures, as is done for the GCM results, may not fully capture the changes in extreme temperatures due to a warming climate (which the RCM may be picking up). And lastly, the RCM summer temperature change is larger than the GCM summer temperature change (Figure B1, Appendix 2; Table 2, top row).

5.2 Projected Rainfall Extremes

Since the water-holding capacity of the atmosphere increases with the temperature (by about 7 - 8% more for every 1°C rise in temperature), it is widely accepted (IPCC, 2007) that extreme rainfalls will also increase in a future warmer climate. The IPCC considers this very likely (>90% probability) in most areas of the world, and it could occur even where the annual rainfall total decreases.

Recent studies have shown that extreme precipitation scales not only with moisture content, but also with the vertical profile of vertical velocity and the moist adiabatic temperature lapse rate (O'Gorman and Schneider, 2009; Sugiyama *et al.*, 2010). This means that the increase in the magnitude of extreme rainfall events may be larger than 7 - 8%/°C in some regions. In a study focusing on the New Zealand region, Carey-Smith *et al*. (2010) found that increases in extreme precipitation are likely to be seen in nearly all regions of the country under a warmer climate. This study also suggested that increases in extreme precipitation may exceed increases in the moisture content of the atmosphere.

In this report, five rainfall stations in the Bay of Plenty region have been examined in detail (Table 8). The generalized extreme-value (GEV) distribution has been used to model the distribution of annual maxima at each site following the method of Ailliot *et al.* (2011). The GEV distribution is a flexible three-parameter distribution that combines three extreme value distributions within a single framework: the Gumbel, Frechet and Weibull. After the parameters have been estimated for a particular site, they can be used to calculate the magnitude (and standard error) of rainfall events for arbitrary return periods.

Table 8: The period of observations for five Bay of Plenty rainfall sites and the number of years used to generate the series of annual maxima.

	Start	Stop	Full years
Omanawa	1968	2004	27
Tauranga (Airport)	1942	2010	63
Waimana	1956	2001	34
Whakarewarewa	1900	2010	104
Whakatane (Airport)	1975	2010	29

The report "Climate change effects and impacts assessment: A guidance manual for local government in New Zealand" provides a method showing how high intensity rainfalls can be adjusted for preliminary scenario studies (MfE, 2008). Table 5.2 of this guidance manual provides the recommended percentage adjustments per degree Celsius of warming to apply to high intensity rainfalls for various durations and average recurrence intervals. In this report we have used the percentage change factors from MfE (2008) to estimate the magnitude of future extreme rainfall events (relevant change factors are repeated in Table 9).

Table 9: Factors (percentages per degree Celsius of warming) for use in deriving high intensity rainfall information for 24 hour duration rainfall events.

Average Return Interval (years)	2	5	10	20	50	100
Change Factor (%/°C)	4.3	5.4	6.3	7.2	8.0	8.0

Table 10 contains 24 hour rainfall depths (in mm) for a selection of average return intervals at Omanawa. The observed values and their standard errors (an indication of the uncertainty range) are calculated from GEV distributions fitted to the annual maxima series. The rainfall depths for the future scenarios are calculated by applying the change factors from Table 9 to the observed values. The temperature changes used in these calculations are taken from the 10 downscaled GCM simulations[16].

[16] The temperature change for each model and scenario (e.g. A1B at 2040) is the difference between the mean Bay of Plenty temperature during the future (e.g. 2030 - 2049) and baseline (1980 - 1999) periods. The 10-model average temperature is used to calculate the future rainfall depth and the rainfall depth standard error is a combination of the observed error and the standard deviation of the set of 10 temperature changes.

Table 10: Depth-frequency table for 24 hour rainfall durations for Omanawa (mm).

ARI	Observed		A1B 2040		A1B 2090		A2 2090	
Years	*mm*	*Std. error*	*mm*	*Std. error*	*mm*	*Std. error*	*mm*	*Std. error*
2	104.7	5.5	110.0	7.3	116.8	8.1	119.2	8.1
5	132.6	9.1	141.0	12.0	151.8	13.4	155.6	13.5
10	153.1	13.8	164.4	17.9	178.9	20.2	184.1	20.4
20	174.4	21.0	189.1	26.8	208.0	30.3	214.7	30.7
50	204.6	35.0	223.8	43.6	248.4	49.3	257.2	50.4
100	229.4	49.5	250.9	60.1	278.5	67.8	288.3	69.5

Figure 20 contains the 2 and 10-year event magnitudes from Table 10 in graphical form. The observed values, while assigned to 1990, include all the available data records (see Table 8). Also included on these graphs are the results from two regional climate model (RCM) simulations. The RCM event magnitudes were obtained by fitting GEV distributions to series of annual maxima taken from daily rainfall time series at the grid point nearest to the site location. These time-series were not downscaled, as this process, while correcting the mean rainfall bias, is not expected to improve the projections of rainfall extremes. The three values for each RCM simulation were calculated using 40 years of simulation each in order to increase the sample size. This means that the time periods for the GCM and RCM are not exactly the same in this extreme rainfall analysis; for the RCM data, 1990 includes 1970 - 2009, 2040 includes 2015 - 2054 and 2090 includes 2060 - 2099.

Due to the resolution of the 30 km RCM simulations, it is not expected that the magnitudes of the extreme events at the nearest grid point will exactly match the observed values. This explains why projections from the RCM do not always lie within the uncertainty estimates of the observed data. Indeed, for some sites they are significantly different (see Appendix 3). In addition, because each RCM simulation is a single realisation of what the weather may do in the future and the actual occurrence of extreme events is quite variable, the projected curves are not necessarily smoothly increasing. However, bearing these caveats in mind, it is apparent that the RCM shows a general increase in the magnitude of extreme events in the future that is largely consistent with the GCM-scaled observations.

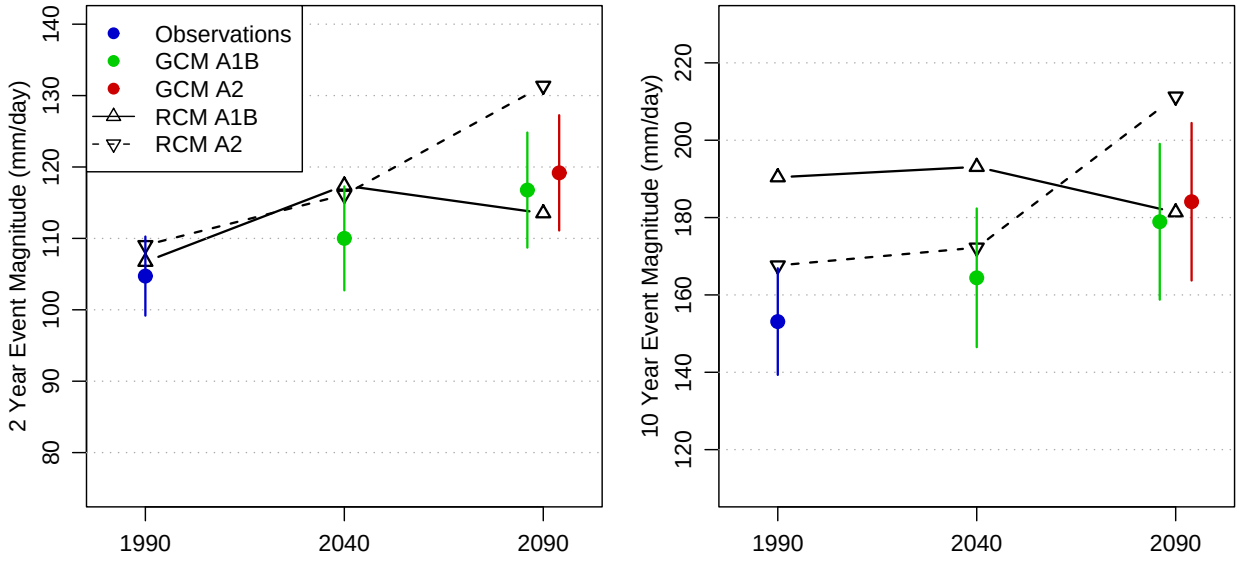

Figure 20: Two and ten year event magnitudes for Omanawa. Observations are shown in blue; projected estimates using observations factored by global climate model temperature changes are shown in green and red; regional climate model results are shown by the dashed and solid black lines.

Table 11 to Table 14 contain 24-hour rainfall depths for the four other sites under consideration.

Table 11: Depth-frequency table for 24 hour rainfall durations for Tauranga Airport (mm).

ARI	Observed		A1B 2040		A1B 2090		A2 2090	
Years	*mm*	*Std. error*	*mm*	*Std. error*	*mm*	*Std. error*	*mm*	*Std. error*
2	93.2	4.3	97.9	5.8	103.9	6.4	106.1	6.4
5	125.3	6.7	133.3	9.4	143.5	10.5	147.1	10.6
10	148.2	9.9	159.1	13.6	173.2	15.5	178.2	15.6
20	171.4	14.7	185.8	19.9	204.4	22.7	211.0	22.9
50	203.3	23.9	222.3	31.4	246.8	35.8	255.5	36.4
100	228.7	33.3	250.1	42.3	277.6	48.0	287.4	49.0

Table 12: Depth-frequency table for 24 hour rainfall durations for Waimana (mm).

ARI	Observed		A1B 2040		A1B 2090		A2 2090	
Years	*mm*	*Std. error*	*mm*	*Std. error*	*mm*	*Std. error*	*mm*	*Std. error*
2	103.3	5.8	108.5	7.5	115.2	8.3	117.6	8.3
5	134.2	8.5	142.7	11.4	153.6	12.8	157.5	12.8
10	154.9	11.8	166.3	15.9	181.0	17.9	186.2	18.1
20	174.9	16.8	189.7	22.3	208.6	25.3	215.3	25.7
50	201.1	26.1	219.9	33.8	244.1	38.5	252.7	39.2
100	220.8	35.2	241.6	44.3	268.1	50.2	277.6	51.2

Table 13: Depth-frequency table for 24 hour rainfall durations for Whakarewarewa (mm).

ARI	Observed		A1B 2040		A1B 2090		A2 2090	
years	*mm*	*Std. error*	*mm*	*Std. error*	*mm*	*Std. error*	*mm*	*Std. error*
2	80.7	2.6	84.8	3.8	90.0	4.3	91.9	4.3
5	105.1	3.9	111.7	6.0	120.3	6.9	123.3	6.8
10	121.9	5.6	130.9	8.5	142.5	9.8	146.6	9.8
20	138.7	8.2	150.4	12.1	165.4	13.9	170.7	14.0
50	161.2	13.0	176.3	18.4	195.7	21.2	202.6	21.4
100	178.7	17.8	195.4	24.1	216.9	27.6	224.6	28.0

Table 14: Depth-frequency table for 24 hour rainfall durations for Whakatane Airport.

ARI	Observed		A1B 2040		A1B 2090		A2 2090	
Years	*mm*	*Std. error*	*mm*	*Std. error*	*mm*	*Std. error*	*mm*	*Std. error*
2	80.4	5.1	84.4	6.5	89.6	7.2	91.5	7.2
5	104.8	7.0	111.5	9.3	120.0	10.4	123.0	10.5
10	120.2	9.2	129.0	12.4	140.4	13.9	144.5	14.1
20	134.3	12.4	145.6	16.6	160.1	18.9	165.3	19.1
50	151.6	18.3	165.8	24.0	184.1	27.3	190.6	27.8
100	164.1	23.9	179.4	30.3	199.2	34.5	206.2	35.1

5.3 Using HIRDS v3 with climate change scenarios

The HIRDS (High Intensity Rainfall Design System) v3 software is available online at http://hirds.niwa.co.nz/. This system produces rainfall depth-frequency tables, given an input location (for example, a latitude/longitude). HIRDS v3 also incorporates the option of inserting up to 3 annual temperature change projections, in order to calculate estimates of projected rainfall depth-frequency under climate change.

For the selected sites given in Section 5.2, the depth-frequency tables given in Section 5.2 should be used preferentially, otherwise the following use of HIRDS v3 is suggested for obtaining a projected depth-frequency rainfall table at a given location:

1. Select the scenario and time slice of interest (the 3 options are A1B at 2040, A1B at 2090, or A2 at 2090).

2. Check whether the location of interest is found in Table 2 (Section 4.2), or Table B1 or Table B2 (both in Appendix 2); if so, use the *annual* temperature change based on the 10-model average as the primary input into the HIRDS v3 website (Figure 21).

3. There is room for up to 3 projected annual temperature changes to be input into HIRDS v3 at any one time – allowing for an envelope approach. If an envelope

approach is desirable, and the location of interest is found in Table 2 (Section 4.2), or Table B1 or Table B2 (both in Appendix 2), then additionally use the *annual* temperature change (lowest) and *annual* temperature change (highest) as inputs.

4. Otherwise, use the 4 seasonal temperature change GIS layers (which have data on a ~5km by 5km grid) associated with the selected scenario/time slice to produce an annual temperature change value, for the nearest grid-point to the location of interest. This is appropriate, even in complex terrain, since projected seasonal mean temperature change across the Bay of Plenty is a "smooth" field which varies only slightly across the region (for example, see Figure 9). For example, if A1B at 2040 is chosen, select the 4 GIS layers which contain the 10-model average temperature change for A1B at 2040 for summer, autumn, winter and spring; utilise GIS software to select the nearest grid point to the location of interest; and calculate an average ((summer value + autumn value + winter value + spring value)/4) at this grid-point. Insert this average value (the 10-model average *annual* temperature change) into HIRDS v3[17].

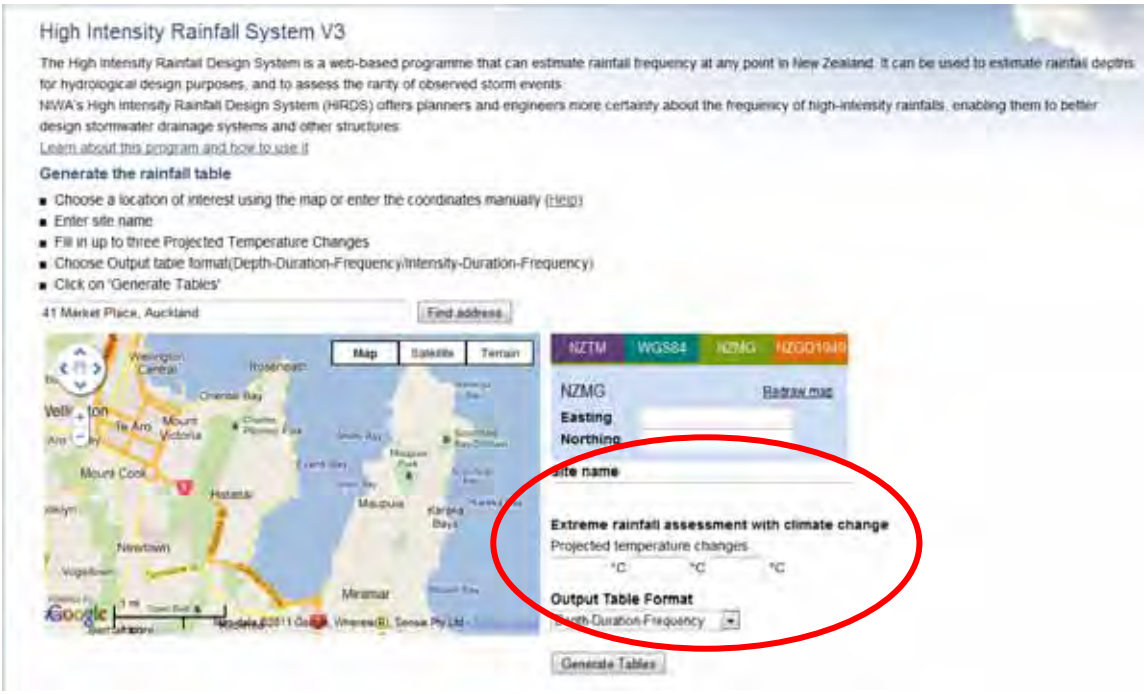

Figure 21: Illustration of the HIRDS v3 website interface, and the insertion area for projected annual temperature changes (circled in red).

5.4 Drought and pasture growth projections

In this section, the current pasture growth profile of the Bay of Plenty region, and its current drought exposure, are assessed, based on station-specific analyses at the 5 sites selected by the Bay of Plenty Regional Council (Katikati, Whakamaramara, Te Puke, Te Teko and Opotiki).

[17] Note that no envelope approach is possible using the GIS seasonal mean temperature layers, since these contain the 10-model average value.

Modelled changes in pasture growth profile and drought exposure at these five sites are then given, under the three differing model and time slice options (A1B at 2040, A1B at 2090, and A2 at 2090) using output from the RCM (see Section 3.4).

5.4.1 How is drought defined?

Drought, or a severe and prolonged water deficit, is a major risk to agriculture, but assessing it objectively can be difficult as there are multiple definitions and approaches to drought analysis. It may be defined meteorologically as a prolonged rainfall deficit, by hydrologists as a prolonged reduction in soil water or river flow, agronomically as a prolonged period of feed deficit or crop loss, or economically as loss of farm income (Wilhite et al., 2000; White, 2000). There are also a range of drought indices that can be used to objectively define droughts, for example the Palmer Drought Severity Index, the Phillips and McGregor Drought Index and other historical comparisons such as decile ranking of indicators. Each have different criteria to define entry, exit (duration) and intensity of drought events, which may be physically based (e.g. crop wilting point) or historically based (e.g. percentiles).

To provide a basis for assessing a broad range of drought types in the Bay of Plenty, the approach described by Clark *et al.* (2011) was taken here, where drought is quantified according to both its duration and intensity using accumulated days of low soil water[18] as the drought indicator. This provides a hydrological indicator suitable for assessing dryland agricultural drought under New Zealand conditions. The historical thresholds and event durations used to characterise drought are summarised in Table 15.

Table 15: Drought intensity "characteristics" used in this report.

		Drought Intensity		
		High (<=10th percentile plant available soil water)	***Moderate*** (<=25th percentile plant available soil water)	***Low*** (<=50th percentile plant available soil water)
Drought Duration	***> 14 days***	High intensity > 14 day	Moderate intensity > 14 day	Low intensity > 14 day
	> 1 month	High intensity > 1 month	Moderate intensity > 1 month	Low intensity > 1 month

To analyse present and projected drought exposure, the following steps were taken at the five sites:

- Low, moderate and high intensity soil water shortages were defined as a function of calendar day as plant available soil water being below the historical 50th, 25th and 10th percentiles respectively for that day of the year.
- Drought was defined as a run of consecutive days where the soil water was below each day's threshold.

[18] Table 15 quantifies "low" in terms of historical percentiles of soil water.

- If a day was within a high intensity drought it was also within a moderate and low intensity drought; and if a day was of duration > 1 month, it was also of duration > 14 days.

- The summer season was analysed for changing drought exposure under the three climate change scenarios using the RCM results, as this is the time when water limitation of pasture growth is likely to occur.

- The percentage of days per summer spent within each of type of drought was calculated over the current (1980-1999) and future periods. These were reported using the 25th, 50th and 75th percentiles. That is, drought exposure in half of all summers is worse than the 50th percentile value, and in the driest quarter of all summers, it is worse than the 75th percentile value.

This approach taken from Clark *et al.* (2011) quantifies relative droughts and assumes that local practices are adjusted to seasonal climatic conditions at any given site. Given this assumption the aim of the drought indicator is to quantify departures from this expected seasonal variability. A number of strengths and limitations need to be considered when interpreting the results:

- The seasonal summer dry experienced in the Bay of Plenty would not be considered a drought, but a normal feature of climate variability;

- The indicator may not reflect a physical threshold such as plant wilting point or hydrological shortage of water; and

- When seasons are historically very wet, such as the winter in the Bay of Plenty, the indicator should be interpreted with caution - a relative drought quantified using this indicator may still be well above plant wilting point with ample supply of water.

5.4.2 Present-day drought exposure

A recent set of scenarios for New Zealand droughts under climate change were developed by Clark *et al.* (2011) in the 'Drought Report', focusing on high intensity droughts persisting longer than 1 month (defined in Table 15). These suggest that under the current climate these events occur, on average, between 5 and 8% of the time in the Bay of Plenty, although there was variation across the region.

A more detailed site-specific analysis was undertaken here examining regional variability across a broad range of drought types. This analysis departs from that presented in the 'Drought Report' in that it focuses on the summer period.

Based on a site-specific analysis (Table 16), Katikati currently experiences, on average[19]:

- high intensity drought, > 14 days, about 5% of the summer
- low intensity drought, > 14 days, about 30% of the summer
- low intensity drought, > 1 month, about 7% of the summer

The driest quarter of all summers at Katikati currently experience:

- high intensity drought, > 14 days, more than 13% of the time.
- low intensity drought, > 14 days, more than 37% of the time
- low intensity drought, > 1 month, more than 31% of the time

Table 16: Base period (1980-1999) percentage of time in drought for different drought intensities and durations at Katikati. The median percentage is bolded [also given are the 25th percentile and 75th percentile].

Katikati 1980-1999	Summer median [25th percentile 75th percentile]		
	High intensity (<=10th percentile)	Moderate intensity (<=25th percentile)	Low intensity (<=50th percentile)
Duration > 14 days	**5.0** [0.0-12.7]	**5.5** [0.0-14.4]	**30.4** [2.2-**36.7**]
Duration > 1 month	0.0 [0.0-0.0]	0.0 [0.0-0.0]	**6.7** [0.0-30.9]

Appendix 4 (Tables D1, D2, D3, D4) shows the results for the other 4 selected sites. For comparison, assessing only the low intensity droughts of longer than 14 days, we see that this type of drought is currently experienced, on average[19]:

- about 30% of the summer at Katikati
- about 18% of the summer at Whakamarama
- about 29% of the summer at Te Puke
- about 20% of the summer at Te Teko
- about 18% of the summer at Opotiki

The results indicate that there is distinct regional variability in summer drought exposure across the Bay of Plenty, given elevation and distance from the coast. The higher elevation site (Whakamarama, near to the Kaimai Ranges) and the eastern sites (Opotiki, Te Teko) have a current (low intensity, > 14 day) summer drought exposure of 18-20%. In contrast, the

[19] This is the median (50th percentile) value. Half of all summers in the historical record experience drought for longer than the value given and there is large variability seen in the historical record.

drier, western/central, coastal sites of Katikati and Te Puke have a current (low intensity, > 14 day) summer drought exposure of about 30%.

Low intensity summer droughts persisting longer than 1 month can also occur at the five sites under current climate (occurring on average[20] about 7% of the summer at Katikati, 16% at Te Puke, 3% at Te Teko, but remain a rare event at Whakamarama and Opotiki).

5.4.3 Modelled changes in drought under climate change

The scenarios developed by Clark et al. (2011) showed that under the mid-range A1B emissions scenario, for the Bay of Plenty, the most likely projection (i.e. the median of 19 different GCMs examined in that study) was for a 2-5% increase in time in high intensity drought (lasting more than a month) by 2040 and a 2-10% increase by 2090, compared with 1990.

In this report, we assess changes in summer drought exposure and pasture production, under A1B at 2040 and 2090, and A2 at 2090, using RCM outputs on a ~30 km scale, which are further downscaled to the five selected sites (Katikati, Whakamarama, Te Puke, Te Teko and Opotiki) using statistical downscaling methods. The resulting site specific daily climate simulations are used to drive a coupled soil-water balance and pasture production model (see Section 5.4.4).

Projections for Katikati at end of century under both A1B and A2 (Table 17, Figure 22, Figure 23) show the largest changes under both scenarios at 2090 occur in droughts lasting longer than 1 month. Table 17 indicates about a 9% (median) increase in time spent in > 1 month, low intensity droughts at Katikati at 2090 under A1B, and an increase of approximately 22% under A2 at 2090. Under A2 at 2090, there is no real change (-0.5% decrease) in the time spent in > 14 day, high intensity droughts at Katikati. But the time spent in moderate intensity and high intensity droughts lasting more than a month is increased under A2 at century-end (with a median change of between 6-8% at Katikati, but ranging between 0-8% across all sites), which is consistent with the predictions in previous national drought analyses, such as Mullan *et al.* (2005) and Clark *et al.* (2011).

Table 17: Projected changes in (median) percentage of time spent in drought at Katikati, at 2090 under both A1B and A2 scenarios.

Katikati, Summer season, A1B at 2090			
Change (% time spent in drought)	High intensity (<=10th percentile)	Moderate intensity (<=25th percentile)	Low intensity (<=50th percentile)
Duration > 14 days	1.6	8.4	7.9
Duration > 1 month	0.0	0.0	9.4
Katikati, Summer season, A2 at 2090			
Change (% time spent in drought)	High intensity (<=10th percentile)	Moderate intensity (<=25th percentile)	Low intensity (<=50th percentile)
Duration > 14 days	-0.5	3.4	14.0
Duration > 1 month	5.6	7.8	21.7

[20] This is the median (50th percentile) value. Half of all summers in the historical record experience drought for longer than the value given and there is large variability seen in the historical record.

For comparison (Appendix 4), assessing the time spent in > 1 month, low intensity summer drought at all five sites, we see an average[21] projected increase at 2090 of:

- about 9% under A1B and about 22% under A2 at Katikati
- about 14% under A1B and about 25% under A2 at Whakamarama
- about 17% under A1B and about 26% under A2 at Te Puke
- about 13% under A1B and about 20% under A2 at Te Teko
- about 11% under A1B and about 2% under A2 at Opotiki

Notably, the five sites on average all show increases in time spent in > 1 month low intensity drought. The magnitudes are fairly similar, except for at Opotiki at 2090 under A2. The smaller Opotiki median result is not in error – it simply reflects that for *most* summers, there are no drought periods of duration exceeding a month – either now or in the future. But for the driest quarter of all summers, Opotiki does show significant increases. The time spent in > 1 month, low intensity summer drought is projected to increase under A2 at 2090 by:

- about 19% at Whakamarama, Katikati, and Te Teko
- about 24% at Te Puke
- about 15% at Opotiki

Figure 22 and Figure 23 show the full range of summer drought projections at Katikati at both mid-century and end of century, in graphical form, under A1B and A2, respectively. Both figures indicate a clear increase in average (median, red line) summer drought exposure by century-end compared to present, for all droughts except high intensity droughts (which are relatively rare).

In contrast, at 2040 under the A1B scenario (Figure 22) a decrease is seen in > 14 day droughts in summer, linked to an absence of low summer rainfall years in the A1B RCM projections at mid-century. This is most likely due to interdecadal variability (i.e. wet decades, dry decades), based on natural climate cycles. By century-end, however, A1B and A2 drought projections are more similar, i.e. the climate change signal dominates by 2100. That is, there is an increase in time spent in > 14 day summer drought of all intensities under A1B at 2090, and also an increase in > 1 month low intensity summer drought.

Appendix 4 shows the projected drought changes for the other 4 selected sites, both in tabular form for 2090 values and graphical form for both mid-century and century-end.

[21] This is the median (50th percentile) increase. Half of all summers are projected to increase time spent in drought for more than the median value given.

Figure 22: Projections of percentage of time spent in drought at Katikati, Summer Season, under A1B. Red line shows the projected median. Blue box indicates 25th and 75th percentile. Projected twenty-year maximum and minimum values are shown as whiskers off the boxplot. Top rows depict droughts lasting more than 14 days; lower rows depict droughts lasting more than a month. Left hand column shows high intensity drought, middle column shows moderate intensity drought, and right hand column shows low intensity droughts. Within each square, present day (1980-1999) estimates (left hand side) are compared to 2040 (centre) and 2090 (right hand side).

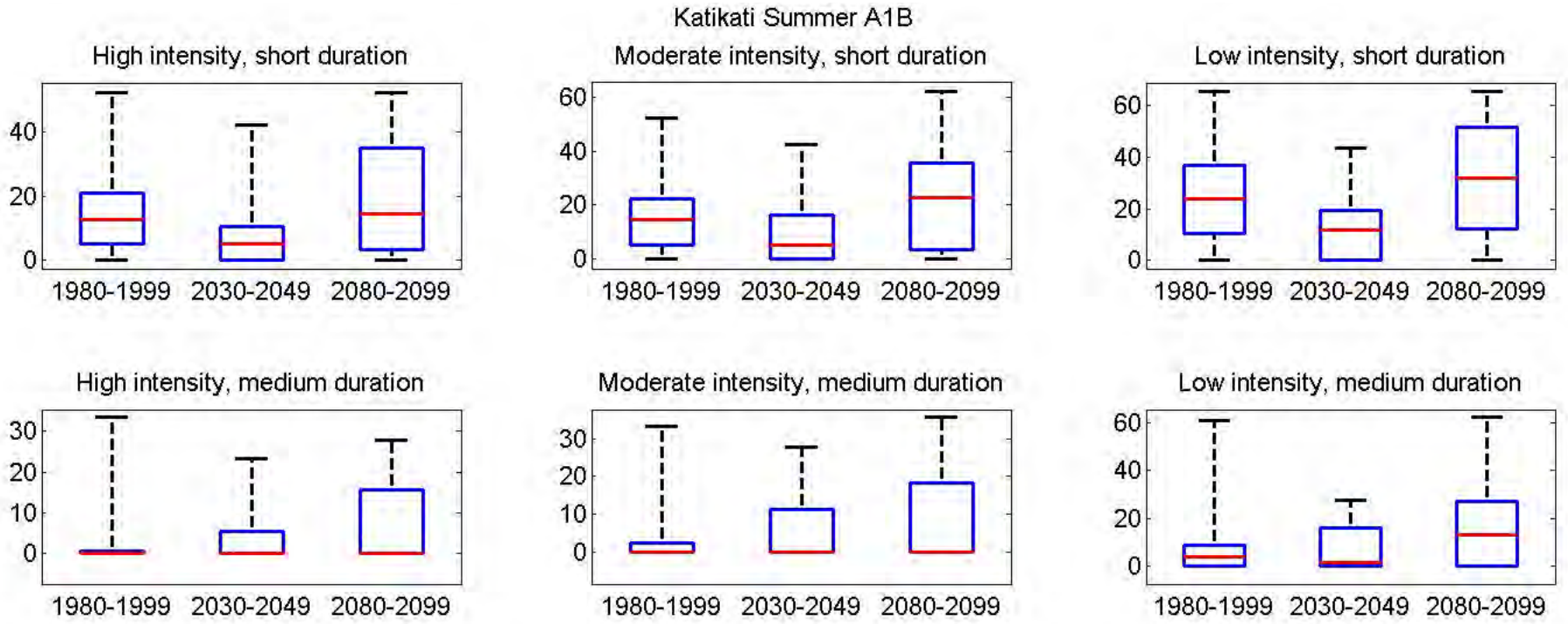

Figure 23: Projections of percentage of time spent in drought at Katikati, Summer Season, under A2. Red line shows the projected median. Blue box indicates 25th and 75th percentile. Projected twenty-year maximum and minimum values are shown as whiskers off the boxplot. Top rows depict droughts lasting more than 14 days; lower rows depict droughts lasting more than a month. Left hand column shows high intensity drought, middle column shows moderate intensity drought, and right hand column shows low intensity droughts. Within each square, present day (1980-1999) estimates (left hand side) are compared to 2040 (centre) and 2090 (right hand side).

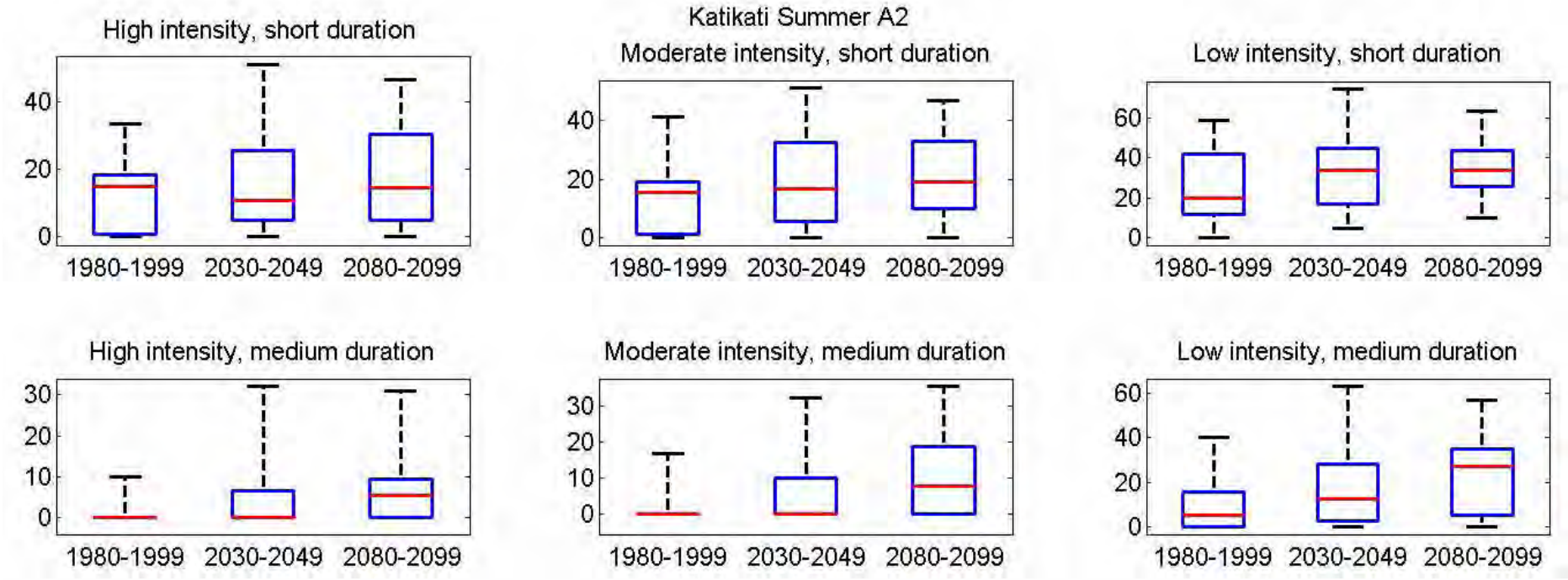

5.4.4 How is pasture growth calculated?

A coupled soil water, pasture growth, grazing model was used to simulate pasture growth rates and profile soil water. The model has four modules: a three layer force-restore water balance (Rickert *et al.*, 2000); a series of phenomenological equations describing plant growth, reproduction and development (based on McCall and Bishop-Hurley, 2003); a simple animal module describing intake of pasture as a function of metabolic weight (Pittroff and Kothmann, 2001); and a management module describing grazing. The water balance component of the model has undergone extensive testing using NIWA's soil moisture modelling network, with results showing that the model is an appropriate choice for use in climate change analyses (Clark *et al.*, 2011).

Daily pasture growth rate (in kg dry matter per hectare per day) is calculated based on McCall's pasture growth equations (McCall and Bishop-Hurley, 2003). The model uses daily rainfall, maximum temperature, minimum temperature, incoming global short wave radiation and evapotranspiration to determine daily pasture growth (these are downscaled from the RCM).

The model uses a 3-layer force-restore water balance (Rickert *et al.*, 2000), where the field capacity of the second layer (the most significant for plant available water) is set from Landcare's fundamental soil layer (fsl) database. The different soil types and their relative areas in each ~5km x 5km VCS grid box were determined from this database by Dr. Anthony Clark (Personal communication, 2011). The third layer field capacity is set at 75 mm.

The model assumes a Ryegrass (*Lolium perenne*) and white clover (*Trifolium repens*) sward. Water availability is determined from input precipitation, and modelled runoff, evapotranspiration and drainage. The model does not consider irrigation, changes in grass species, or management options to adapt to future climate conditions. A fixed stocking rate and grazing regime is assumed, nominally three New Zealand stock units per hectare. It is assumed that feed is provided to stock whenever there is insufficient pasture biomass to feed them. The model does not include carbon dioxide fertilisation effects. The model does not include an explicit nutrient cycle but assumes that adequate nutrients are available and the pasture is not nutrient limited.

5.4.5 Current pasture growth in the Bay of Plenty

The relatively warm, dry summers and cool, wet winters in the Bay of Plenty yield an annual pasture growth curve with a distinct spring growth peak, a more variable autumn growth peak, low winter growth and highly variable summer growth. Growth is generally water-limited through summer (day 0 to day 50 of the calendar year, Figure 24), but storms (bringing significant rainfall) can yield periods of high growth at that time of the year and there is high year to year variability in summer pasture growth. An autumn growth peak begins between day 50 and 100 (late February to early April), lasting until about day 150, with high inter-annual variability. Cool temperatures limit growth rates over winter, between day 150 and 250 (June to August). As temperatures increase in spring, pastures take advantage of water

stored in the soil over winter, and growth rates increase to a maximum around day 270 to 320 (early October to late November). Spring growth is generally reliable with little interannual variability.

Figure 24 shows the pasture growth curve at Katikati under current climate, being very similar to the growth curves modelled at the other sites. The only exception is at Whakamarama, which is at an elevation of 300 m amsl just east of the Kaimai divide, so receives higher summer rainfall, and lower summer temperatures, than the lower elevation sites – such that more reliable summer pasture growth, but lower winter growth, is estimated at Whakamarama (compare Table 18 and Table 19).

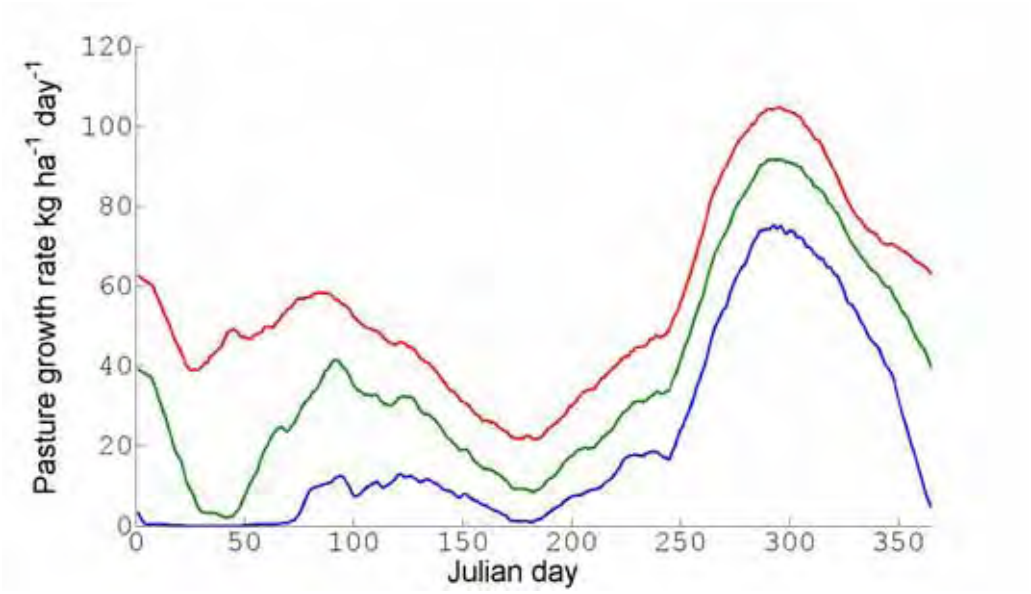

Figure 24: Pasture growth curve for Katikati under current climatic conditions. Simulations are run with meteorological observations for the period 1980-1999. Green lines represent the median pasture growth for that Julian day. Julian day 1 equates to 1 January; Julian day 365 equates to 31 December. Blue lines represent the 25th percentile and red lines the 75th percentile of growth for that Julian day.

Table 18: Katikati pasture biomass for 1980-1999 from RCM reanalysis data, median value (25th percentile-75th percentile). Summer value calculated from contiguous Dec-Feb values and is for the 19 years 1981-1999.

Katikati Reanalysis Biomass production in kg per hectare 1980-1999	
Annual biomass	14144 (13095-15171)
Summer biomass	2666 (1470-3503)
Autumn biomass	2697 (1876-3457)
Winter biomass	2045 (1833-2386)
Spring biomass	6705 (6430-7144)

Table 19: Whakamarama pasture biomass for 1980-1999 from RCM reanalysis data, median (25th percentile-75th percentile). Summer value calculated from contiguous Dec-Feb values and is for the 19 years 1981-1999.

Whakamarama Reanalysis	Biomass production in kg per hectare 1980-1999
Annual biomass	14529 (14108-14712)
Summer biomass	5446 (4646-5872)
Autumn biomass	2739 (2490-3023)
Winter biomass	1048 (745-1230)
Spring biomass	5374 (5025-5722)

5.4.6 Modelled changes in pasture growth under climate change

Modelling of future pasture growth under a changing climate (with no adaptation) shows little change in annual pasture biomass but significant changes in the seasonality of pasture growth in the Bay of Plenty.

By century-end, higher summer temperatures reduce summer pasture growth significantly at the five sites analysed but milder winter temperatures result in large increases in winter pasture growth (Figure 25 - Figure 29 and Appendix 4). The spring peak in growth shifts little (Figure 25), but there is greater spring growth prior to the peak and earlier onset of the summer growth restriction period. Total spring growth and reliability of spring growth are unchanged. Autumn growth continues to have high interannual variability with little change in its magnitude or spread. The onset and end of the autumn growth peak shift later by approximately 3 weeks by the end of the century under A2 (Figure 25).

Under A2 (Figure 25, Figure 28, Figure 29, Appendix 4) at both 2040 and 2090, all sites show a clear decreasing summer pasture growth, with a decrease in the median and range. By 2040 at all sites except Whakamarama (which shows the same pattern of change, just smaller), half of all summers show pasture growth lower than the least-productive quarter (25%) of summers under today's climate. At Katikati, for example (Figure 25), half of all summers show no pasture growth during January or February by 2040 under the A2 scenario[22]. By 2090 at all sites, at least three-quarters (75%) of all summers have lower pasture growth than the least-productive quarter (25%) of summers currently.

In contrast, under A1B at mid-century there is a *reduction* of low growth years, giving a slightly higher median summer pasture growth (Appendix 4). Again, this simply reflects the RCM and GCM model (Figure 13) projections of increased summer rainfall under A1B at 2040. It is likely that this difference is due to inter-decadal climate variability (i.e. wet decades, dry decades), based on natural climate cycles. By century-end, the climate change signal dominates, with A1B projections having a similar pattern to A2 pasture growth projections, but a smaller magnitude of change.

[22] The A1B scenario has more rainfall at 2040 (due to natural decadal variability), but there is only a slight improvement in summer pasture growth.

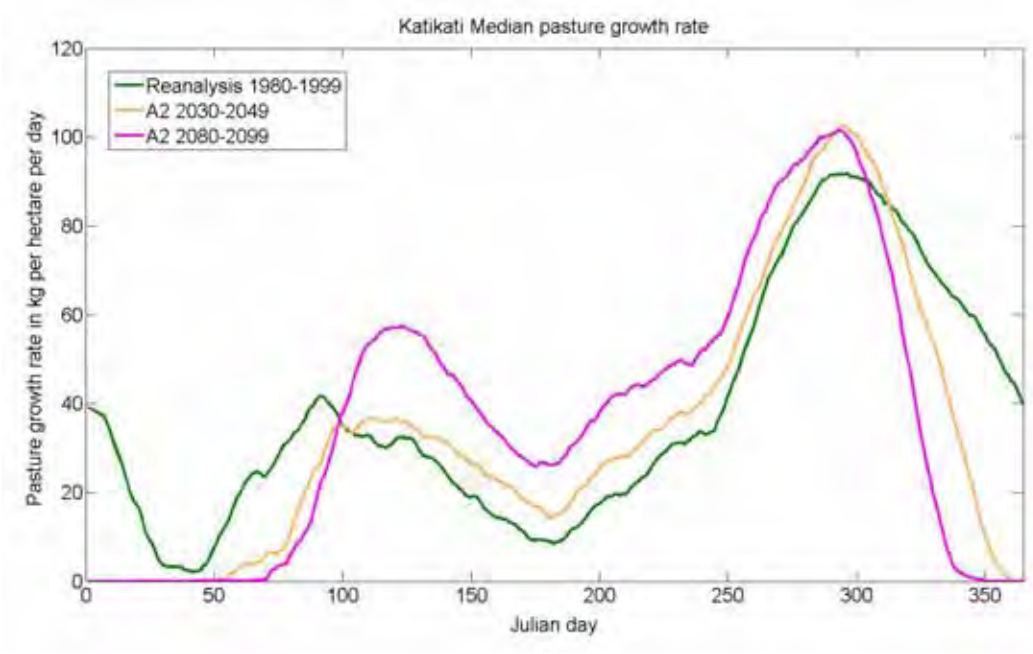

Figure 25: Median pasture growth curves for Katikati under current climatic conditions and under future A2 projections, as a function of Julian day. Julian day 1 equates to 1 January; Julian day 365 equates to 31 December. The green line represents the median pasture growth under current conditions (based on the reanalysis-driven RCM) and is the same as in Figure 23. The light brown and magenta lines represent median pasture growth at 2040 and 2090, respectively, under the A2 scenario.

Pasture growth changes were also mapped across the entire Bay of Plenty under A1B and A2, for summer versus winter (Figure 26 to Figure 29), as a percentage of historical (1980-1999) median growth. The scales differ from summer to winter. In the summer maps, 100% of median (i.e. the same as current conditions) is shown in a red colour, whilst 50% of median, or less, is shown in a dark blue colour. In the winter maps, red colours indicate in the order of 300% of median (i.e. three times current levels), aqua represents about 200% of median (i.e. twice current levels), and dark blue under 180% of current median.

From Figure 26 - Figure 29, we can see the largest decreases in summer pasture growth are in low lying areas with lower annual rainfall, along the coast and extending up major river systems. Under the A2 scenario, median summer pasture growth decreases significantly at all locations at both 2040 and 2090, with larger decreases seen at all locations at 2090 compared to 2040. Under the A1B scenario, little change or slight increases in median summer pasture growth are seen at all locations by 2040 (Figure 26); this is most likely due to interdecadal variability dominating the projections at this time for this scenario, as mentioned previously.

Winter pasture growth shows large increases under both scenarios, with around double current levels along the coast, and treble inland, at 2090 (noting that winter growth at elevation is relatively lower than at the coast).

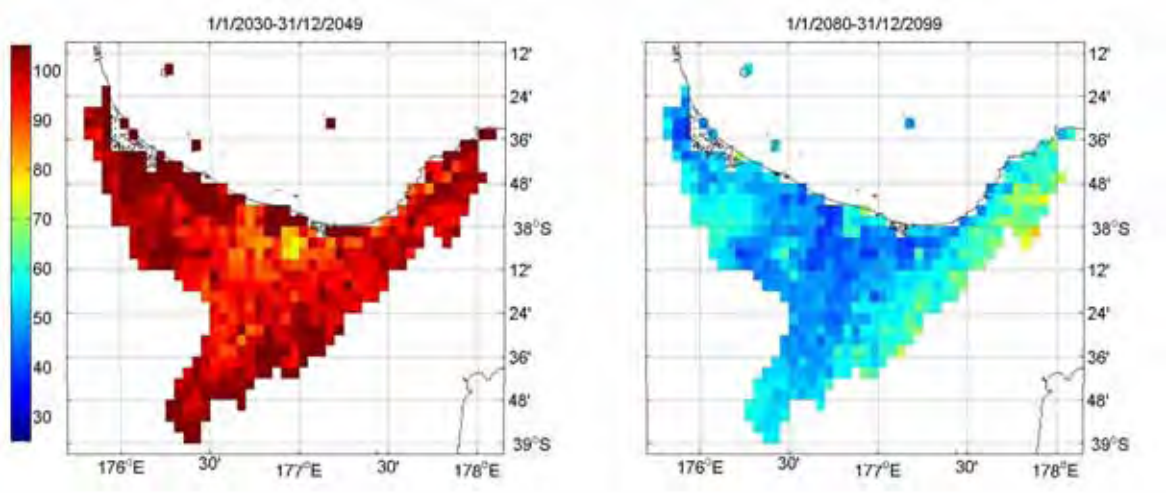

Figure 26: Projected future median summer pasture growth (at 2040, left hand side and 2090, right hand side) as a percentage of historical 1980-1999 median summer pasture growth on ~5km x 5km VCS grid for the A1B scenario.

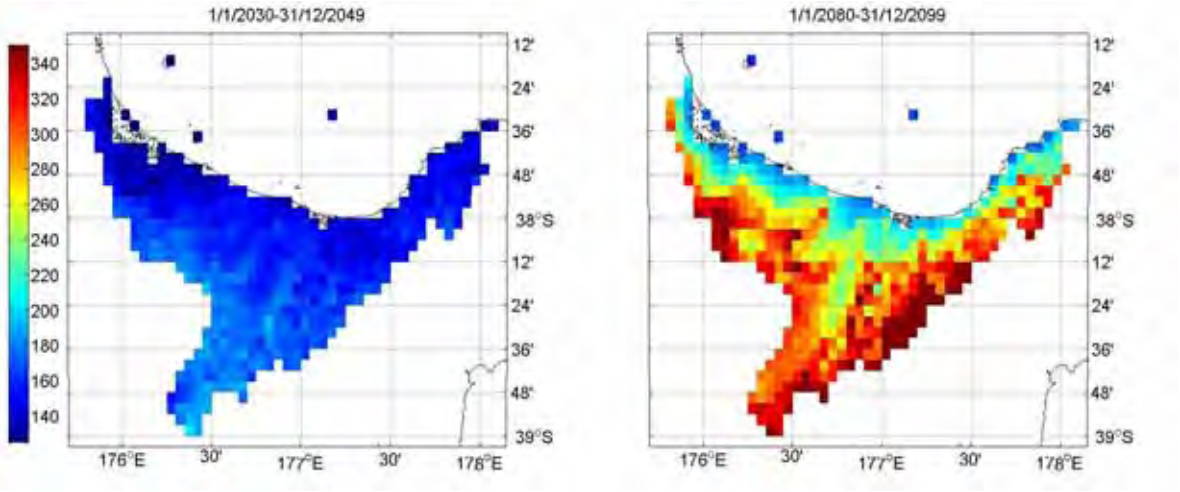

Figure 27: Projected future median winter pasture growth (at 2040, left hand side and 2090, right hand side) as a percentage of historical 1980-1999 median summer pasture growth on ~5km x 5km VCS grid for the A1B scenario.

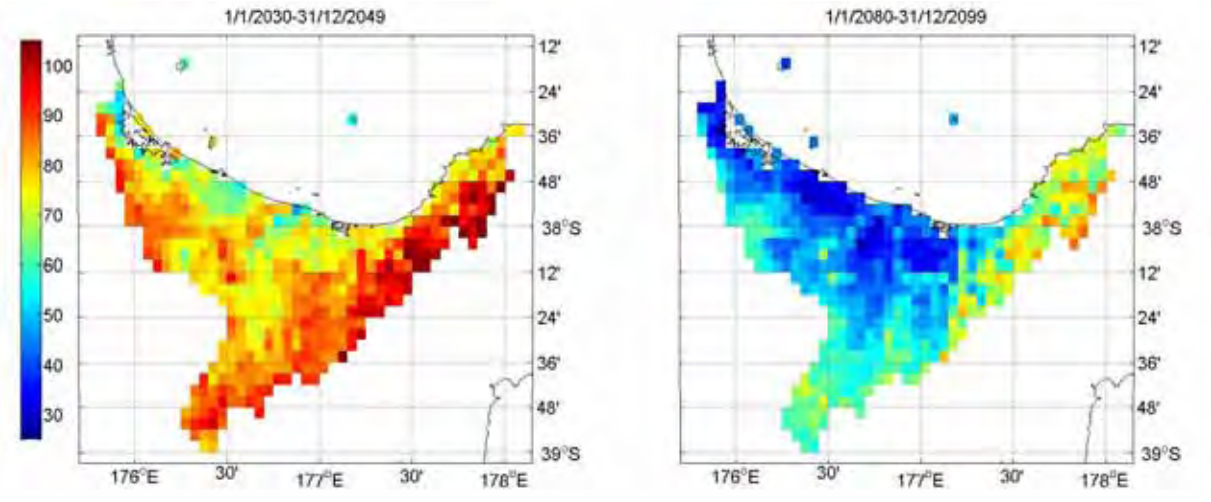

Figure 28: Projected future median summer pasture growth (at 2040, left hand side and 2090, right hand side) as a percentage of historical 1980-1999 median summer pasture growth on ~5km x 5km VCS grid for the A2 scenario.

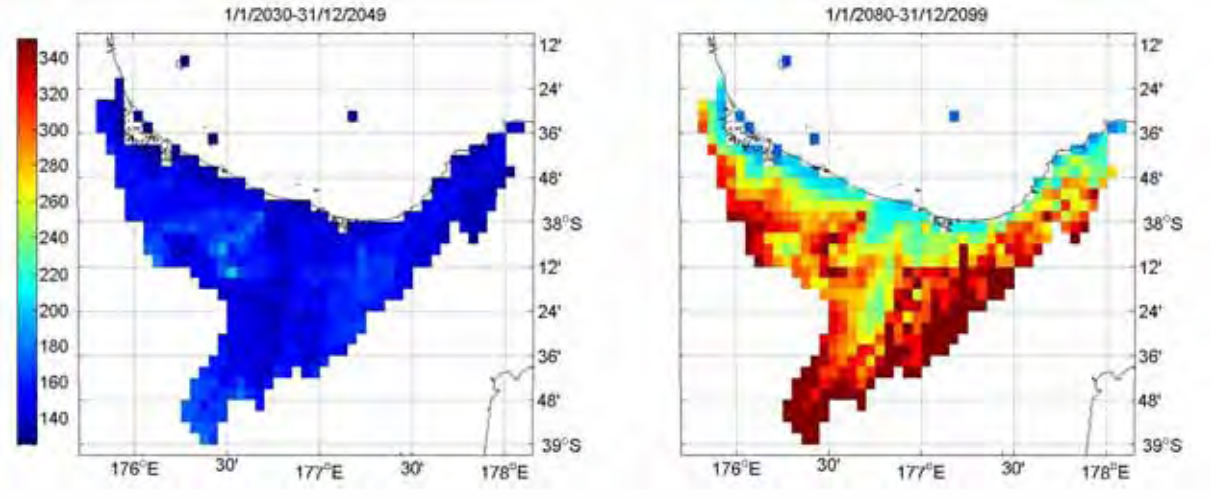

Figure 29: Projected future median winter pasture growth (at 2040, left hand side and 2090, right hand side) as a percentage of historical 1980-1999 median summer pasture growth on ~5km x 5km VCS grid for the A2 scenario.

6. A Synthesis of Results

6.1 Introduction

Bay of Plenty Regional Council has requested an update of the climate change assessment that was undertaken for the region in 2003 (Griffiths *et al.*, 2003). This updated report draws on a significant body of climate change modelling and knowledge undertaken internationally and by NIWA over the intervening eight years. Important New Zealand climate change reports produced since 2003 include a national guidance manual on climate change prepared for the Ministry for the Environment (MfE, 2008), a drought report (Clark *et al.*, 2011), a wind report (Mullan *et al.*, 2011), and a publication on extreme rainfalls (Carey-Smith *et al*., 2010).

6.2 Modelling information

The climate change modelling used in this report is based on (greenhouse gas) emission scenarios described in the Intergovernmental Panel on Climate Change Fourth Assessment Report (commonly abbreviated as IPCC AR4). These scenarios are divided into "storylines" that describe distinctly different future developments of economic growth, global population, and technological change. The three most comprehensively investigated storylines are known as: B1 (low emissions), A1B (mid-range emissions), and A2 (high emissions). The IPCC does not attach any probabilities to these emission scenarios; in other words, they do not see any one scenario as being more likely than any other. The AR4 scenarios form the basis of all the climate change reports listed above.

The projections for this Bay of Plenty Regional Council report focus on the A1B (mid-range) and A2 (high) scenarios, and two time slices: mid-century (2030-2049) and century-end (2080-2099), relative to present day (1980-1999).

The primary set of future projections described in this report are calculated from 10 Global Climate Models (GCMs) that have been empirically downscaled to a ~5km x 5km grid across New Zealand, which is known as the Virtual Climate Station (VCS) network (Tait *et al.*, 2006). There are approximately 500 VCS grid-points covering the Bay of Plenty, of the 11,500 VCS grid-points over the New Zealand land mass.

Empirical downscaling is a technique for building in local scale detail that is consistent with the much larger-scale global climate model output. Statistical relationships that link large-scale atmospheric variables with local/regional climate variables are developed using several decades of past climatic data. These relationships are then applied to the large-scale projections from the GCMs. For example, large-scale pressure patterns might be related to local (station) observations of rainfall. In the past year, NIWA has developed a new, improved empirical/statistical downscaling approach, as described in Clark *et al.* (2011). The new technique is used here in this report, and supersedes the downscaling used in previous

publications, such as the Ministry for the Environment guidance manual (MfE, 2008). However, the new empirically downscaled climate change patterns are very similar to the earlier patterns of change, in the Bay of Plenty and for the rest of New Zealand. In particular, the direction of rainfall change (wetter/drier) is the same, although the magnitude of the changes tends to be slightly smaller under the new downscaling.

Other differences between this report and the Ministry for the Environment guidance manual include that the downscaling has been applied directly to both A1B and A2 GCM output here, instead of estimating A2 changes by a simple scaling of the A1B results (as was done in MfE, 2008). This means that the A2 rainfall change at 2090, say, may not only be a different magnitude to A1B but may have a different spatial pattern. In addition, a slightly different set of GCMs was used (10 GCMs here, of which only 7 are common to the 12 used in the guidance manual). An important consequence of the differing GCMs for this report is that the extreme top end of the temperature range will be smaller than in MfE (2008) and the model spread will be tighter.

In addition, NIWA also runs a high-resolution climate model in the New Zealand region, known as a Regional Climate Model (RCM), which is "nested" in one particular GCM. This approach is often called dynamical downscaling. To run the RCM, the GCM must be run first to provide the boundary conditions at the edges of the RCM domain, containing information on wind, pressure, temperature and moisture that allow weather systems to pass from the lower resolution GCM into the higher resolution RCM. The RCM method provides a more physics-based approach for developing future climate change scenarios at the meso-scale compared to empirical downscaling, but requires considerable computational resources. The result is a huge archive of daily weather data at about 300 grid-points (~30km grid) over the New Zealand land mass, covering a 130-year period. There are two such data sets, one under the A1B scenario and the other under A2. Downscaling of the RCM datasets enabled drought and pasture modelling in this report, since the RCM outputs provide daily data and contain many more variables than just rainfall and temperature, as provided by the GCMs. In addition, it enabled comparison to the empirically downscaled GCM projections.

The primary results produced in this report are the '10-model averages' of the empirically downscaled GCM data, since comparisons between observational data and multiple climate models have shown that the group average tends to have a lower error than most, if not all, of the individual models. The 10-model average seasonal temperature and seasonal rainfall projections have been provided as GIS layers to the Council (~5km x 5km gridded data). In addition, to cater for an "envelope" approach, the lowest and highest response from the empirically downscaled GCM models, as well as the single result from the dynamical RCM projection driven by a single GCM (the United Kingdom Met Office HadAM3P model), were also given for each scenario/time slice, for a selection of key sites.

6.3 Key temperature projections

Projections show an increase in temperature with time for the Bay of Plenty. The warming at 2040 is similar for A1B and A2, but A2 has clearly promoted more warming by 2090 than A1B. There is very little spatial variation in the temperature projections within the Bay of Plenty (meaning Tauranga warms about the same as Whakatane, under A2 at 2090, for example). There is, however, a difference in the degree of warming from one season to another as well as a considerable difference between models. The *range* of warming seen across the models increases with time (i.e. the differences between the 10 models are larger by 2090 than at 2040). The RCM annual warming lies very close to the average warming from the 10 GCMs for all of the scenarios/time slices.

In terms of the GCM 10-model average warming, temperatures are projected to increase slightly faster for the autumn and winter seasons than for spring and summer. For the RCM, however, warming is faster in the summer and autumn seasons than for winter and spring.

In summary, the Bay of Plenty region is projected to:

- warm by about 1.2 °C (relative to 1990) by 2040 under the A1B scenario, in the annual mean, as an average across the 10 GCMs, with a range between 0.5 and 1.5 °C;
- warm by about 2.7 °C (range 1.7 to 3.2 °C) by 2090 under A1B (annual mean);
- warm by about 3.2 °C (range 2.5 to 3.6 °C) by 2090 under the higher A2 emission scenario (annual mean); and
- warm slightly more in winter than the annual mean (at 2090 under A1B, 7 of the 10 GCMs warm most in winter, 2 warm most in autumn, and 1 warms most in summer. The RCM warms most in summer).

6.4 Key rainfall projections

In contrast to projected temperature changes, the projected rainfall changes show marked spatial variation across the Bay of Plenty region.

In summer, the GCM 10-model average projects rainfall increases over almost the entire Bay of Plenty region, being largest (~10%) in the far east and northeast of the district, as well as inland between Rotorua and Edgecumbe. The 10-model average shows almost no rainfall change along the south-western boundary with Waikato Regional Council. The autumn rainfall projected changes are similar to those in summer. The summer-autumn rainfall projected ‘increases’ are primarily a reflection of increased variability; in the projected future climate, very dry summer-autumn seasons become more common as do extremely wet ones, with the net effect of increased rainfall in a long-term average sense.

There is a complete contrast in winter, when the 10-model average projects rainfall decreases of about 10% along the coast and the south-eastern boundary of the Bay of Plenty region. The spring rainfall changes are similar to those in winter.

Overall, there is little change in the annual rainfall projections, owing to the opposing rainfall trends in summer/autumn and winter/spring.

In summary, rainfall projections for the Bay of Plenty include:

- for the region as a whole, virtually no change relative to 1990 levels in the 10-model average annual precipitation by century-end, but there is a range across the models from a 10% decrease to a 15-20% increase (A1B and A2 combined);
- a weak tendency for decreased precipitation by century end along the coast (about 5%);
- a marked trend to winter rainfall decreases, especially for coastal locations (at 2090, 8 of the 10 GCMs show a winter rainfall decrease under A1B, and 7 under A2);
- a similar rainfall trend in spring to that in winter (i.e., a decrease);
- a trend to increasing rainfall in the summer season, which is more marked for inland locations than at the coast (at 2090, 7 of the 10 GCMs are projecting a summer rainfall increase under A1B, and 7 under A2); and
- a similar rainfall trend in autumn to that in summer (i.e., an increase).

6.5 Key circulation, storminess and extreme wind results

A poleward shift in the low pressure/storm track in a future, warmer climate is likely, meaning a reduction in the number of lows over the North Island and to the east of the country in winter, with the chance of slightly increased low pressure frequency to the south of the country. In summer, however, an opposite pattern is likely, with increased low pressure activity over the Tasman Sea and a decrease in activity south of New Zealand.

This pressure pattern is meteorologically consistent with the likely drier winters, and wetter (more variable rainfall) summers, discussed above.

Projected seasonal mean winds in the future for the Bay of Plenty show an increase in easterly days in summer and autumn, and an increase in westerly days in winter and spring. Daily extreme winds generated by large-scale weather systems (such as fronts and lows) are projected to decrease in summer but increase in winter, based on an analysis of weather map "types" which have historically produced extreme winds in the Bay of Plenty. Atmospheric stability indices suggest an increase in small-scale convection under climate change (all year round, but particularly important in the warmer part of the year), which is likely to affect small-scale extreme winds associated with thunderstorms and gust fronts.

6.6 Extreme temperature projections

The projected frequency of an air frost (i.e. when air temperature measured at ~1.5 metres above the ground drops below 0°C) becomes vanishing small by century-end across the Bay of Plenty region, under GCM projections. At present, the frequency of air frosts ranges from about 5 per year in Opotiki to 20 per year in Rotorua. However, by the end of the century under the A1B scenario, Rotorua is projected to experience an air frost only 1 to 2 times a year and under the A2 scenario, is projected to go some years without seeing a frost at all. The frequency of cold nights also becomes significantly smaller in all the future scenarios.

Hot days (recording 25°C or more) are projected to become the norm during the summer months by the end of the century. For example, at Whakatane, on average about 22 hot days currently occur per year, but by 2090 between 80 and 100 hot days per year are projected. At Opotiki, the end of century A2 scenario projects a more than 8 fold increase in the number of hot days.

Compared to the GCM results, the RCM estimates a larger number of both air frosts and hot days at selected sites in the Bay of Plenty, under current climate and into the future.

6.7 Extreme rainfall projections

Since the water-holding capacity of the atmosphere increases with the temperature (by about 7 - 8% more for every 1°C rise in temperature), it is widely accepted (IPCC, 2007) that extreme rainfalls will also increase in a future warmer climate. Recent studies have shown that extreme precipitation scales not only with moisture content, but also with upward velocity and atmospheric stability. In a New Zealand study, Carey-Smith *et al.* (2010) found that increases in extreme precipitation events are likely to be seen in nearly all regions of the country under a warmer climate, and suggested that increases in extreme precipitation may exceed increases in the moisture content of the atmosphere (i.e. exceed 7 - 8% more for every 1°C rise in temperature).

The distribution of annual rainfall maxima was calculated at five sites within the Bay of Plenty, following the method of Ailliot *et al.* (2011), and rainfall depth-duration tables were produced under future climate. Although there are differences between the GCM and RCM projections at each site, it is apparent that the RCM shows a general increase in the magnitude of extreme events in the future that is largely consistent with the GCM increases.

6.8 Key drought results

On average, under current climate, droughts lasting more than a month are infrequent in the Bay of Plenty. Low intensity droughts lasting more than 14 days are currently experienced in summer (on average) around 30% of the time at Katikati and Te Puke, and about 20% of the time at Whakamarama, and the eastern sites Te Teko and Opotiki.

Projections under both A1B and A2 by century-end show the largest changes are likely to occur in droughts lasting longer than a month. At the five sites analysed, increases of

between 9% and 17% in time spent in low intensity summer drought, lasting 1 month or more, are likely at 2090 under A1B (compared to 20-26% under A2, with the exception of Opotiki). Notably, under A2 at 2090, the time spent in moderate intensity and high intensity droughts lasting a month or more is also generally increased (by between 0-8% across all five sites), which is consistent with the predictions in previous national drought analyses.

6.9 Key pasture growth modelling results

The relatively warm, dry summers and cool, wet winters in the Bay of Plenty currently yield an annual pasture growth curve with a distinct, reliable, spring growth peak, variable autumn growth peak, and low winter growth (due to cool temperatures limiting growth rates). Pasture growth is generally water-limited through summer but storms (bringing significant rainfall) can yield periods of high growth at that time of the year and there is high year to year variability in summer growth. Near the ranges, winter growth is lower and summer growth is higher than that seen along the coast, due to the lower temperatures and higher summer rainfall observed at higher elevations.

A coupled soil-water balance and pasture production model of stock-grazed ryegrass pasture was used to model future pasture growth under a changing climate (with no adaptation). Projections at 2090 show little change in *annual* pasture biomass but significant changes in the *seasonality* of pasture growth in the Bay of Plenty. Projected higher summer temperatures reduce summer pasture growth significantly at 2090 under either A1B or A2. Milder winter temperatures result in large increases in winter growth (double current levels along the coast, and treble inland) by 2090 (noting that the inland areas currently have relatively low winter growth compared to the coast). The spring peak in growth shifts little, but there is greater spring growth prior to the peak and earlier onset of the summer growth restriction period. Total spring growth and reliability of spring growth are unchanged.

In contrast, under A1B at mid-century there is a reduction of low growth years, giving a slightly higher median summer pasture growth, which reflects the RCM and GCM projection of increased summer rainfall under A1B at 2040. This is likely to be due to inter-decadal climate variability (i.e. wet decades, dry decades), based on natural climate cycles such as El Nino/La Nina, for example.

6.10 Use of these results

Climate change science is complex, as is interpreting and using the results found. The science answers “what might” questions (such as “what might winter rainfall in the Bay of Plenty do in a warmer future?”), and there is often a large spread in results from model to model, even under the same climate change scenario and at the same time slice. This is particularly true for rainfall projections.

This report should initially be used in a qualitative sense i.e. for “big-picture” understanding of the likely climate of a future, warmer Bay of Plenty - such as understanding, for example, that drier winters are likely, overall. In addition, there are a large number of quantitative

results available within this report, both for the Bay of Plenty (the region as a whole), or for selected sites, using both GCM and RCM results, contained in Tables and Figures in the main body of the report, as well as the four Appendices. To cater for an "envelope" approach, the lowest and highest responses from the GCM models, as well as the single result from the RCM, are given for a selection of sites and variables in many of the Tables.

In addition to this report, the present-day climatological fields (seasonal mean temperature, seasonal mean rainfall), and the GCM 10-model average projected changes, have been provided to the Council in GIS format, on a ~5km x 5km grid. These 32 layers will prove useful over time when investigating possible opportunities, or risks, in the Bay of Plenty under climate change.

7. Acknowledgements

The authors would like to sincerely thank Dr. Anthony Clark (Dairy NZ) for expert review and commentary on Section 5.4.

8. References

Ailliot, P., C. Thompson and P. Thomson, (2011). Mixed methods for fitting the GEV distribution, *Water Resour. Res.*, **47**, W05551.

Benestad, R.E; Hanssen-Bauer, I.; Chen, D. (2008). Empirical-Statistical Downscaling. World Scientific Publishing Co., Singapore, 215 p.

Bhaskaran, B., Mullan, A.B. and George, S.E. (1999). Modelling of atmospheric climate variations at NIWA. *Weather and Climate*, **19**, 23-36.

Bhaskaran, B., Renwick, J. and Mullan A.B.(2002). On the application of the Unified Model to produce finer scale climate information for New Zealand. *Weather and Climate*, **22**, 19-27.

Carey-Smith, T., S. Dean, J. Vial, and C. Thompson (2010): Changes in precipitation extremes for New Zealand: climate model predictions. *Weather and Climate*, **30**, 23-48.

Clark, A.; Mullan, B.; Porteous, A. (2011). Scenarios of regional drought under climate change. Client Report WLG2010-32 for Ministry of Agriculture and Forestry, 135p., June 2011.

Drost, F., Renwick, J.A., Bhaskaran, B., Oliver, H., McGregor, J.L. (2007). Simulation of NZ's climate using a high-resolution nested regional climate model. *International Journal of Climatology*. **27**:1153-1169. DOI: 10.1002/joc.1461.

Griffiths, G., Mullan, B., Thompson, C., Burgess, S., and Tait, A. (2003). The Climate of the Bay of Plenty: Past and Future? NIWA Client Report AKL2003-044, prepared for Environment Bay of Plenty, June 2003.

Gordon, C., Cooper, C., Senior, C.A., Banks, H., Gregory, J.M., Johns, T.C., Mitchell, J.F.B. and Wood, R.A. (2000). The simulation of SST, sea ice extents and ocean heat transports in a version of the Hadley Centre coupled model without flux adjustments. *Climate Dynamics*, **16***:* 147-168.

IPCC (2007). Climate Change (2007). The Physical Science Basis. Contribution of Working Group I to the Fourth Assessment Report of the Intergovernmental Panel on Climate Change. Solomon, S.; Qin, D.; Manning, M.; Chen, Z. Marquis, M., Averyt, K.B., Tignor, M. and Miller, H.L. (Eds.), Cambridge University Press, Cambridge, United Kingdom and New York, NY, USA, 996 p. Available at http://ipcc-wg1.ucar.edu/wg1/wg1-report.html.

Kidson, J.W. (2000). An analysis of New Zealand synoptic types and their use in defining weather regimes. *International Journal of Climatology*, **20:** 299–316.

Lambert , S. J., and G.J. Boer. (2001). CMIP1 evaluation and intercomparison of coupled climate models. *Climate Dyn.*, **17**, 83-106.

Manning, M. R., Edmonds, J., Emori, S., Grubler, A., Hibbard, K., Joos, F., Kainuma, M., Keeling, R. F., Kram, T., Manning, A. C., Meinshausen, M., Moss, R., Nakicenovic, N., Riahi, K., Rose, S. K., Smith, S., Swart, R., van Vuuren, D. P., (2010). Misrepresentation of the IPCC CO2 emission scenarios, *Nature Geoscience*, **3,** 376-377. doi:10.1038/ngeo880

McCall, D. G., and Bishop-Hurley G. J., (2003). A pasture growth model for use in a whole farm dairy production model. *Agricultural Systems*, **76**: 1183-1205.

Meehl, G.A;, Covey, C.; Delworth, T.; Latif, M.; McAvaney, B.; Mitchell, J.F.B.; Stouffer, R.J.; Taylor, K.E. (2007). The WCRP CMIP3 multimodel dataset: A new era in climate change research. *Bulletin American Meteorological Society*, *88:* 1383–1394.

Ministry for the Environment (MfE), (2008). *Climate Change Effects and Impacts Assessment. A Guidance Manual for Local Government in New Zealand.* 2nd Edition. Prepared by Mullan, B; Wratt, D; Dean, S; Hollis, M. (NIWA); Allan, S; Williams, T. (MWH NZ Ltd), and Kenny, G. (Earthwise Consulting Ltd), in consultation with Ministry for the Environment. NIWA Client Report WLG2007/62, February 2008, 156p. Report available from: http://www.mfe.govt.nz/publications/climate/climate-change-effect-impacts-assessments-may08/index.html

Mullan, A.B.; Wratt, D.S.; Renwick, J.A. (2001). Transient model scenarios of climate changes for New Zealand. *Weather and Climate* **21:** 3–34.

Mullan, B, Porteous, A. Wratt, D. and Hollis, M. (2005). Changes in drought risk with climate change, NIWA Project MFE05305, Report Prepared for the Ministry for the Environment and Ministry for Agriculture and Forestry.

Mullan, B.; Carey-Smith, T.; Griffiths, G.; Sood, A. (2011). Scenarios of storminess and regional wind extremes under climate change. Client Report WLG2010-31 for Ministry of Agriculture and Forestry, 80p., March 2011.

Nakicenovic, N.; Swart, R (Eds). (2000). Special Report on Emissions Scenarios. A Special Report of Working Group III of the Intergovernmental Panel on Climate Change. Cambridge University Press, Cambridge, United Kingdom and New York, NY, USA, 599 p.

O'Gorman, P. A. and T. Schneider, (2009). The physical basis for increases in precipitation extremes in simulations of 21st-century climate change. *Proceedings of the National Academy of Sciences of the United States of America,* **106,** 14773-14777.

Pittroff, W., and Kothmann, M. M., (2001). Quantitative prediction of feed intake in ruminants: I. Conceptual and mathematical analysis of models for sheep. *Livestock Production Science*, **71**: 131-150.

Pope, V.D., Gallani, M.L., Rowntree, P.R. and Stratton, R.A., (2000). The impact of new physical parametrizations in the Hadley Centre climate model: HadAM3. *Climate Dynamics*. **16**. 123-146.

Reisinger, A., Mullan, A.B., Manning, M., Wratt, D.W., Nottage, R.A.C. (2010). Global and local climate change scenarios to support adaptation in New Zealand. *In:* Climate change adaptation in New Zealand: Future scenarios and some sectoral perspectives. Nottage, R.A.C., Wratt, D.S., Bornman, J.F., Jones, K. (eds). New Zealand Climate Change Centre, Wellington, pp 26-43.

Rickert, K.G., Stuth, J.W,. and McKeon, G.M., (2000). Chapter 3. Modelling pasture and animal production. In: Field and laboratory methods for grassland and animal production research. L. 't Mannetje and R.M. Jones, CABI Publishing.

Rowell, D.P. (2005). A scenario of European climate change for the late twenty-first century: seasonal means and interannual variability. *Climate Dynamics*, **25**, 837-849.

Stone, M. and Brooks, R. (1990). Continuum regression: Cross-validated sequentially constructed prediction embracing ordinary least squares, partial least squares, and principal components regression. *Journal of the Royal Statistical Society, Series B,* **52(2):** 237-269.

Sugiyama, M., H. Shiogama, and S. Emori, 2010: Precipitation extreme changes exceeding moisture content increases in MIROC and IPCC climate models. *Proceedings of the National Academy of Sciences of the United States of America,* **107**, 571-575.

Tait, A.; Henderson, R.; Turner, R.; Zheng, X. (2006). Thin plate smoothing splines interpolation of daily rainfall for New Zealand using a climatological rainfall surface. *International Journal of Climatology,* **26:** 2097-2116.

White, David H. (2000). 'Implementing Drought Policy in Australia' Agricultural Science, Vol 13, No.2.

Wilhite, D.A., Hayes, M.J., Knutson, C., Helm Smith, K (2000). Planning for drought: moving from crisis to risk management. *Journal of the American Water Resources Association.* **36**, 697–710.

Appendix 1

Figure A1: A1B 2030-2049 - rainfall (% change): Autumn

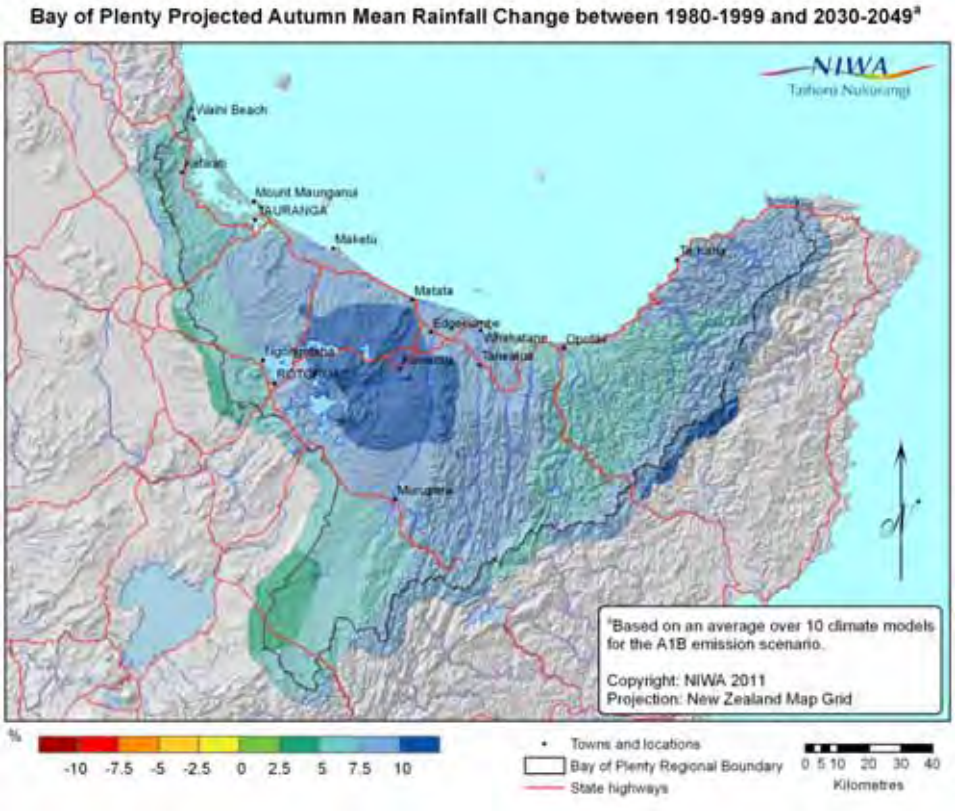

Figure A2: A1B 2030-2049 - rainfall (% change): Winter

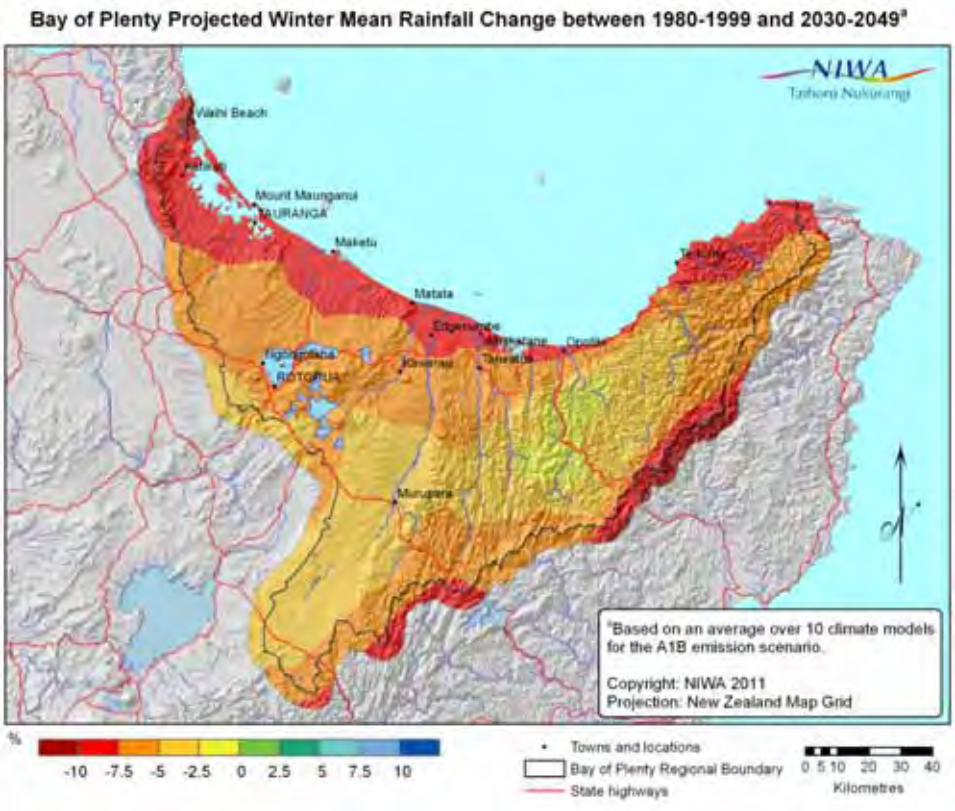

Figure A3: A1B 2030-2049 - rainfall (% change): Spring

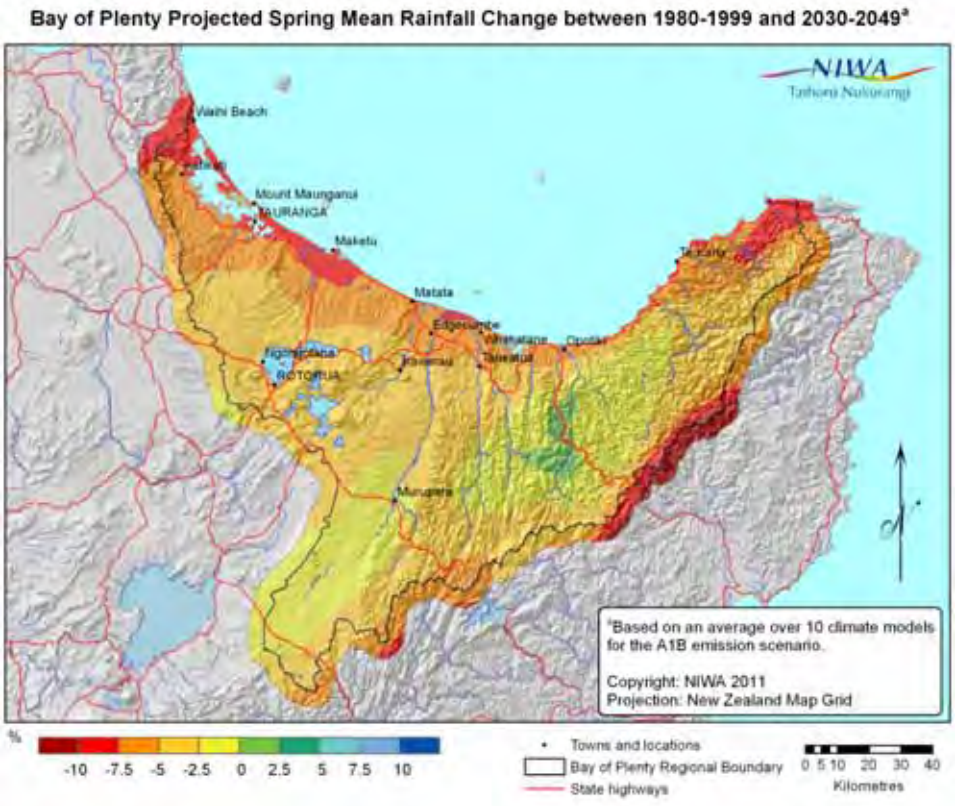

Figure A4: A1B 2030-2049 - rainfall (% change): Summer

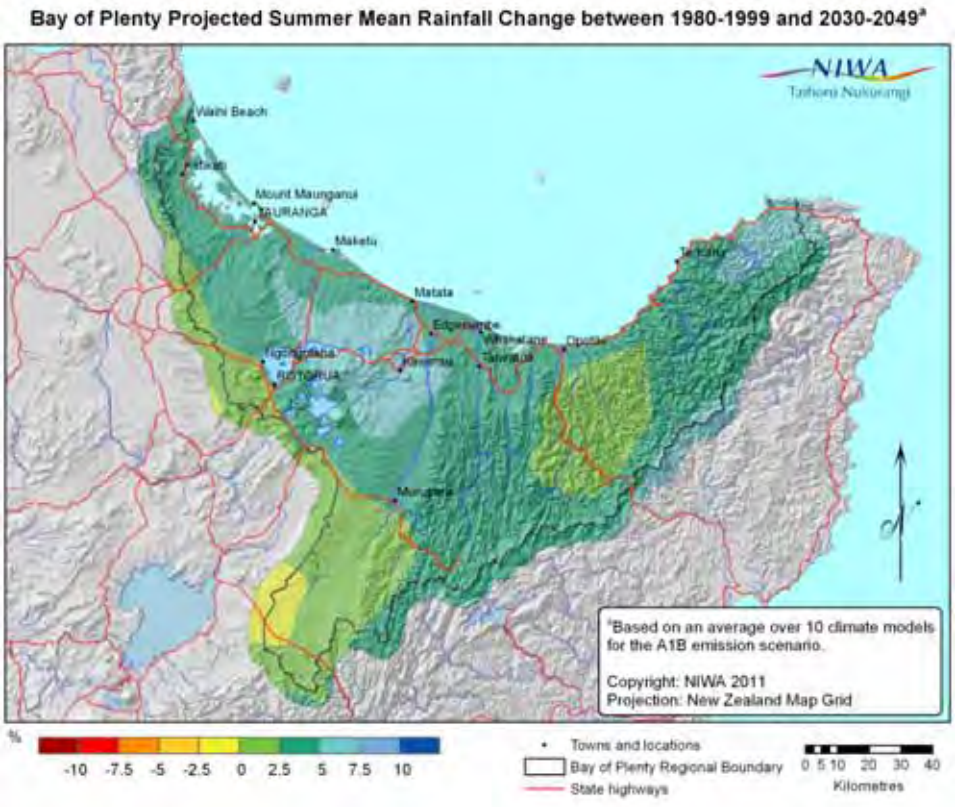

Figure A5: A1B 2030-2049 - temperature (°C change): Autumn

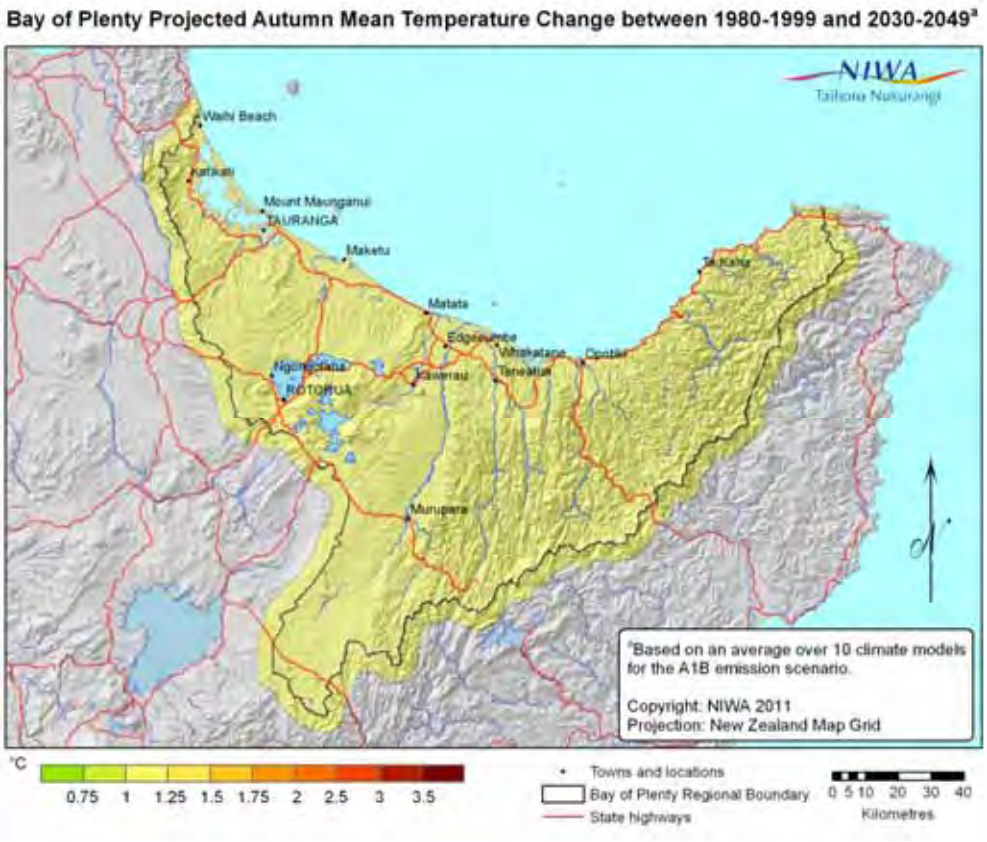

Figure A6: A1B 2030-2049 - temperature (°C change): Winter

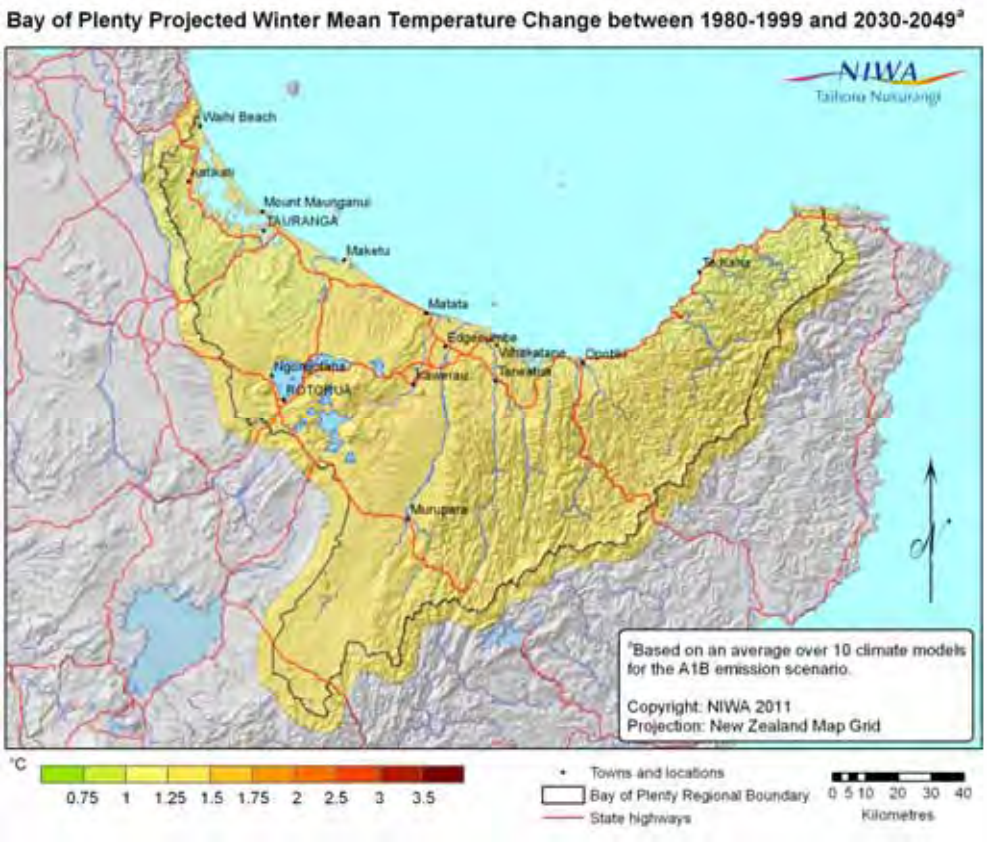

Figure A7: A1B 2030-2049 - temperature (°C change): Spring

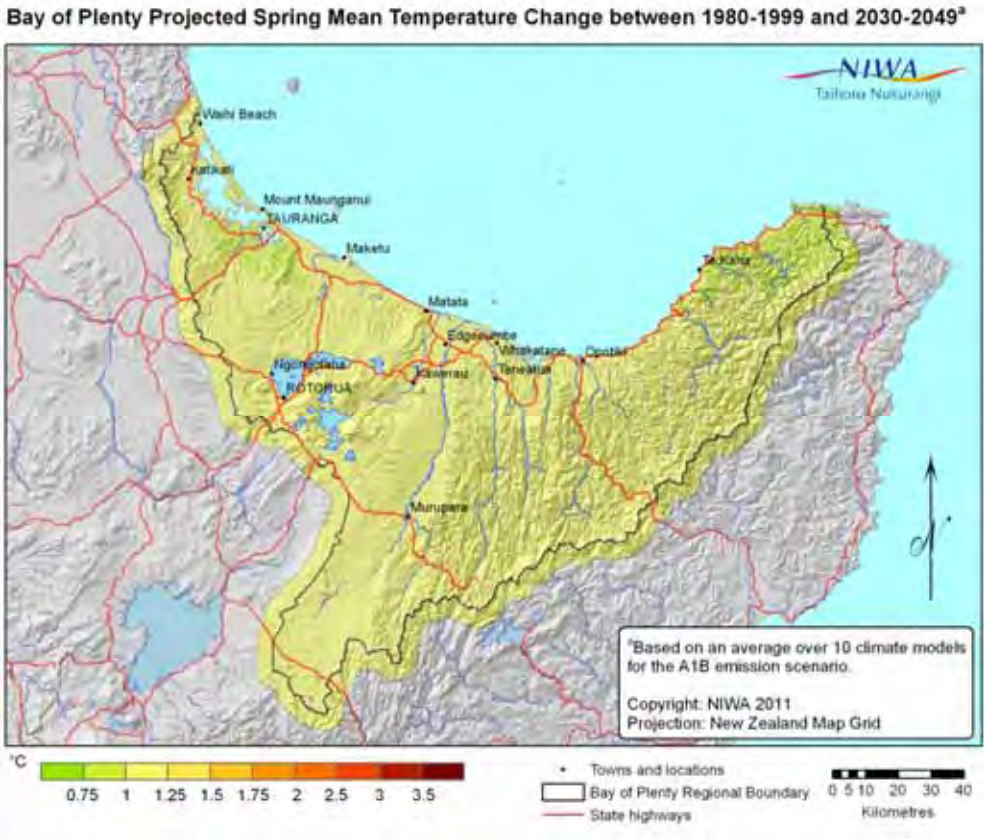

Figure A8: A1B 2030-2049 - temperature (°C change): Summer

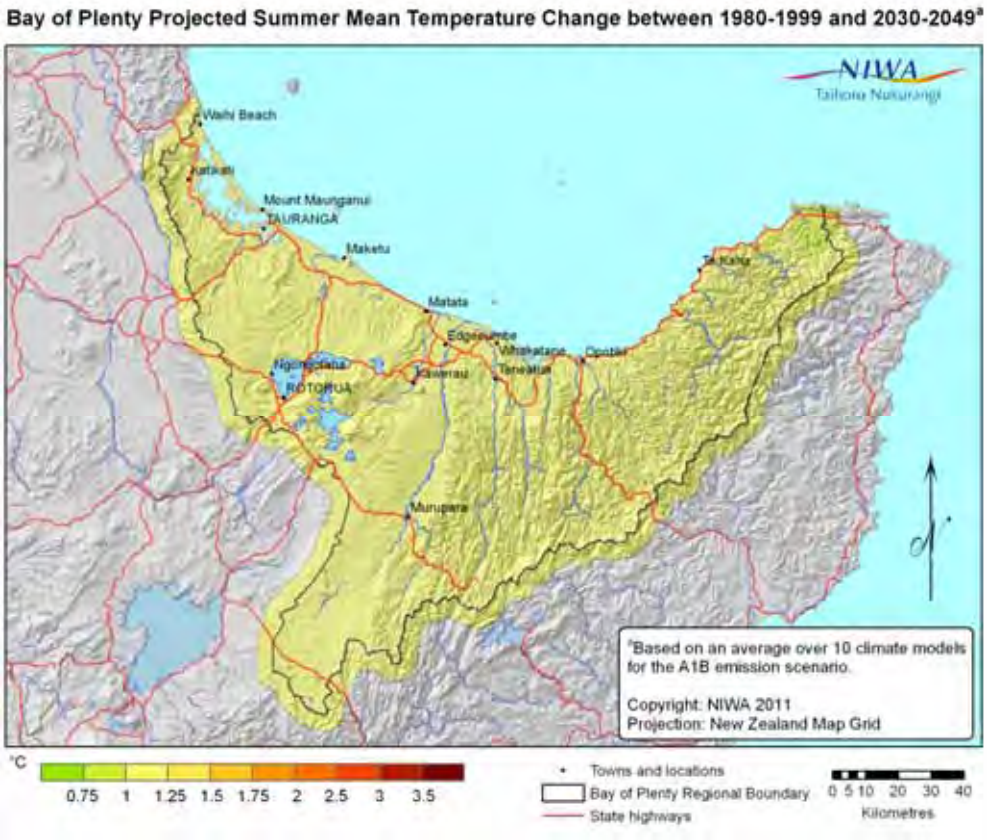

Figure A9: A1B 2080-2099 - rainfall (% change): Autumn

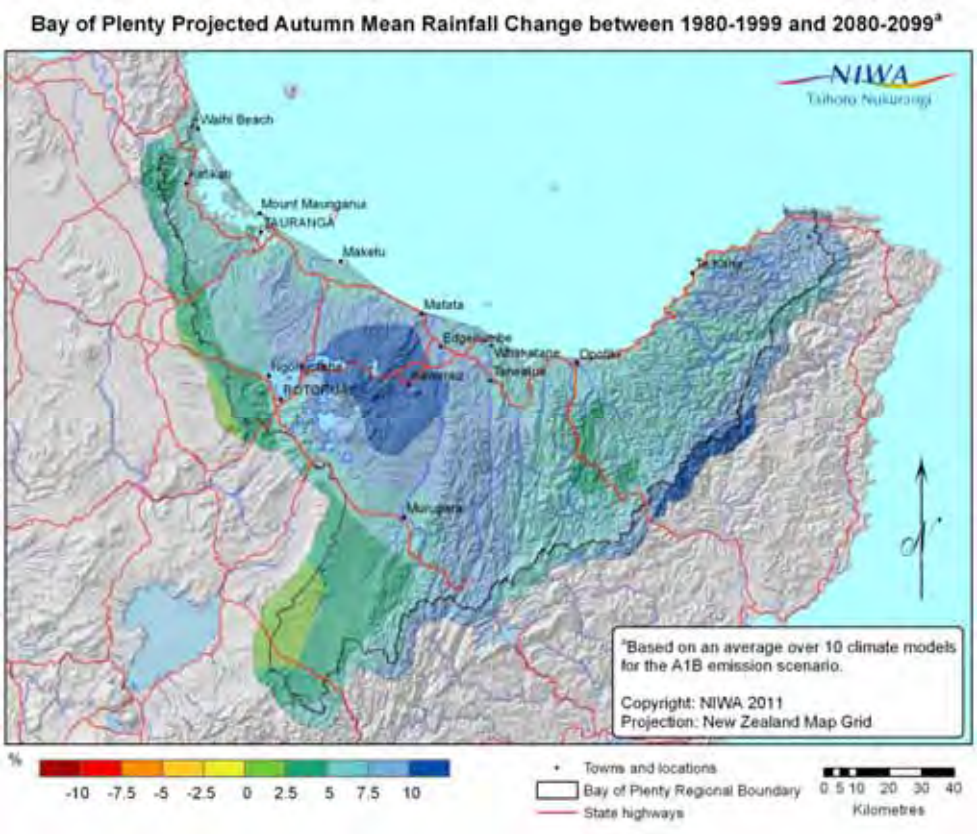

Figure A10: A1B 2080-2099 - rainfall (% change): Winter

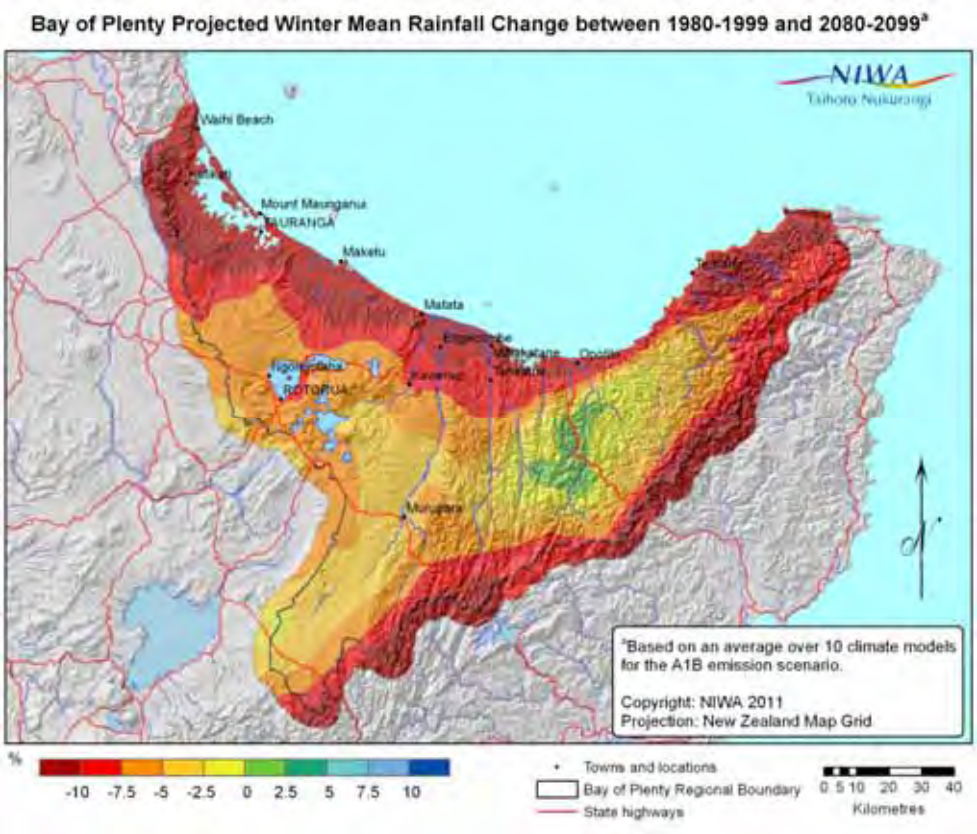

Figure A11: A1B 2080-2099 - rainfall (% change): Spring

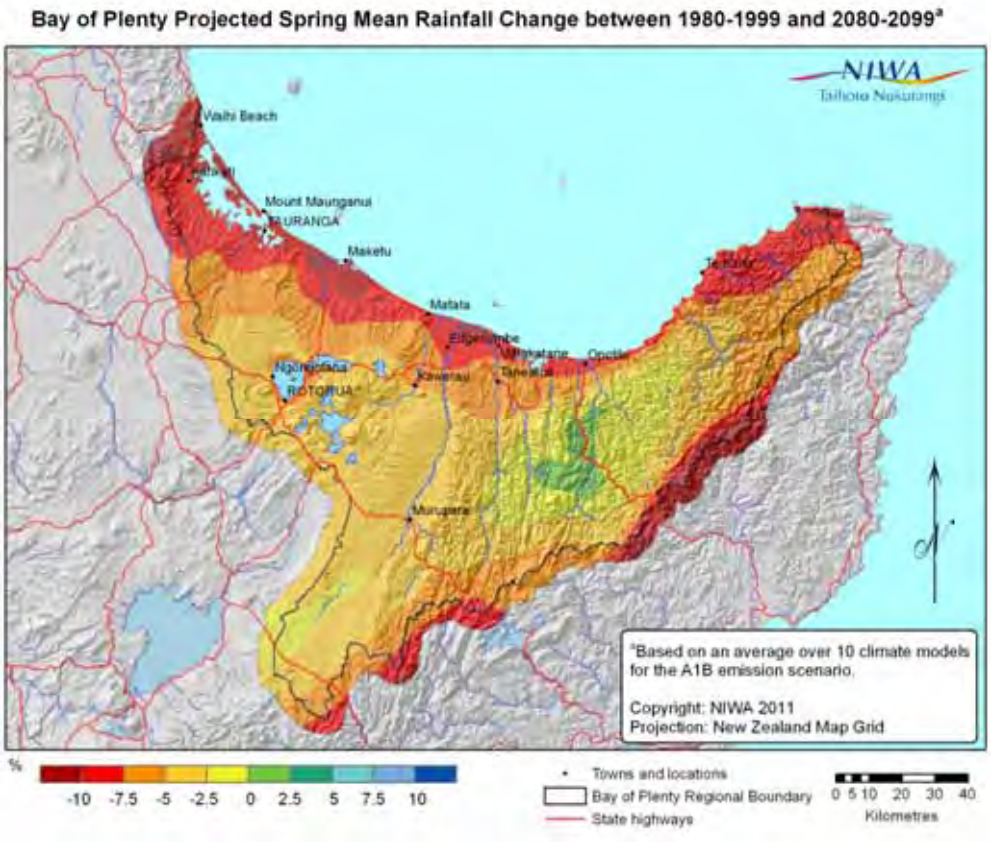

Figure A12: A1B 2080-2099 - rainfall (% change): Summer

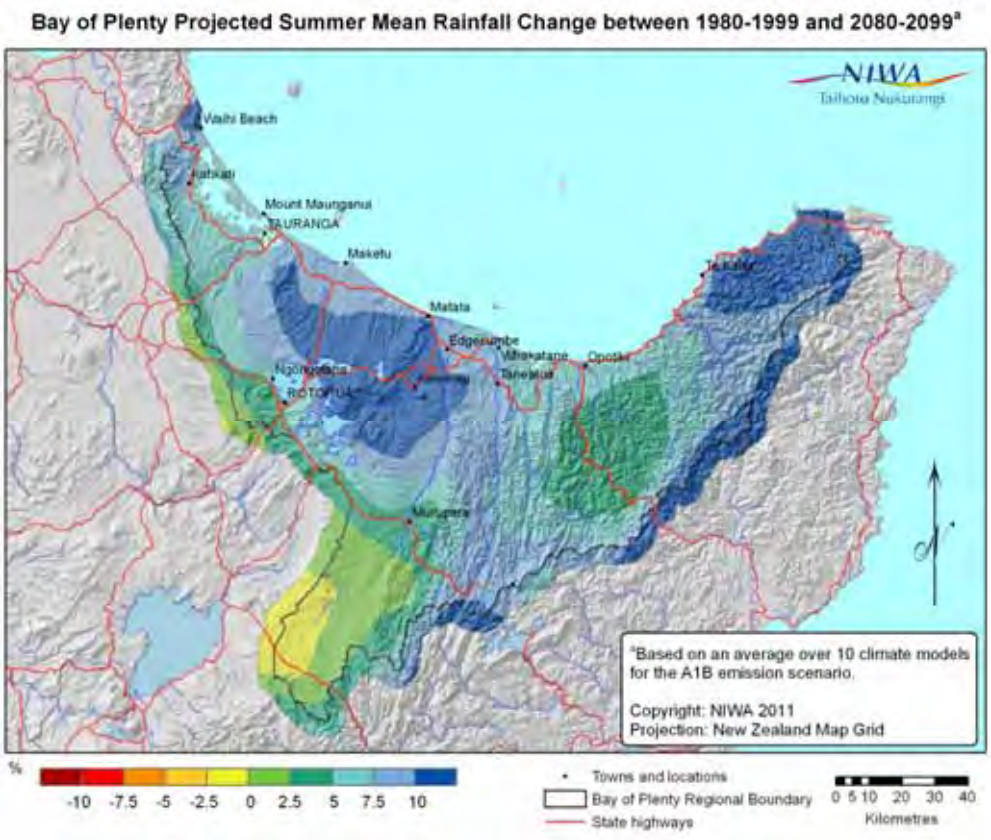

Figure A13: A1B 2080-2099 - temperature (°C change): Autumn

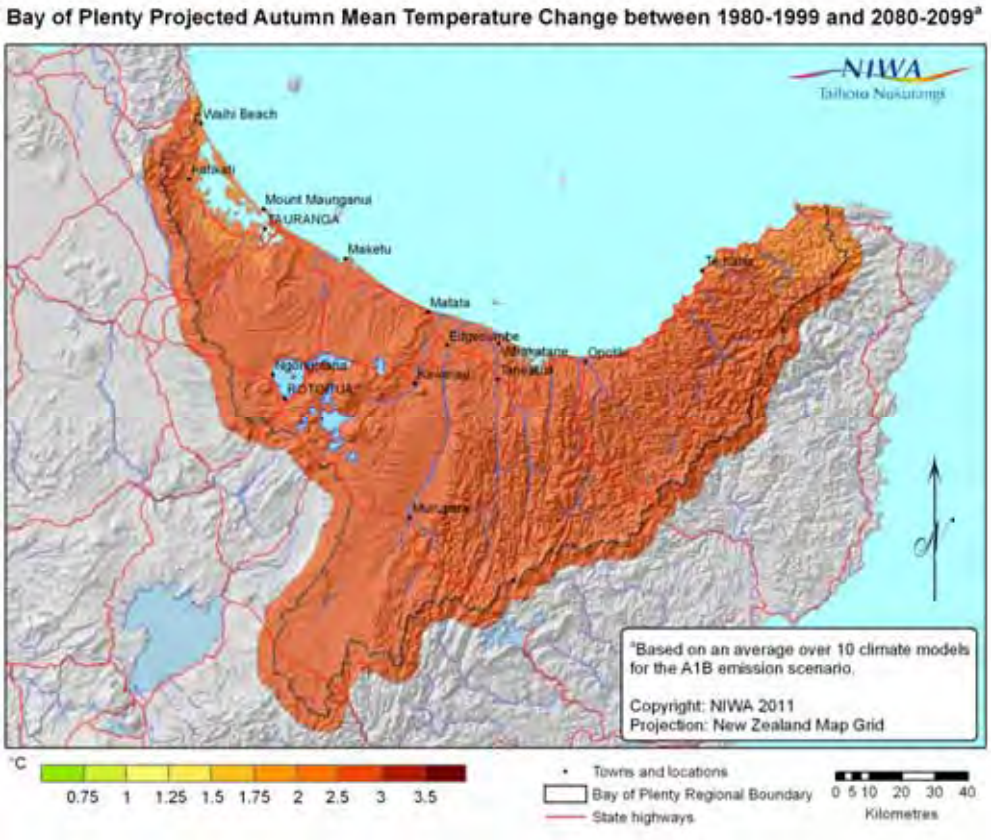

Figure A14: A1B 2080-2099 - temperature (°C change): Winter

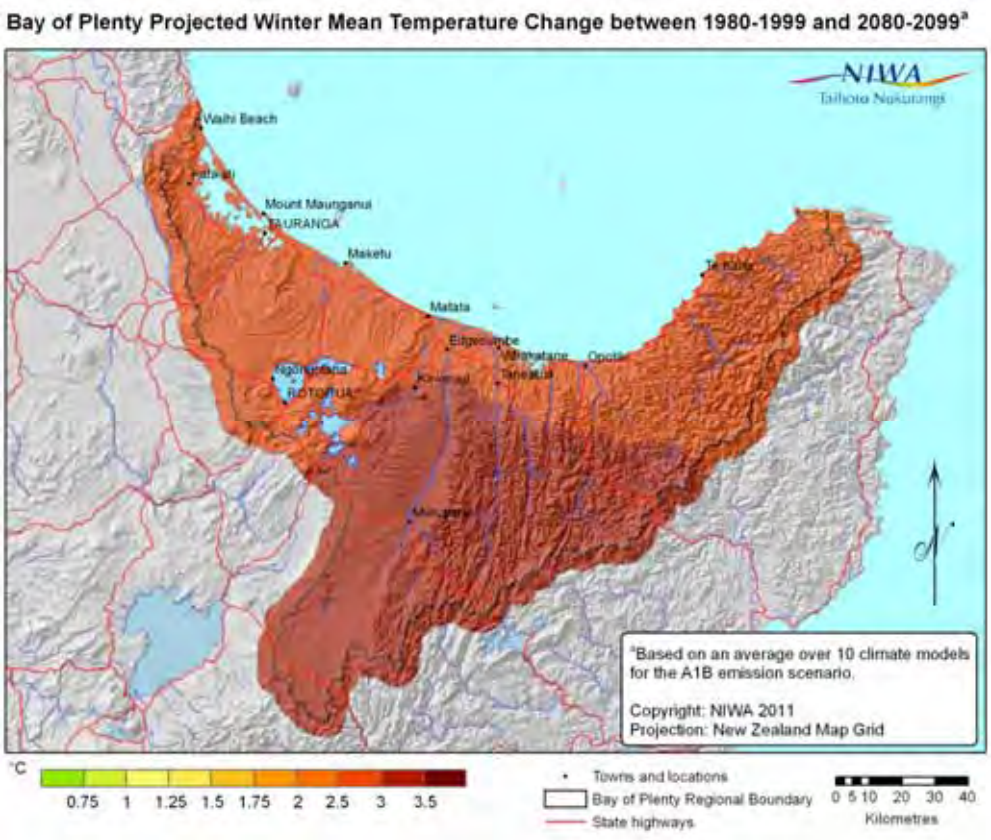

Figure A15: A1B 2080-2099 - temperature (°C change): Spring

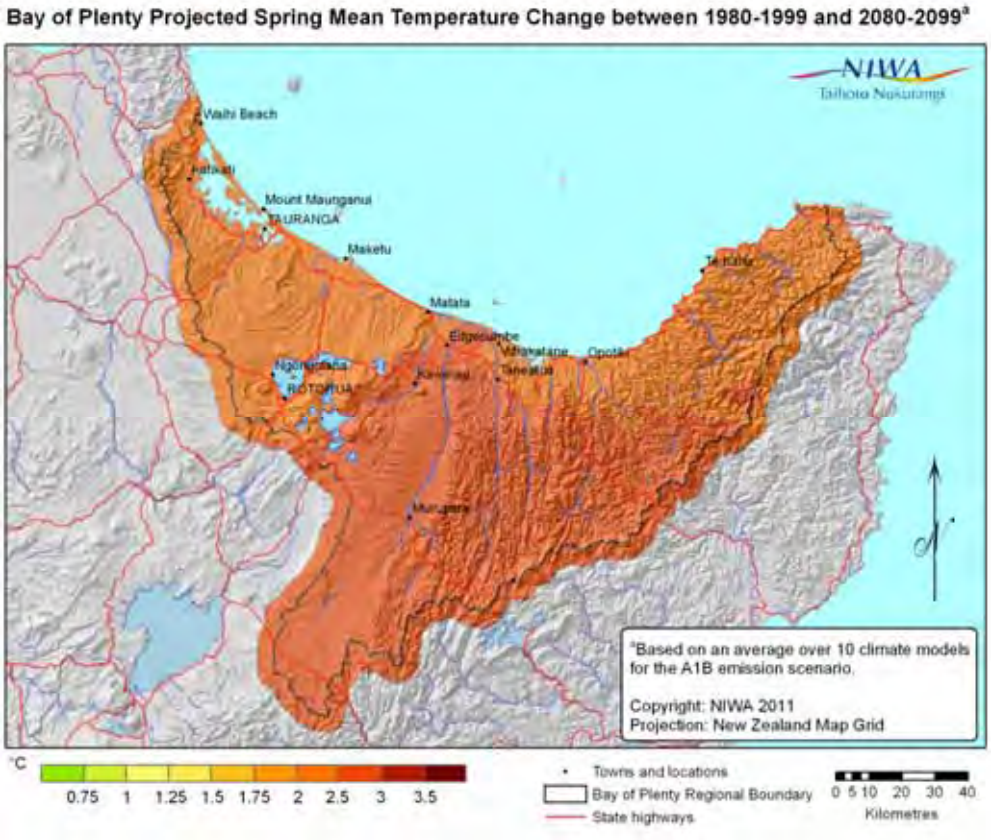

Figure A16: A1B 2080-2099 - temperature (°C change): Summer

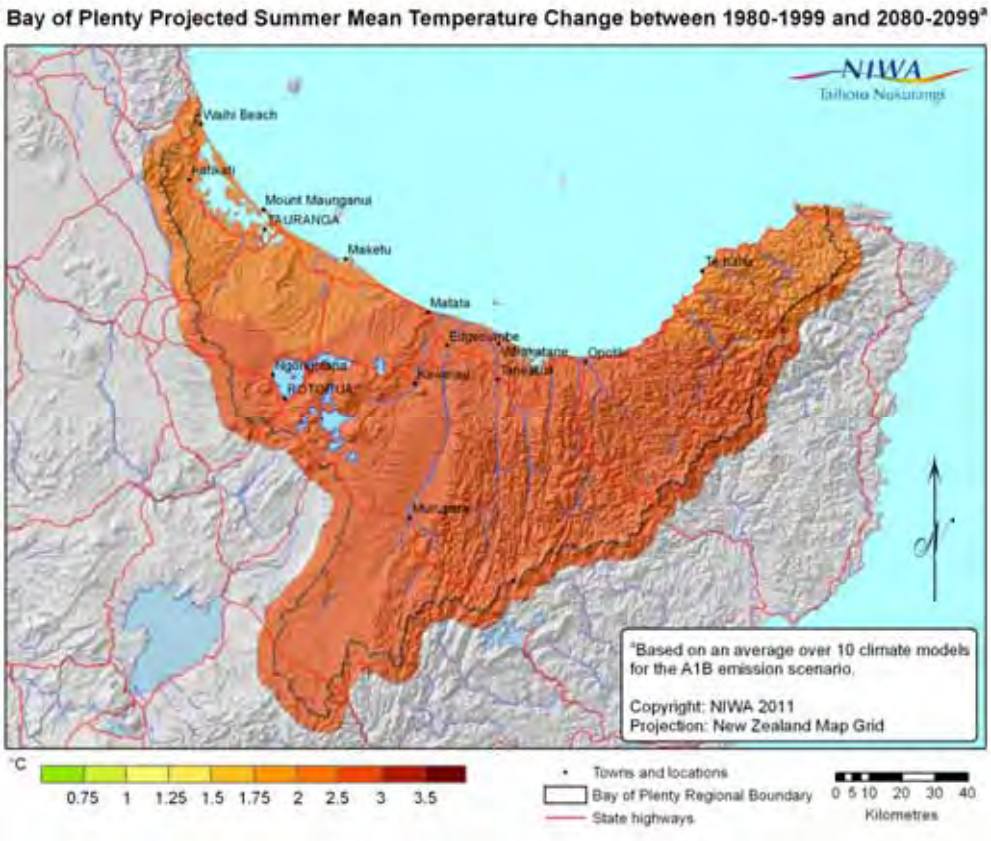

Figure A17: A2 2080-2099 - rainfall (% change): Autumn

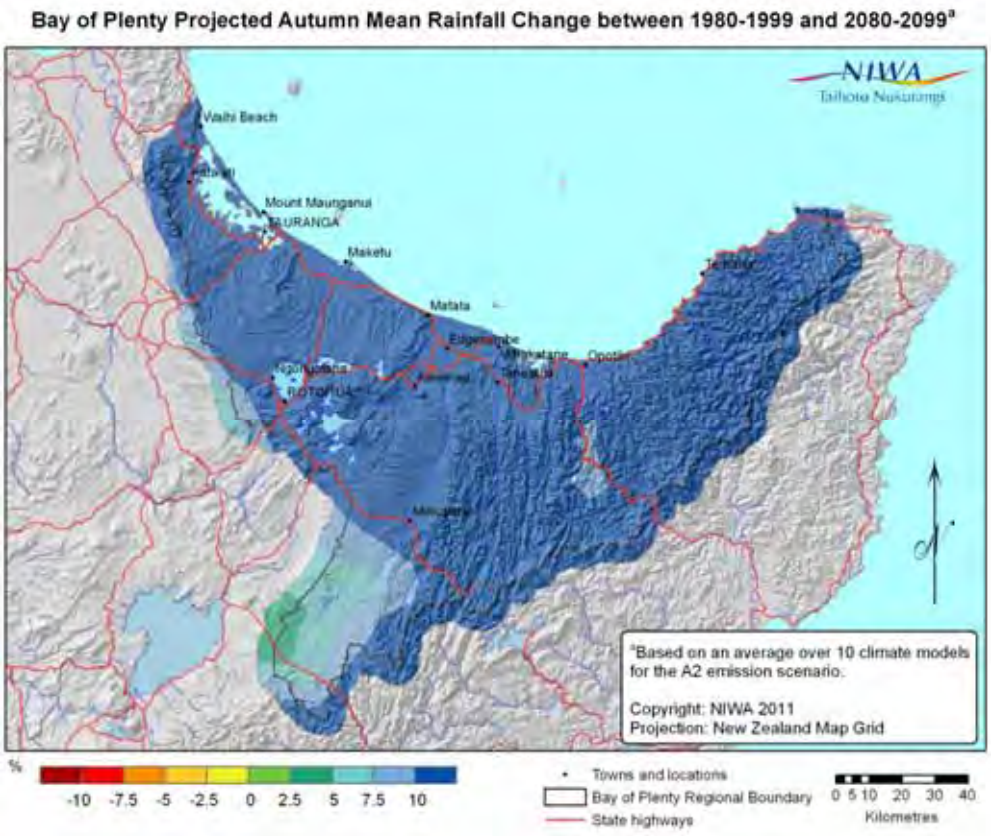

Figure A18: A2 2080-2099 - rainfall (% change): Winter

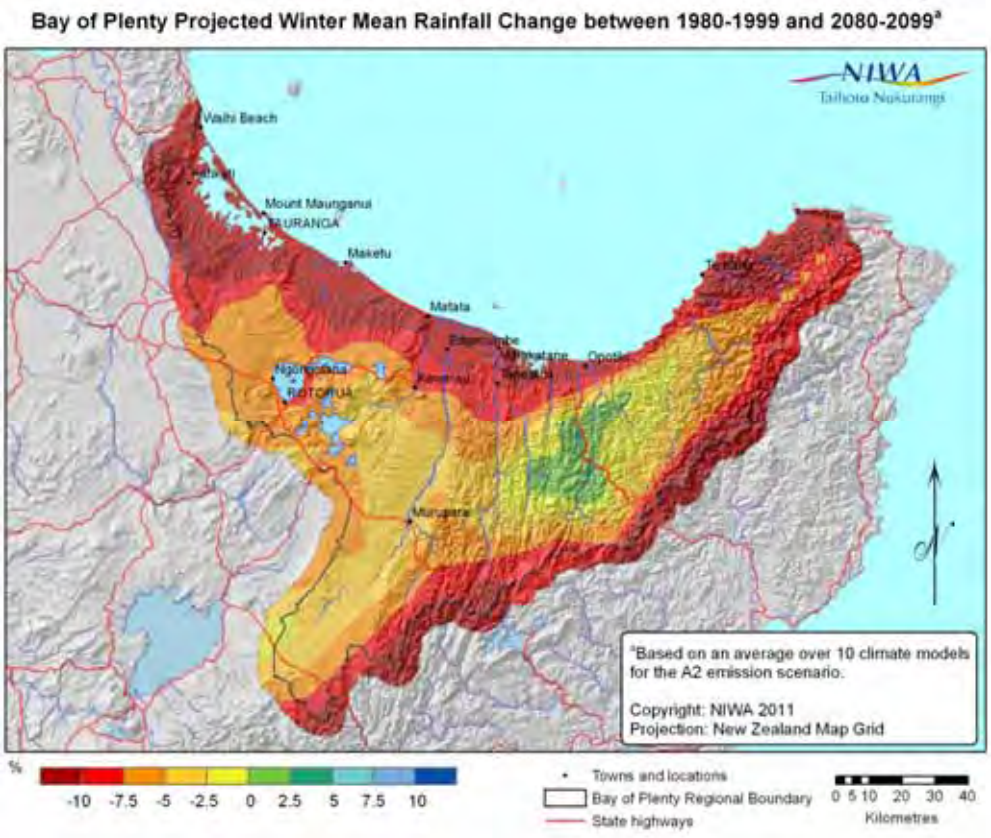

Figure A19: A2 2080-2099 - rainfall (% change): Spring

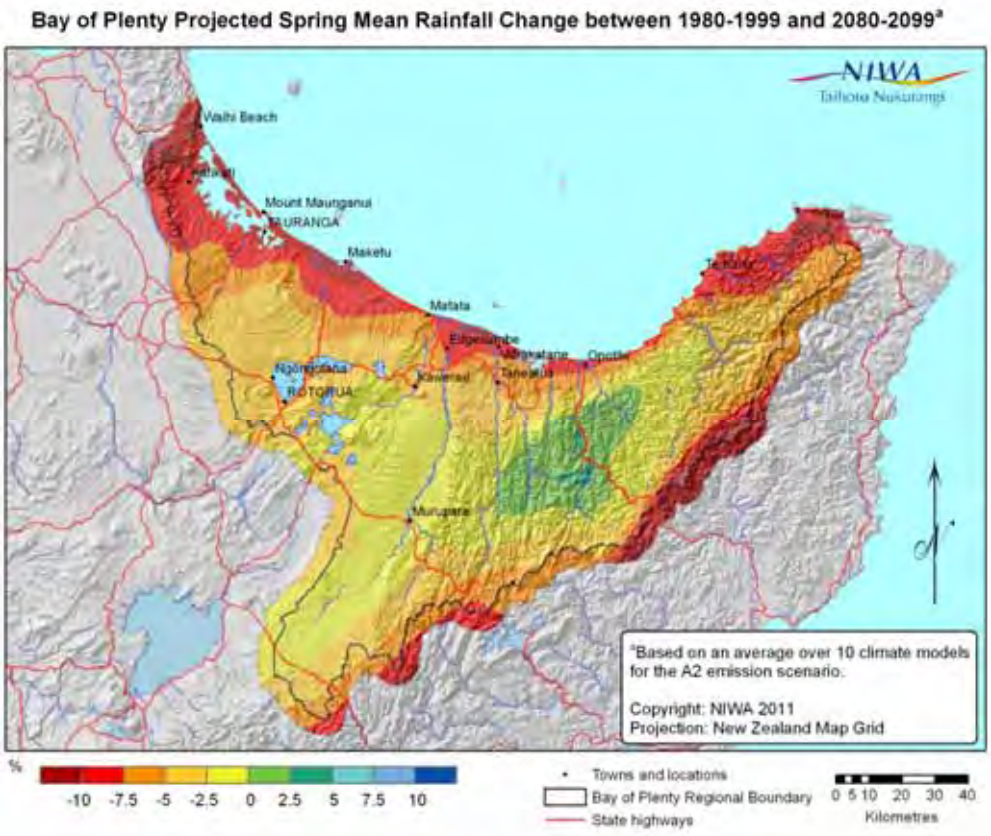

Figure A20: A2 2080-2099 - rainfall (% change): Summer

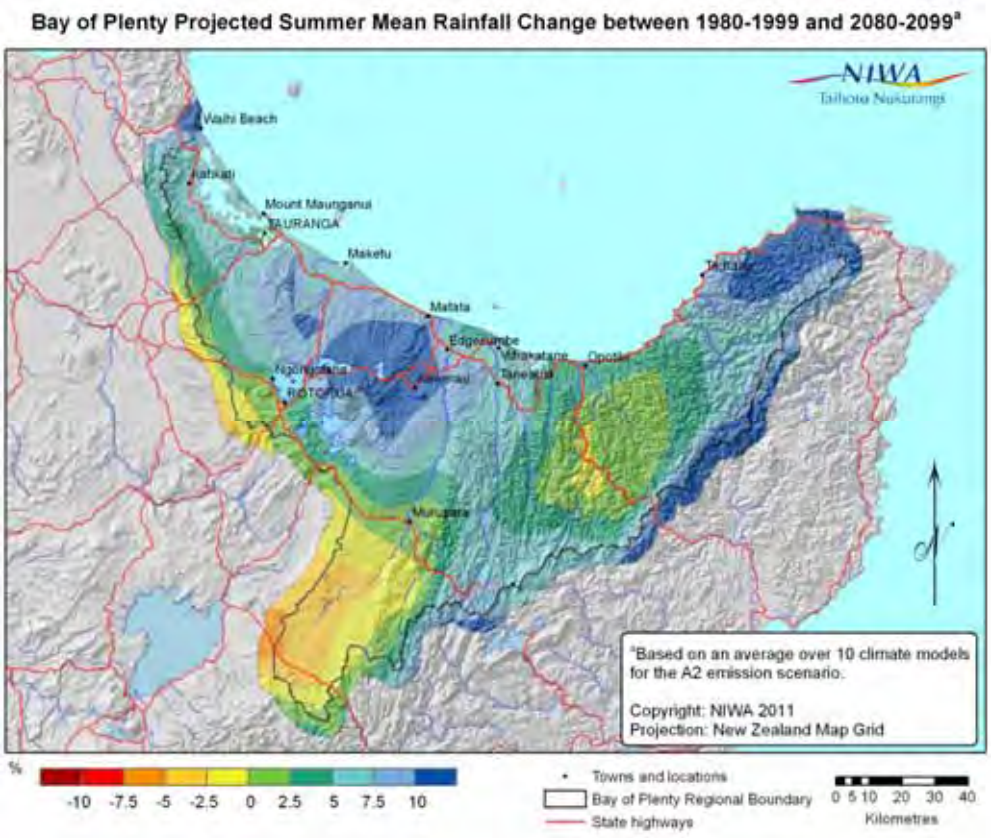

Figure A21: A2 2080-2099 - temperature (°C change): Autumn

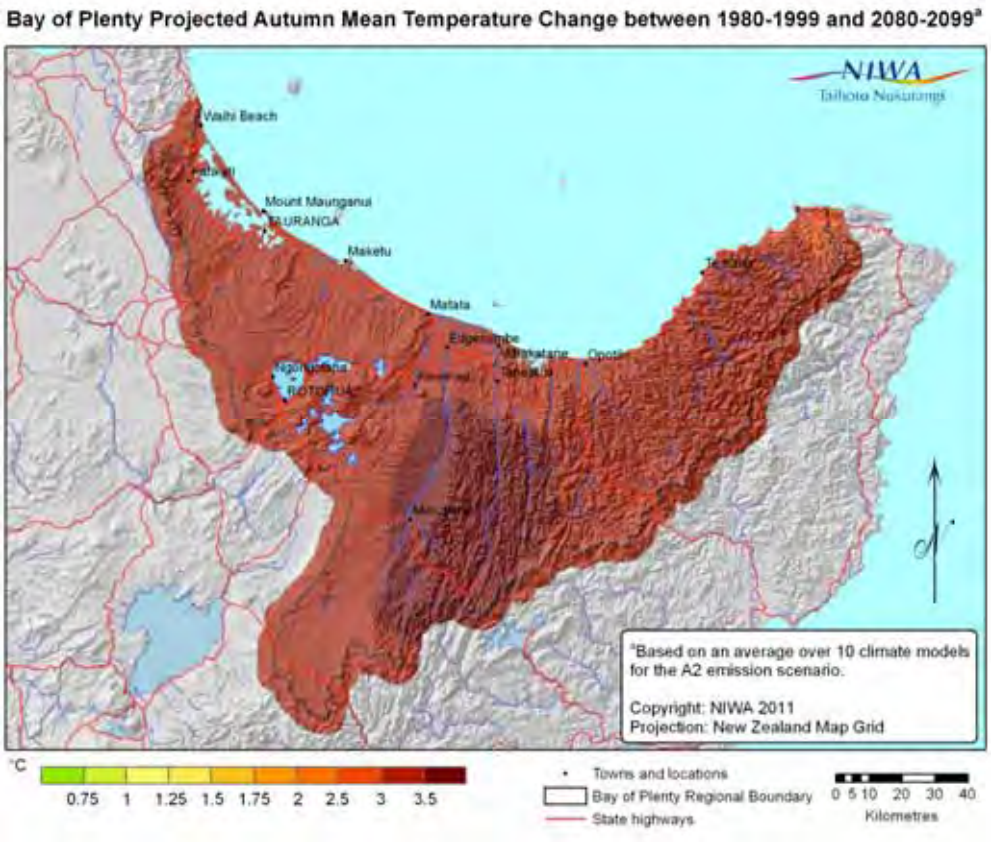

Figure A22: A2 2080-2099 - temperature (°C change): Winter

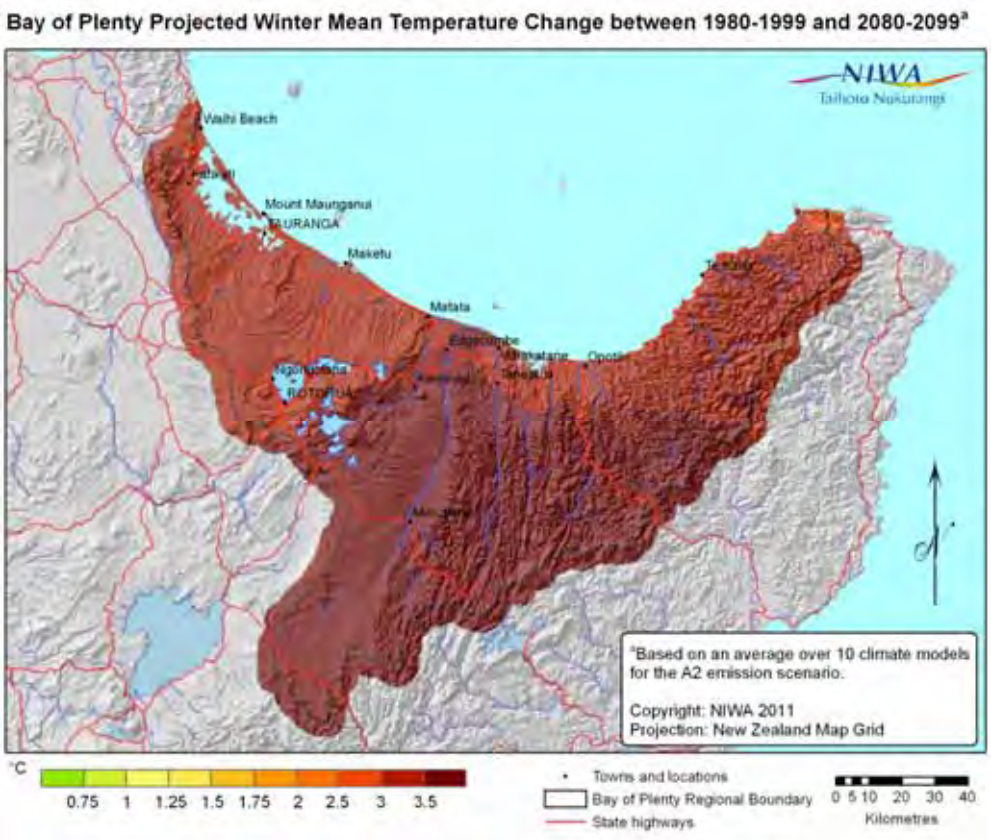

Figure A23: A2 2080-2099 - temperature (°C change): Spring

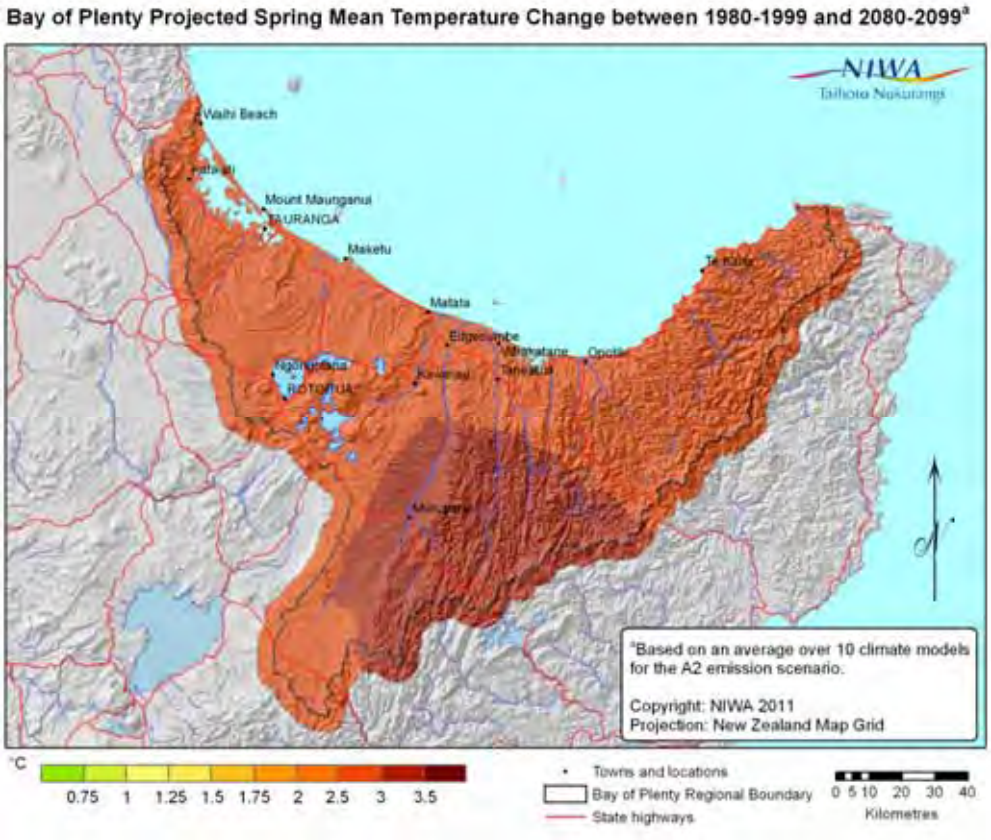

Figure A24: A2 2080-2099 - temperature (°C change): Summer

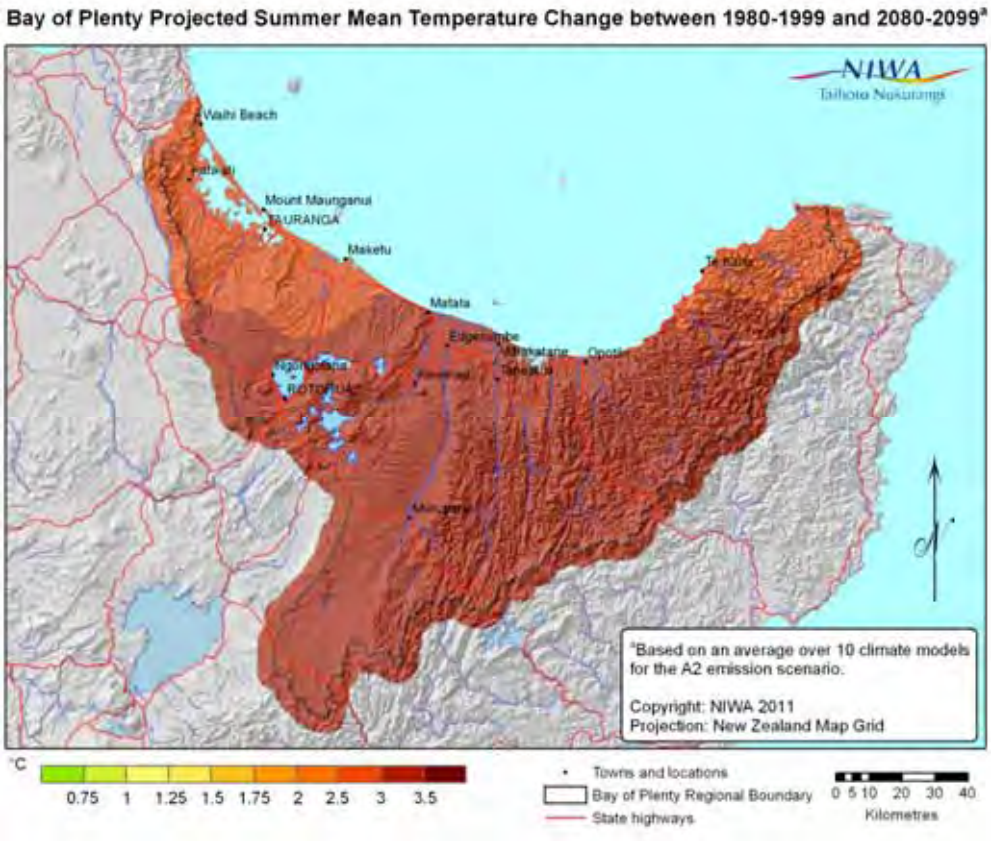

Appendix 2 – Material related to GCM projections

Figure 10 in the main body of the report shows annual temperature projections (displayed as box and whisker plots) for the Bay of Plenty from 10 climate models, averaged over all VCS grid-points within the Bay of Plenty Regional Council Boundary. Results for four seasons are shown here, separately, in Figure B1. In both Figure 10 and Figure B1, the range of warming projected by the 10 models for the 2030-2049 ('2040') and 2080-2099 ('2090') periods, for the two emission scenarios A1B and A2, is shown. The RCM result is shown with a red arrow. For explanation of the box and whisker plot, see Figure 10.

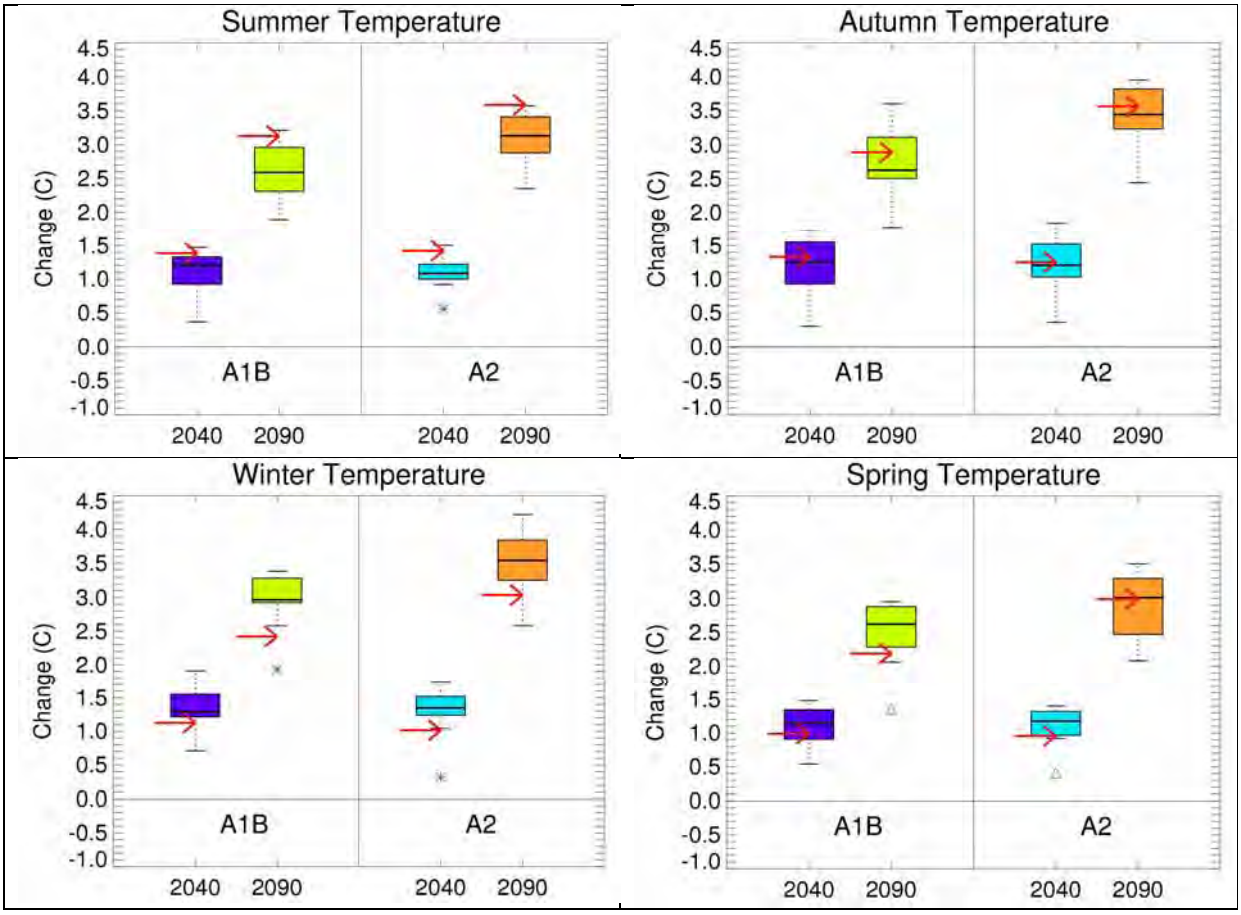

Figure B1: Downscaled temperatures by season, similar to Figure 10 in main report.

Projected temperature changes for Bay of Plenty at 2040 under the A1B emission scenario, as represented by 10 downscaled GCMs, are given in Table B1. Table B2 gives projected temperature changes at 2090 under A2. For the region as a whole (i.e., average across all VCS grid-points within the region), and for selected grid-points co-located with named towns, the following information is given: the 10-model average, the extreme low and high values from the model distribution, and the single projected value for the RCM. Changes are shown for the four seasons and for the annual average.

Table B1: Projected temperature change (°C) at 2040 under A1B, similar to Table 2.

Region or Site	Summer	Autumn	Winter	Spring	Annual
Region average:					
10-model average	1.1	1.2	1.3	1.1	1.2
Lowest, Highest	0.4, 1.5	0.3, 1.7	0.7, 1.9	0.5, 1.5	0.5, 1.5
RCM	1.4	1.3	1.1	1.0	1.2
Katikati:					
10-model average	1.0	1.1	1.2	1.0	1.1
Lowest, Highest	0.4, 1.4	0.3, 1.6	0.7, 1.7	0.5, 1.4	0.5, 1.4
RCM	1.3	1.3	1.2	1.0	1.2
Tauranga:					
10-model average	1.0	1.1	1.2	1.0	1.1
Lowest, Highest	0.4, 1.4	0.3, 1.6	0.6, 1.7	0.5, 1.4	0.5, 1.4
RCM	1.2	1.3	1.1	1.0	1.2
Te Puke:					
10-model average	1.0	1.1	1.2	1.0	1.1
Lowest, Highest	0.4, 1.4	0.3, 1.6	0.7, 1.8	0.5, 1.4	0.5, 1.4
RCM	1.3	1.3	1.1	1.0	1.2
Whakatane:					
10-model average	1.1	1.2	1.3	1.1	1.2
Lowest, Highest	0.4, 1.5	0.3, 1.7	0.7, 1.9	0.5, 1.5	0.5, 1.5
RCM	1.2	1.3	1.2	0.9	1.2
Opotiki:					
10-model average	1.1	1.2	1.2	1.0	1.1
Lowest, Highest	0.4, 1.5	0.3, 1.7	0.6, 1.8	0.5, 1.4	0.4, 1.5
RCM	1.2	1.3	1.1	0.8	1.1
Rotorua:					
10-model average	1.1	1.2	1.3	1.1	1.2
Lowest, Highest	0.4, 1.5	0.3, 1.7	0.7, 1.9	0.5, 1.5	0.5, 1.5
RCM	1.5	1.3	1.1	1.0	1.2
Kawerau:					
10-model average	1.1	1.2	1.4	1.1	1.2
Lowest, Highest	0.4, 1.5	0.3, 1.8	0.7, 1.9	0.5, 1.5	0.5, 1.6
RCM	1.4	1.3	1.1	1.0	1.2

Table B2: Projected temperature change (°C) at 2090 under A2, similar to Table 2.

Region or Site	Summer	Autumn	Winter	Spring	Annual
Region average:					
10-model average	3.1	3.4	3.5	2.9	3.2
Lowest, Highest	2.4, 3.6	2.4, 4.0	2.6, 4.2	2.1, 3.5	2.5, 3.6
RCM	3.6	3.6	3.0	3.0	3.3
Katikati:					
10-model average	2.8	3.1	3.2	2.7	3.0
Lowest, Highest	2.2, 3.3	2.3, 3.6	2.4, 3.9	1.9, 3.2	2.3, 3.3
RCM	3.7	3.4	3.1	3.0	3.3
Tauranga:					
10-model average	2.9	3.1	3.2	2.7	3.0
Lowest, Highest	2.2, 3.3	2.3, 3.7	2.3, 3.8	1.9, 3.2	2.3, 3.3
RCM	3.6	3.4	2.9	3.0	3.2
Te Puke:					
10-model average	2.9	3.1	3.2	2.7	3.0
Lowest, Highest	2.2, 3.3	2.3, 3.7	2.4, 3.9	2.0, 3.3	2.3, 3.4
RCM	3.6	3.5	2.9	3.0	3.2
Whakatane:					
10-model average	3.1	3.4	3.5	2.9	3.2
Lowest, Highest	2.4, 3.6	2.5, 4.0	2.6, 4.3	2.1, 3.5	2.6, 3.6
RCM	3.6	3.5	3.1	3.1	3.3
Opotiki:					
10-model average	3.1	3.3	3.3	2.8	3.1
Lowest, Highest	2.3, 3.5	2.4, 3.9	2.5, 3.9	2.0, 3.4	2.4, 3.6
RCM	3.4	3.4	2.9	2.8	3.1
Rotorua:					
10-model average	3.1	3.4	3.4	2.9	3.2
Lowest, Highest	2.3, 3.5	2.4, 3.9	2.5, 4.2	2.0, 3.4	2.5, 3.6
RCM	3.7	3.6	3.0	3.0	3.3
Kawerau:					
10-model average	3.1	3.4	3.6	2.9	3.3
Lowest, Highest	2.4, 3.6	2.5, 4.0	2.6, 4.3	2.1, 3.5	2.6, 3.7
RCM	3.7	3.6	3.0	3.1	3.3

Projected rainfall changes for Bay of Plenty at 2040 under the A1B emission scenario, as represented by 10 downscaled GCMs, are given in Table B3. Table B4 gives projected rainfall changes at 2090 under A2. For the region as a whole (i.e., average across all VCS grid-points within the region), and for selected grid-points co-located with named towns, the following information is given: the 10-model average, the extreme low and high values from the model distribution, and the single projected value for the RCM. Changes are shown for the four seasons and for the annual average.

Table B3: Projected rainfall change (%) at 2040 under A1B, similar to Table 3.

Region or Site	Summer	Autumn	Winter	Spring	Annual
Region average:					
10-model average	3	8	-6	-4	0
Lowest, Highest	-7, 13	-10, 26	-19, 9	-10, 7	-9, 7
RCM	5	8	2	-10	1
Katikati:					
10-model average	3	7	-9	-8	-3
Lowest, Highest	-8, 13	-13, 29	-21, 4	-17, 6	-11, 7
RCM	18	8	1	-12	3
Tauranga:					
10-model average	3	6	-9	-8	-3
Lowest, Highest	-9, 11	-14, 27	-21, 4	-17, 5	-12, 6
RCM	19	10	2	-13	4
Te Puke:					
10-model average	4	8	-9	-7	-2
Lowest, Highest	-8, 13	-13, 30	-22, 7	-16, 8	-12, 7
RCM	11	11	1	-10	3
Whakatane:					
10-model average	3	7	-9	-8	-3
Lowest, Highest	-10, 12	-13, 28	-22, 3	-16, 6	-12, 6
RCM	12	8	5	-14	3
Opotiki:					
10-model average	3	7	-8	-6	-2
Lowest, Highest	-9, 12	-12, 27	-19, 5	-13, 6	-11, 6
RCM	10	7	4	-13	2
Rotorua:					
10-model average	3	8	-7	-5	-1
Lowest, Highest	-9, 13	-11, 27	-20, 8	-12, 7	-10, 7
RCM	7	10	2	-10	2
Kawerau:					
10-model average	6	12	-7	-5	0
Lowest, Highest	-7, 18	-10, 40	-21, 13	-15, 13	-11, 9
RCM	8	11	4	-10	4

Table B4: Projected rainfall change (%) at 2090 under A2, similar to Table 3.

Region or Site	Summer	Autumn	Winter	Spring	Annual
Region average:					
10-model average	5	15	-7	-4	1
Lowest, Highest	-21, 24	-8, 49	-24, 12	-19, 13	-10, 15
RCM	14	-23	3	-11	-5
Katikati:					
10-model average	6	15	-15	-10	-3
Lowest, Highest	-19, 24	-13, 54	-31, 12	-24, 9	-16, 15
RCM	18	-19	-10	-12	-8
Tauranga:					
10-model average	4	14	-15	-11	-4
Lowest, Highest	-22, 24	-14, 50	-30, 12	-26, 8	-17, 15
RCM	20	-20	-6	-12	-6
Te Puke:					
10-model average	7	16	-13	-9	-2
Lowest, Highest	-20, 27	-12, 55	-28, 13	-25, 11	-15, 16
RCM	17	-19	-2	-10	-4
Whakatane:					
10-model average	4	14	-15	-11	-4
Lowest, Highest	-23, 23	-15, 52	-30, 11	-26, 9	-17, ,14
RCM	20	-21	-3	-12	-5
Opotiki:					
10-model average	4	14	-12	-8	-2
Lowest, Highest	-22, 22	-12, 50	-27, 11	-22, 10	-14, 14
RCM	25	-24	2	-12	-4
Rotorua:					
10-model average	4	15	-9	-5	-1
Lowest, Highest	-24, 23	-10, 50	-27, 12	-20, 12	-12, 15
RCM	14	-22	3	-8	-4
Kawerau:					
10-model average	12	22	-8	-4	4
Lowest, Highest	-17, 32	-5, 47	-25, 12	-20, 14	-11, 18
RCM	12	-18	5	-8	-3

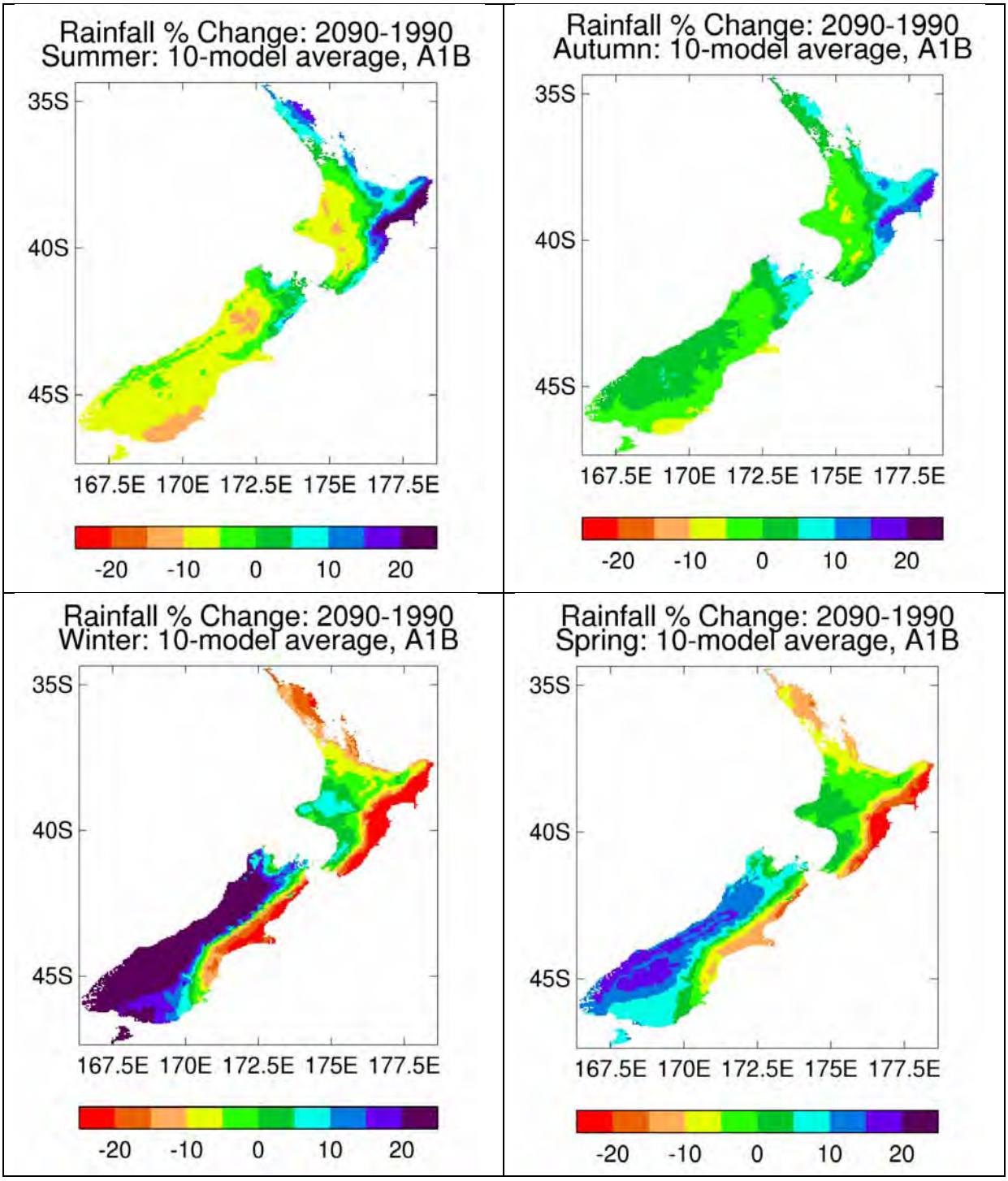

Figure B2: Projected changes in New Zealand seasonal rainfall (%), between 1980-1999 and 2080-2099 under the A1B emission scenario, as an average over the 10 GCMs of this study.

From a national perspective, using the same 10-model average as employed in this report, Figure B2 shows the modelled rainfall changes across New Zealand at 2090 under A1B are clearly strongest during winter, followed by spring (showing increases in the south and west of the South Island, but decreases on the east coast of both islands). The summer and autumn patterns are somewhat in contrast, showing increases in eastern Northland, Coromandel, Bay of Plenty, Gisborne, Hawkes Bay and coastal Wairarapa.

Appendix 3 – Material related to site-specific projections

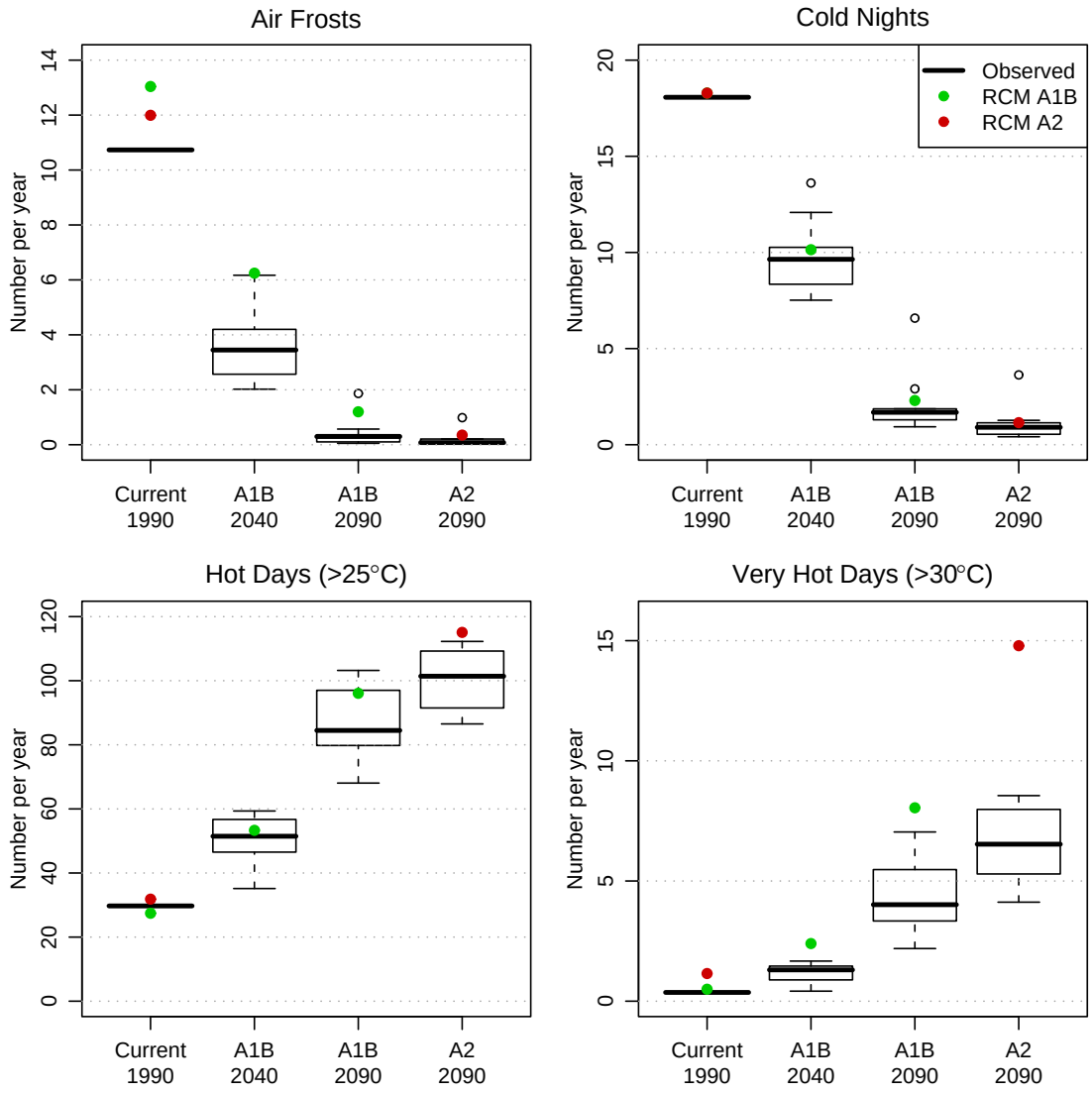

Figure C1: Projected changes in the occurrence of extreme temperatures at Katikati. The box and whisker plots show the spread in the projections from the 10 GCM ensemble members. The red and green dots are the projections from the RCM.

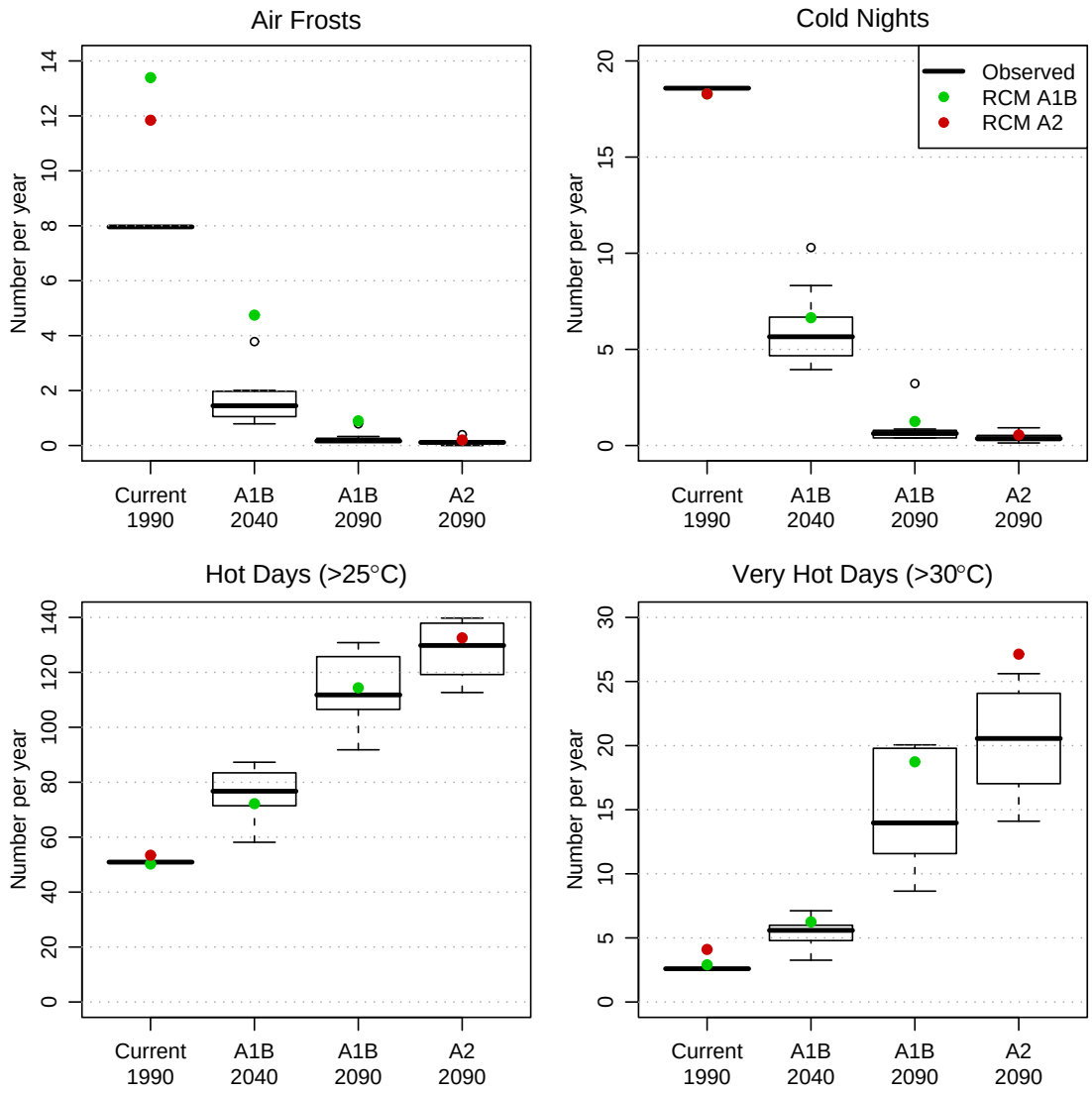

Figure C2: Projected changes in the occurrence of extreme temperatures at Kawerau. The box and whisker plots show the spread in the projections from the 10 GCM ensemble members. The red and green dots are the projections from the RCM.

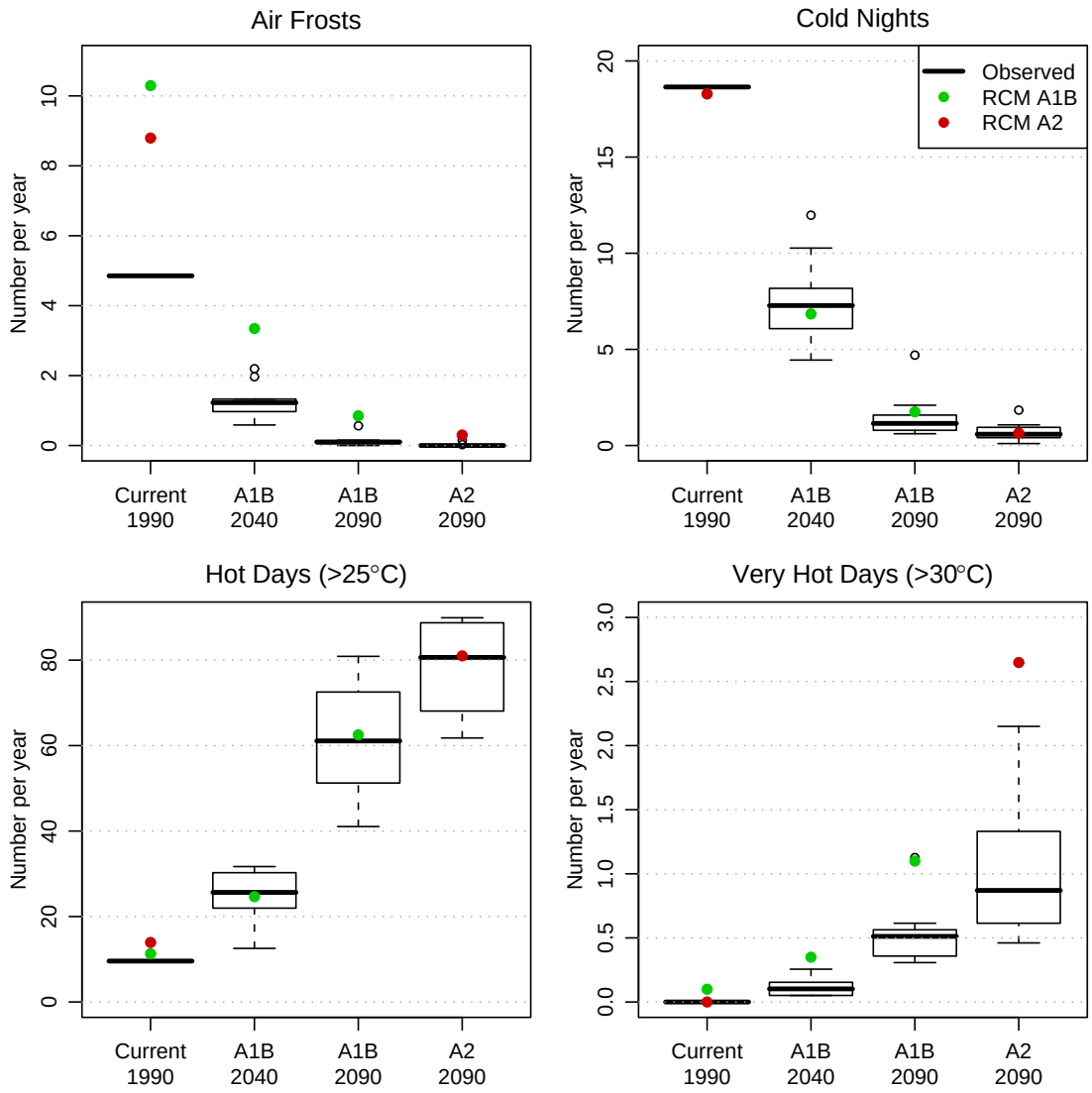

Figure C3: Projected changes in the occurrence of extreme temperatures at Opotiki. The box and whisker plots show the spread in the projections from the 10 GCM ensemble members. The red and green dots are the projections from the RCM.

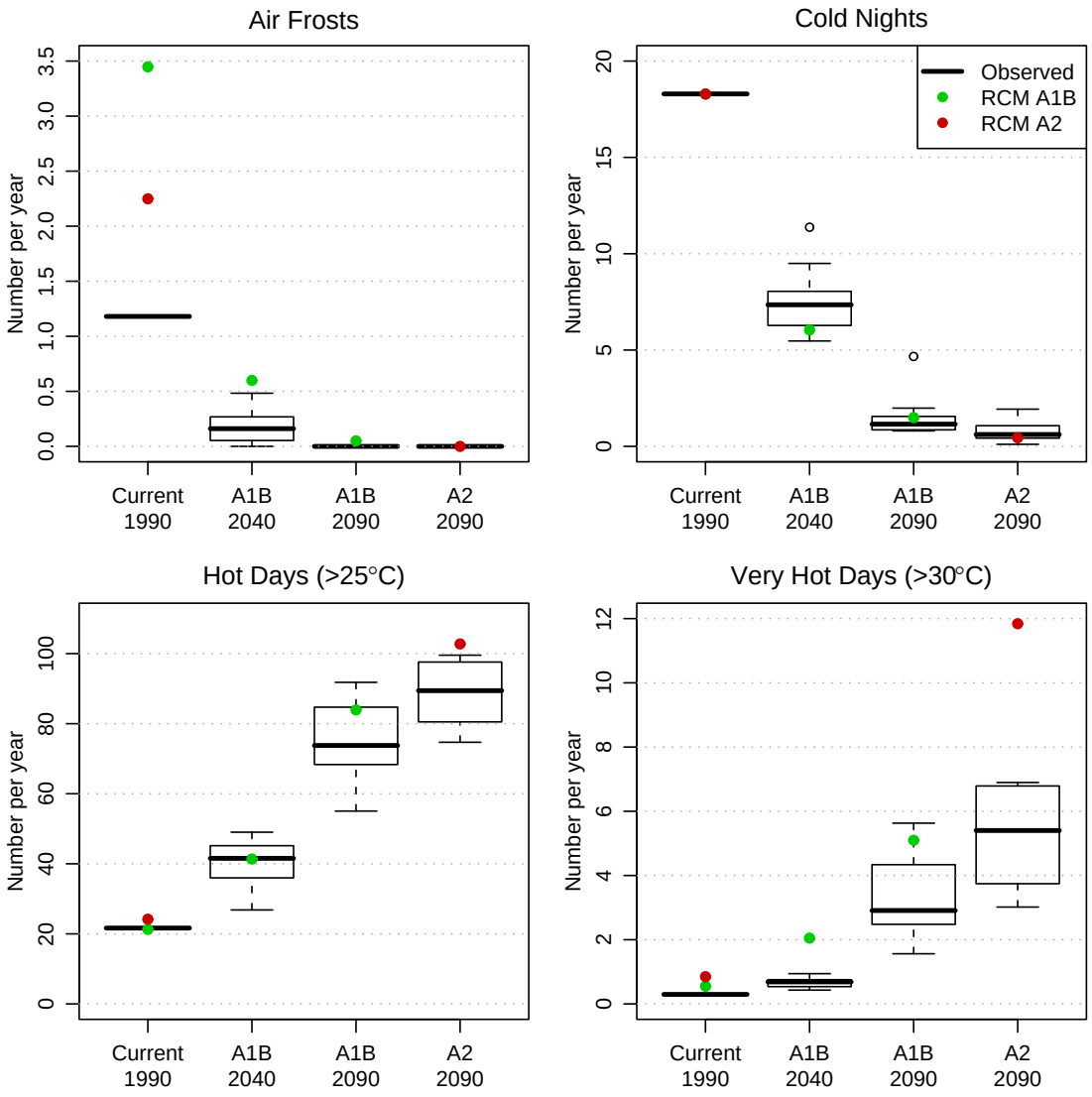

Figure C4: Projected changes in the occurrence of extreme temperatures at Tauranga Airport. The box and whisker plots show the spread in the projections from the 10 GCM ensemble members. The red and green dots are the projections from the RCM.

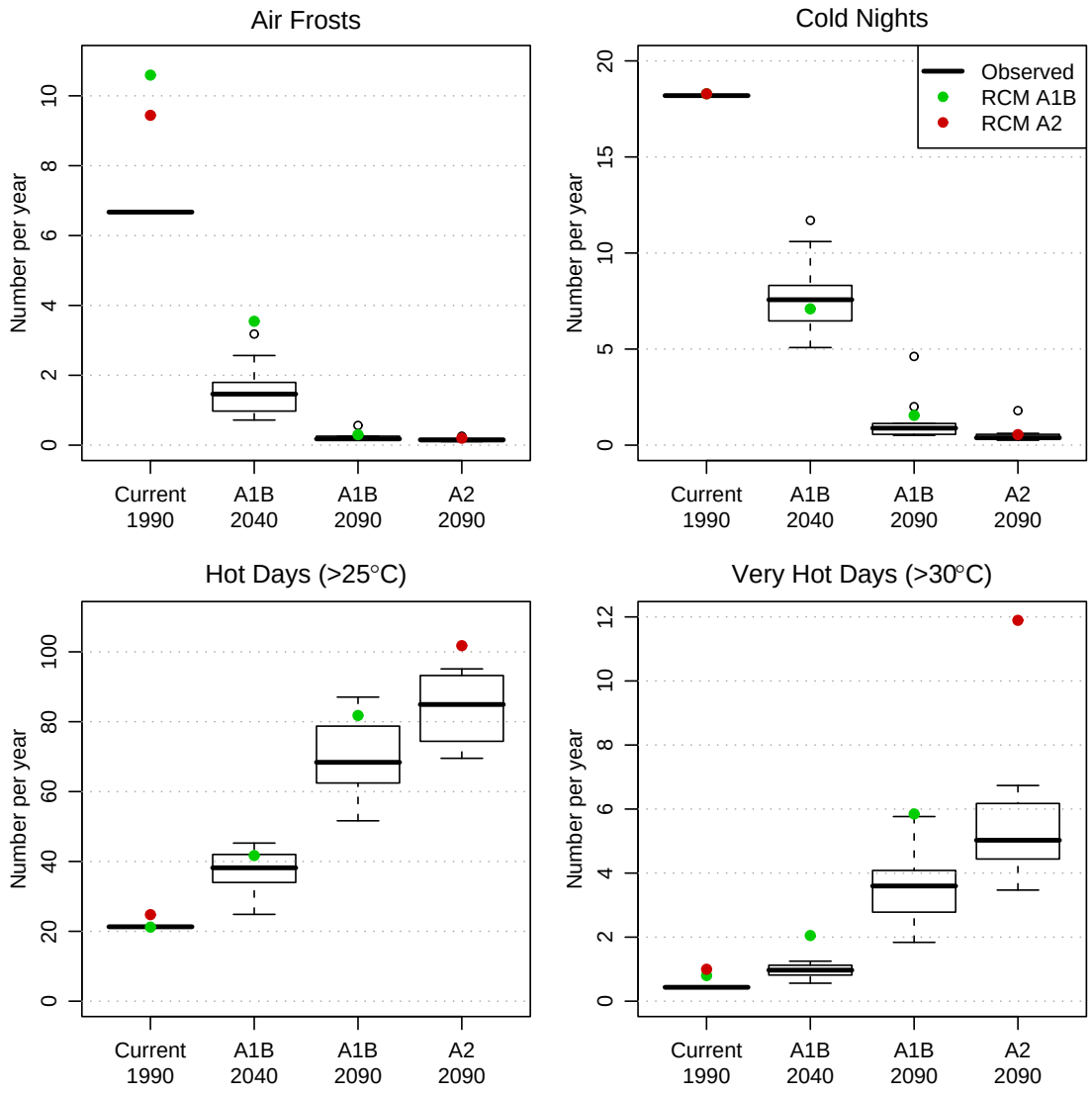

Figure C5: Projected changes in the occurrence of extreme temperatures at Te Puke. The box and whisker plots show the spread in the projections from the 10 GCM ensemble members. The red and green dots are the projections from the RCM.

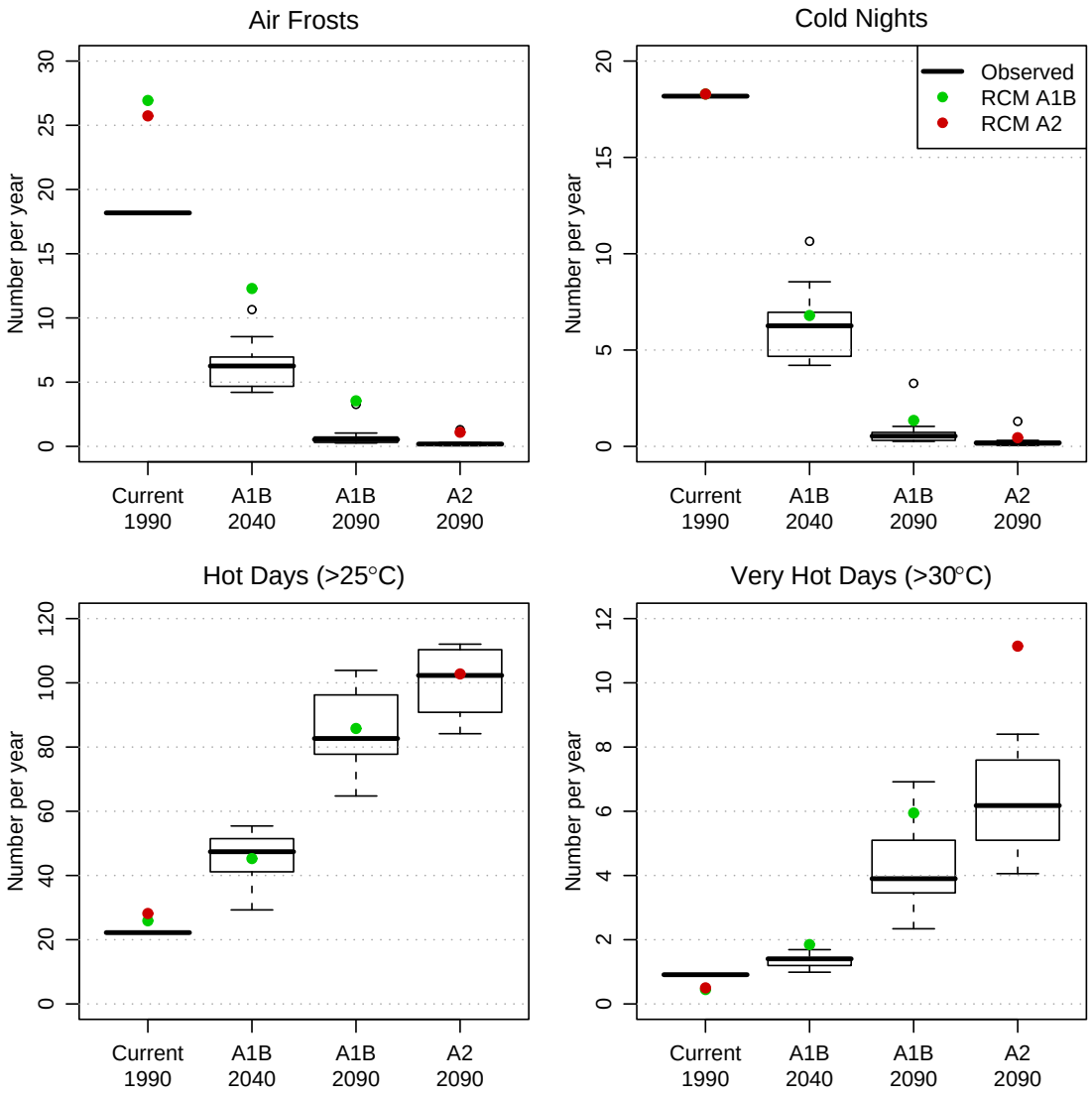

Figure C6: Projected changes in the occurrence of extreme temperatures at Whakatane Airport. The box and whisker plots show the spread in the projections from the 10 GCM ensemble members. The red and green dots are the projections from the RCM.

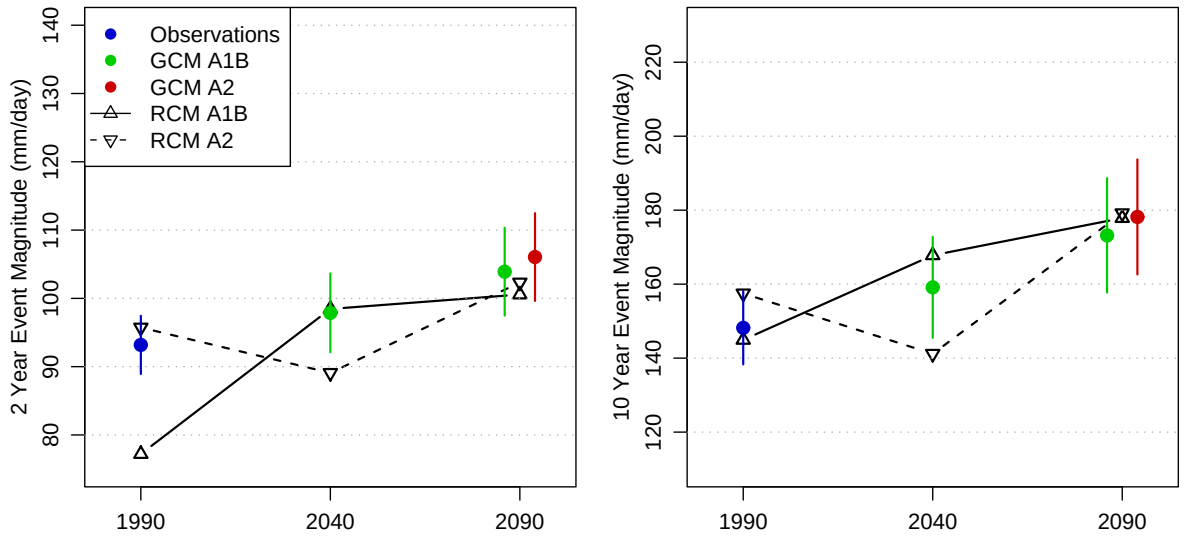

Figure C7: Two and ten year event magnitudes for Tauranga Airport. Observations are shown in blue; projected estimates using observations factored by global climate model temperature changes are shown in green and red; regional climate model results are shown by the dashed and solid black lines.

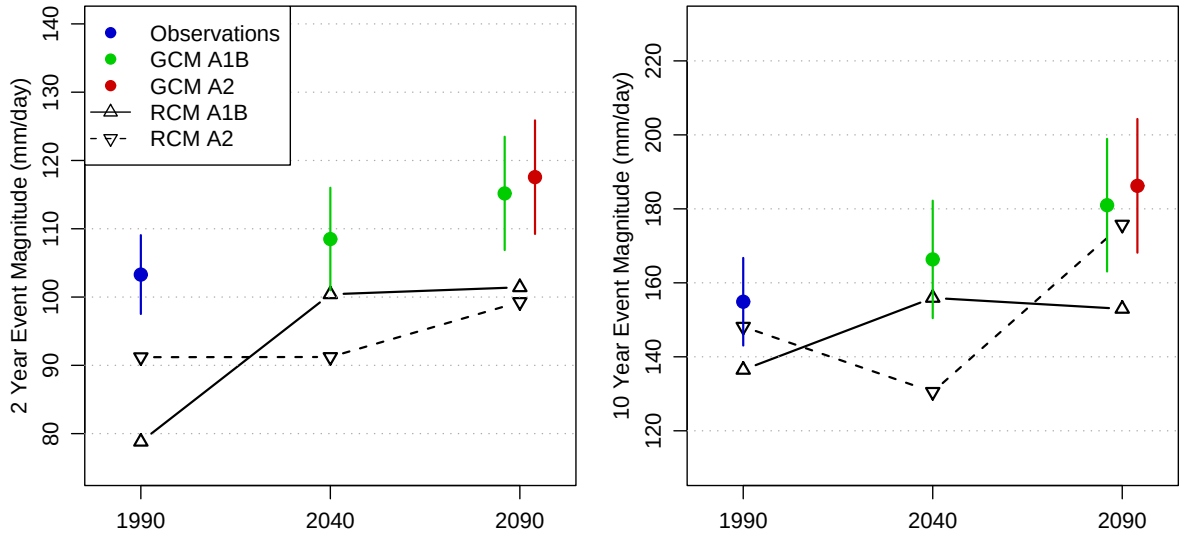

Figure C8: Two and ten year event magnitudes for Waimana. Observations are shown in blue; projected estimates using observations factored by global climate model temperature changes are shown in green and red; regional climate model results are shown by the dashed and solid black lines.

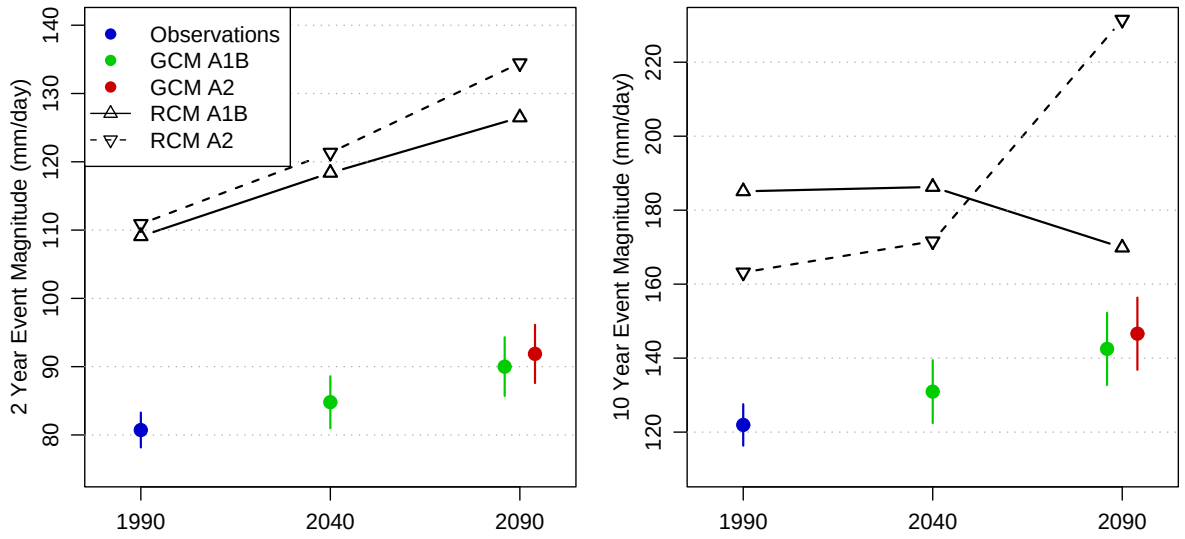

Figure C9: Two and ten year event magnitudes for Whakarewarewa. Observations are shown in blue; projected estimates using observations factored by global climate model temperature changes are shown in green and red; regional climate model results are shown by the dashed and solid black lines.

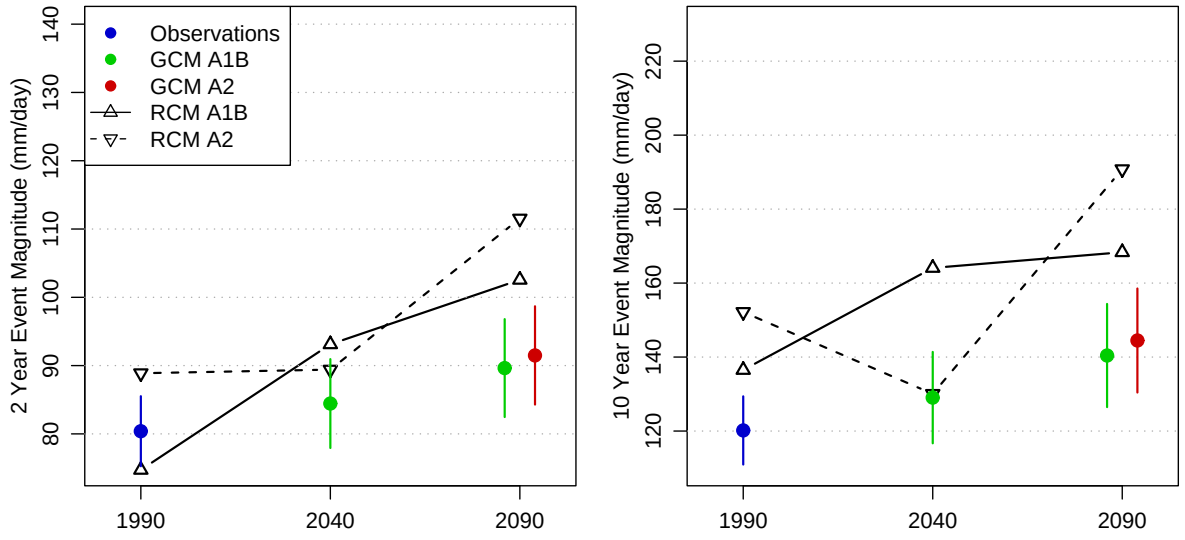

Figure C10: Two and ten year event magnitudes for Whakatane Airport. Observations are shown in blue; projected estimates using observations factored by global climate model temperature changes are shown in green and red; regional climate model results are shown by the dashed and solid black lines.

Appendix 4 – Material related to drought and pasture growth projections

Table D1: Base period (1980 - 1999) percentage of time in summer drought for different drought intensities and durations at Whakamarama. The median percentage is bolded [also given are the 25th percentile and 75th percentile].

Whakamarama Reanalysis 1980-1999	Summer median [25th percentile 75th percentile]		
	High intensity (<=10th percentile)	Moderate intensity (<=25th percentile)	Low intensity (<=50th percentile)
Duration > 14 days	**0.0** [0.0-0.0]	**1.7** [0.0-14.4]	**17.7** [1.1-27.2]
Duration > 1 month	0.0 [0.0-0.0]	0.0 [0.0-0.0]	0.0 [0.0-8.8]

Table D2: Base period (1980 - 1999) percentage of time in summer drought for different drought intensities and durations at Te Puke. The median percentage is bolded [also given are the 25th percentile and 75th percentile].

Te Puke Reanalysis 1980-1999	Summer median [25th percentile 75th percentile]		
	High intensity (<=10th percentile)	Moderate intensity (<=25th percentile)	Low intensity (<=50th percentile)
Duration > 14 days	**0.0** [0.0-6.1]	**5.0** [0.0-14.3]	**28.9** [8.3-38.3]
Duration > 1 month	0.0 [0.0-0.0]	0.0 [0.0-0.0]	**16.1** [0.0-34.3]

Table D3: Base period (1980 - 1999) percentage of time in summer drought for different drought intensities and durations at Te Teko. The median percentage is bolded [also given are the 25th percentile and 75th percentile].

Te Teko Reanalysis 1980-1999	Summer median [25th percentile 75th percentile]		
	High intensity (<=10th percentile)	Moderate intensity (<=25th percentile)	Low intensity (<=50th percentile)
Duration > 14 days	**0.0** [0.0-4.4]	**0.0** [0.0-9.9]	**20.4** [4.4-32.0]
Duration > 1 month	0.0 [0.0-0.0]	0.0 [0.0-0.0]	**2.8** [0.0-14.4]

Table D4: Base period (1980 - 1999) percentage of time in summer drought for different drought intensities and durations at Opotiki. The median percentage is bolded [also given are the 25th percentile and 75th percentile].

Opotiki Reanalysis 1980-1999	Summer median [25th percentile 75th percentile]		
	High intensity (<=10th percentile)	Moderate intensity (<=25th percentile)	Low intensity (<=50th percentile)
Duration > 14 days	**6.1** [0.0-12.7]	**7.8** [0.0-13.7]	**18.2** [7.7-26.1]
Duration > 1 month	0.0 [0.0-0.0]	0.0 [0.0-0.0]	0.0 [0.0-8.3]

Table D5: Projected changes in (median) percentage of time spent in summer drought at Whakamarama, at 2090 under both A1B and A2 scenarios.

Whakamarama, Summer season, A1B at 2090			
Change (% time spent in drought)	High intensity (<=10th percentile)	Moderate intensity (<=25th percentile)	Low intensity (<=50th percentile)
Duration > 14 days	7.7	24.3	24.3
Duration > 1 month	0.0	8.9	14.4
Whakamarama, Summer season, A2 at 2090			
Change (% time spent in drought)	High intensity (<=10th percentile)	Moderate intensity (<=25th percentile)	Low intensity (<=50th percentile)
Duration > 14 days	13.2	30.6	15.8
Duration > 1 month	1.1	7.8	24.5

Table D6: Projected changes in (median) percentage of time spent in summer drought at Te Puke at 2090 under both A1B and A2 scenarios.

Te Puke, Summer season, A1B at 2090			
Change (% time spent in drought)	High intensity (<=10th percentile)	Moderate intensity (<=25th percentile)	Low intensity (<=50th percentile)
Duration > 14 days	7.2	15.0	13.3
Duration > 1 month	0.0	0.0	17.2
Te Puke, Summer season, A2 at 2090			
Change (% time spent in drought)	High intensity (<=10th percentile)	Moderate intensity (<=25th percentile)	Low intensity (<=50th percentile)
Duration > 14 days	1.6	7.7	19.1
Duration > 1 month	0.0	5.0	25.9

Table D7: Projected changes in (median) percentage of time spent in summer drought at Te Teko at 2090 under both A1B and A2 scenarios.

Te Teko, Summer season, A1B at 2090			
Change (% time spent in drought)	High intensity (<=10th percentile)	Moderate intensity (<=25th percentile)	Low intensity (<=50th percentile)
Duration > 14 days	8.4	7.8	13.8
Duration > 1 month	0.0	0.0	13.3
Te Teko, Summer season, A2 at 2090			
Change (% time spent in drought)	High intensity (<=10th percentile)	Moderate intensity (<=25th percentile)	Low intensity (<=50th percentile)
Duration > 14 days	6.1	10.5	14.4
Duration > 1 month	2.8	5.6	20.0

Table D8: Projected changes in (median) percentage of time spent in summer drought at Opotiki at 2090 under both A1B and A2 scenarios.

Opotiki, Summer season, A1B at 2090			
Change (% time spent in drought)	High intensity (<=10th percentile)	Moderate intensity (<=25th percentile)	Low intensity (<=50th percentile)
Duration > 14 days	10.0	10.0	2.8
Duration > 1 month	6.1	6.7	10.5
Opotiki, Summer season, A2 at 2090			
Change (% time spent in drought)	High intensity (<=10th percentile)	Moderate intensity (<=25th percentile)	Low intensity (<=50th percentile)
Duration > 14 days	0.7	1.7	5.2
Duration > 1 month	1.1	3.9	2.3

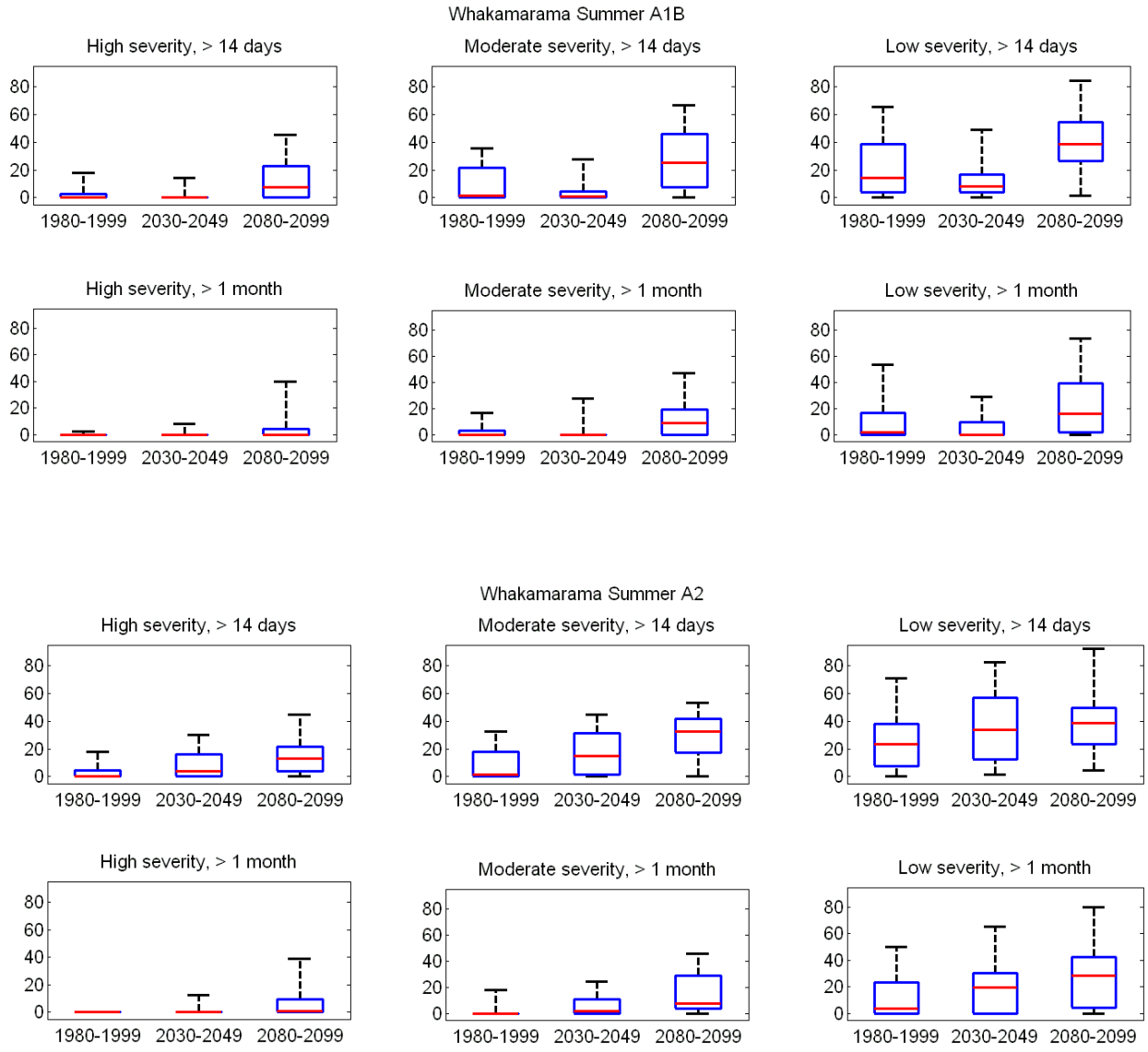

Figure D1: Projections of percentage of time spent in drought at Whakamarama, Summer Season, under A1B (top) and A2 (bottom). Red line shows the projected median. Blue box indicates 25th and 75th percentile. Projected twenty-year maximum and minimum values are shown as whiskers off the boxplot.

Top rows depict droughts lasting more than 14 days; lower rows depict droughts lasting more than a month. Left hand column shows high intensity drought, middle column shows moderate intensity drought, and right hand column shows low intensity droughts. Within each square, present day (1980-1999) estimates (left hand side) are compared to 2040 (centre) and 2090 (right hand side).

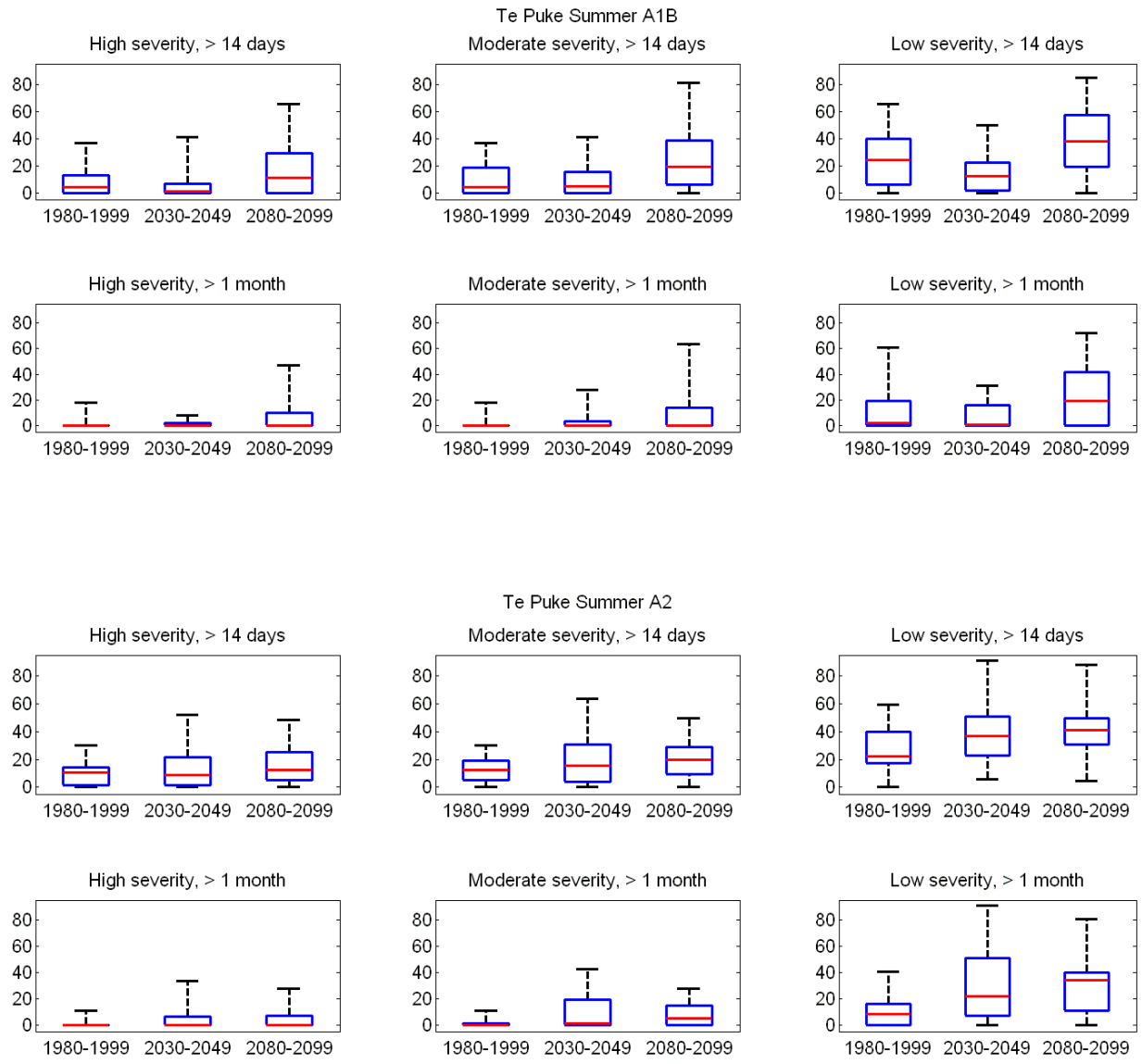

Figure D2: Projections of percentage of time spent in drought at Te Puke, Summer Season, under A1B (top) and A2 (bottom). Red line shows the projected median. Blue box indicates 25th and 75th percentile. Projected twenty-year maximum and minimum values are shown as whiskers off the boxplot.

Top rows depict droughts lasting more than 14 days; lower rows depict droughts lasting more than a month. Left hand column shows high intensity drought, middle column shows moderate intensity drought, and right hand column shows low intensity droughts. Within each square, present day (1980-1999) estimates (left hand side) are compared to 2040 (centre) and 2090 (right hand side).

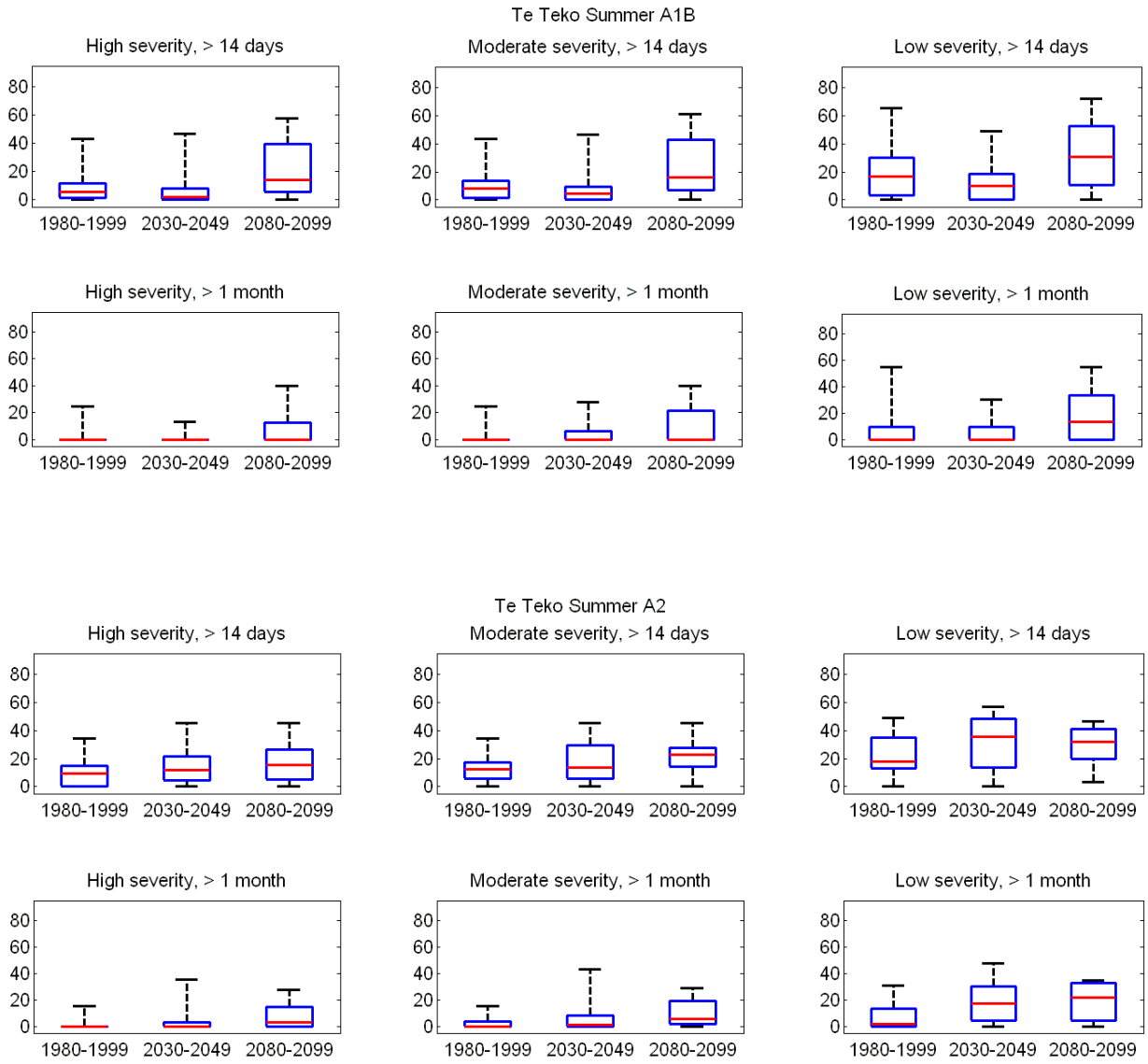

Figure D3: Projections of percentage of time spent in drought at Te Teko, Summer Season, under A1B (top) and A2 (bottom). Red line shows the projected median. Blue box indicates 25th and 75th percentile. Projected twenty-year maximum and minimum values are shown as whiskers off the boxplot.

Top rows depict droughts lasting more than 14 days; lower rows depict droughts lasting more than a month. Left hand column shows high intensity drought, middle column shows moderate intensity drought, and right hand column shows low intensity droughts. Within each square, present day (1980-1999) estimates (left hand side) are compared to 2040 (centre) and 2090 (right hand side).

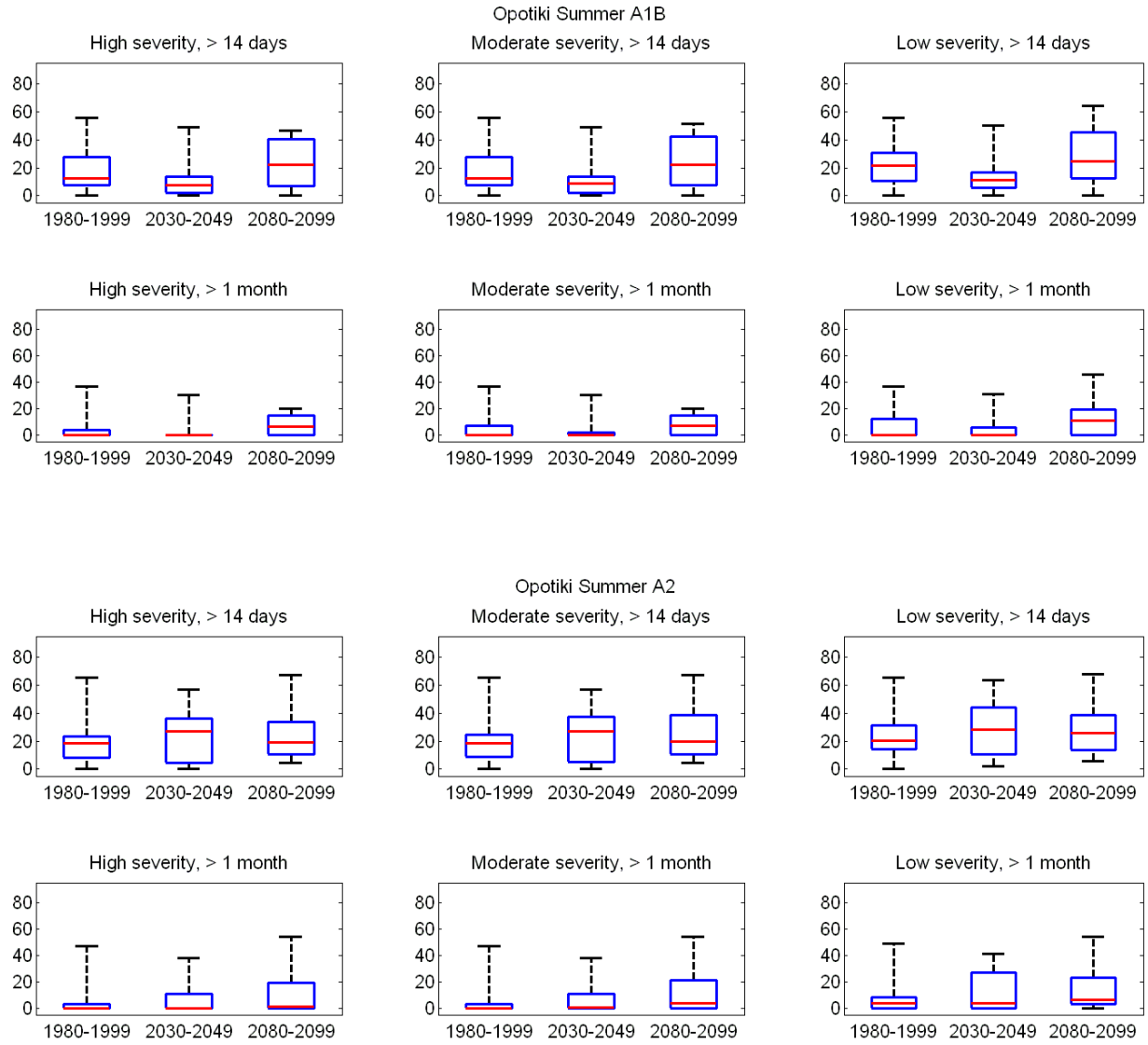

Figure D4: Projections of percentage of time spent in drought at Opotiki, Summer Season, under A1B (top) and A2 (bottom). Red line shows the projected median. Blue box indicates 25th and 75th percentile. Projected twenty-year maximum and minimum values are shown as whiskers off the boxplot.

Top rows depict droughts lasting more than 14 days; lower rows depict droughts lasting more than a month. Left hand column shows high intensity drought, middle column shows moderate intensity drought, and right hand column shows low intensity droughts. Within each square, present day (1980-1999) estimates (left hand side) are compared to 2040 (centre) and 2090 (right hand side).

Table D9: Te Puke pasture biomass for 1980-1999 from reanalysis data, median value (25th percentile-75th percentile). Summer value calculated from contiguous Dec-Feb values and is for the 19 years 1981-1999.

Te Puke Reanalysis Biomass production in kg per hectare 1980-1999	
Annual biomass	14188 (13226-15267)
Summer biomass	3868 (3048-4590)
Autumn biomass	2950 (2283-3302)
Winter biomass	1634 (1367-1886)
Spring biomass	6043 (5857-6421)

Table D10: Te Teko pasture biomass for 1980-1999 from reanalysis data, median value (25th percentile-75th percentile). Summer value calculated from contiguous Dec-Feb values and is for the 19 years 1981-1999.

Te Teko Reanalysis Biomass production in kg per hectare 1980-1999	
Annual biomass	13709 (12729-14496)
Summer biomass	2329 (1596-3141)
Autumn biomass	2297 (1886-2834)
Winter biomass	2009 (1635-2265)
Spring biomass	6926 (6284-7030)

Table D11: Opotiki pasture biomass for 1980-1999 from reanalysis data, median value (25th percentile-75th percentile). Summer value calculated from contiguous Dec-Feb values and is for the 19 years 1981-1999.

Opotiki Reanalysis Biomass production in kg per hectare 1980-1999	
Annual biomass	13813 (13123-14417)
Summer biomass	2614 (1625-3379)
Autumn biomass	2352 (2011-3101)
Winter biomass	2128 (1727-2259)
Spring biomass	6454 (5936-6809)

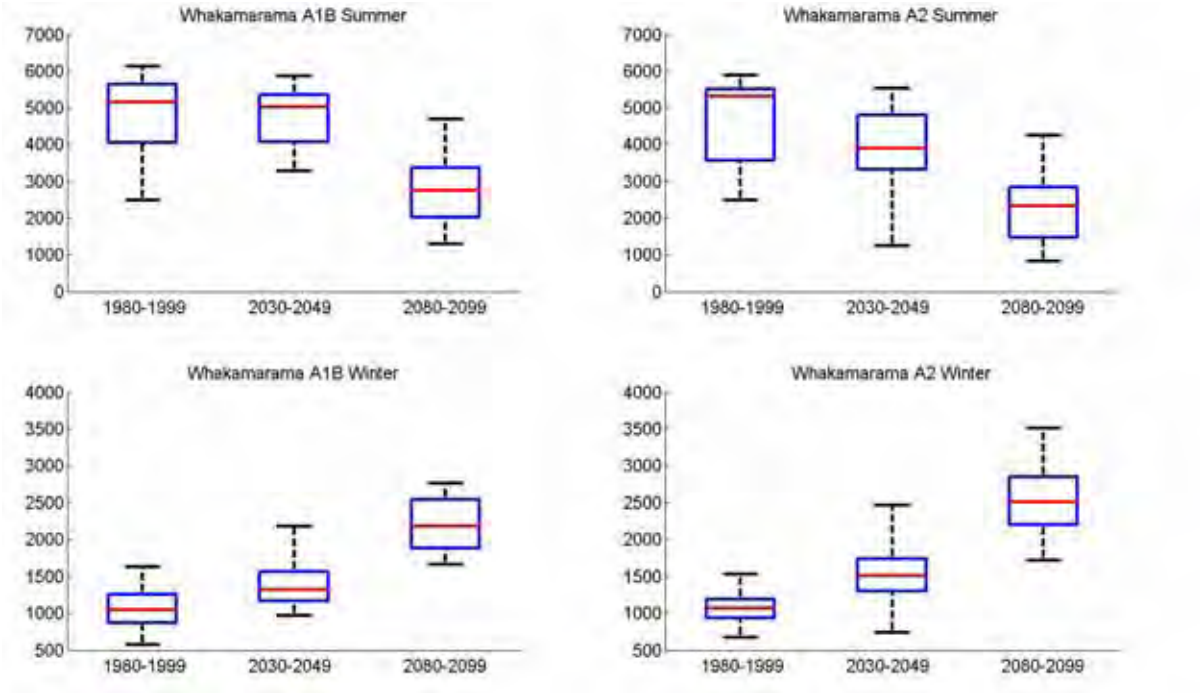

Figure D5: Boxplot of seasonal pasture biomass production in kg per hectare for Whakamarama. The red line indicates the median while the blue box indicates the seasonal 25th – 75th percentiles. In a quarter (25%) of seasons, the seasonal biomass produced is less than the seasonal 25th percentile value (i.e. these are the low-production seasons). In a quarter (25%) of seasons, the seasonal biomass produced is more than the seasonal 75th percentile value (i.e. these are the high-production seasons).

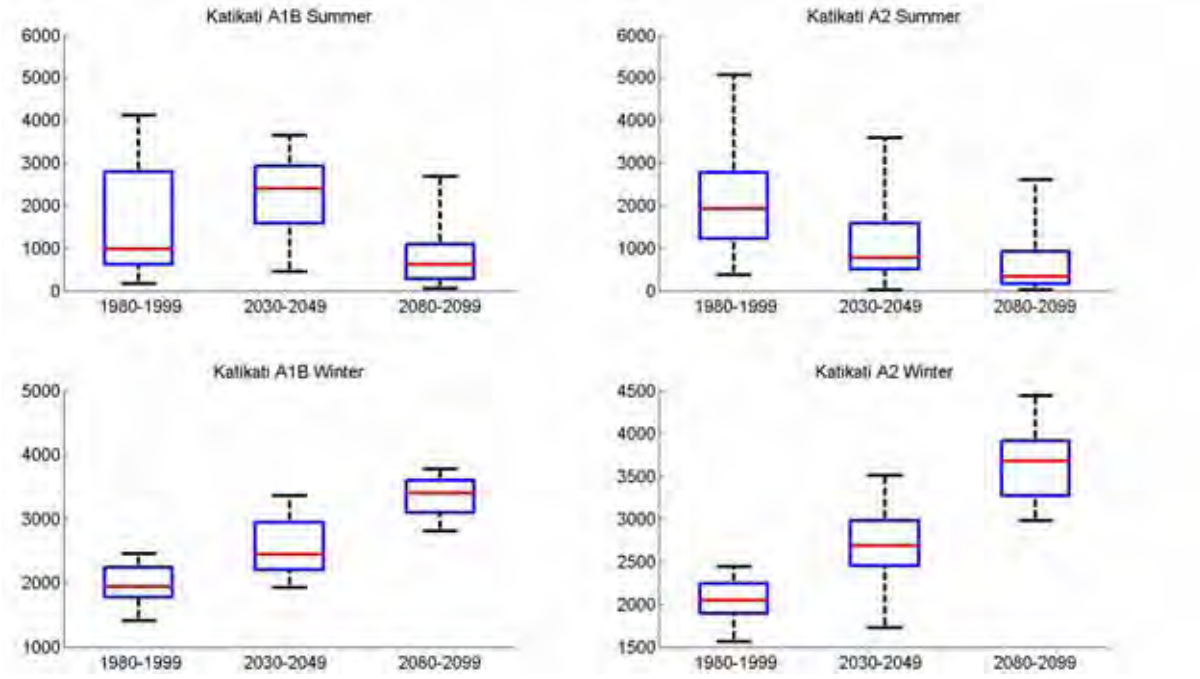

Figure D6: Boxplot of seasonal pasture biomass production in kg per hectare for Katikati. Boxplots as per Figure D5.

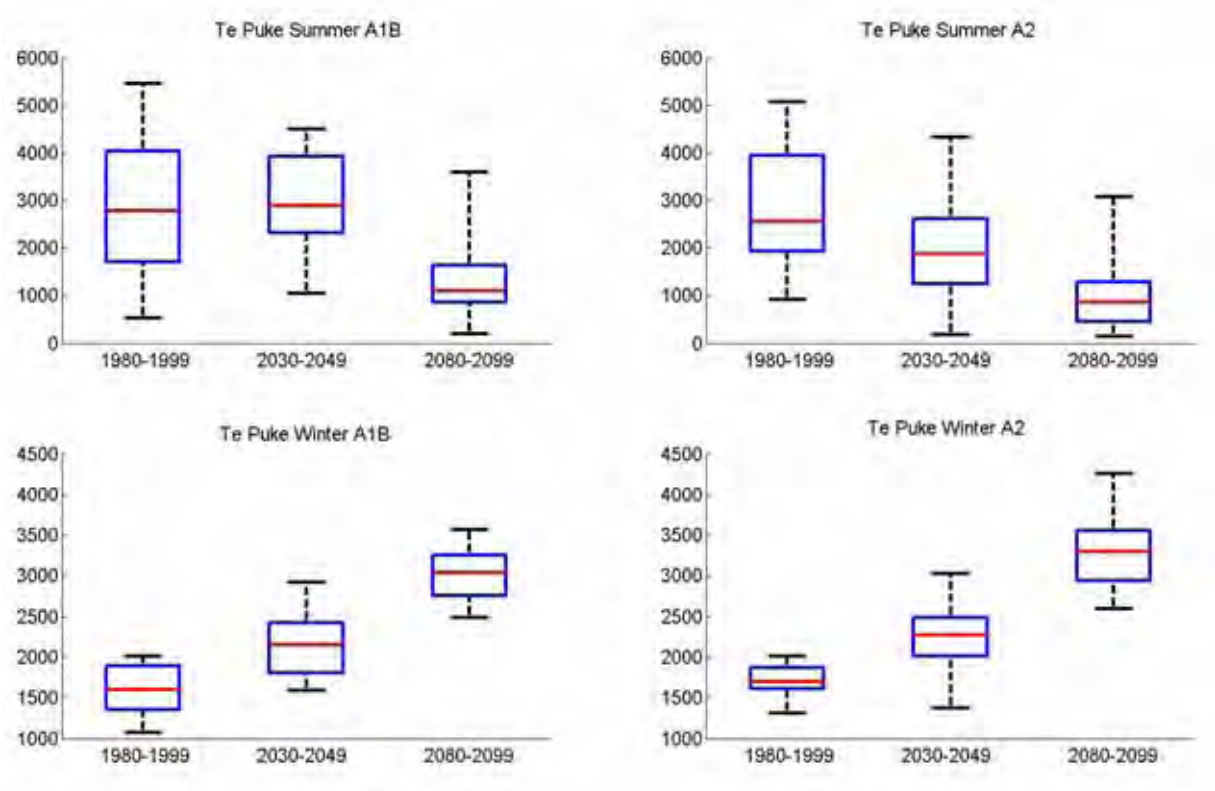

Figure D7: Boxplot of seasonal pasture biomass production in kg per hectare for Te Puke. Boxplots as per Figure D5.

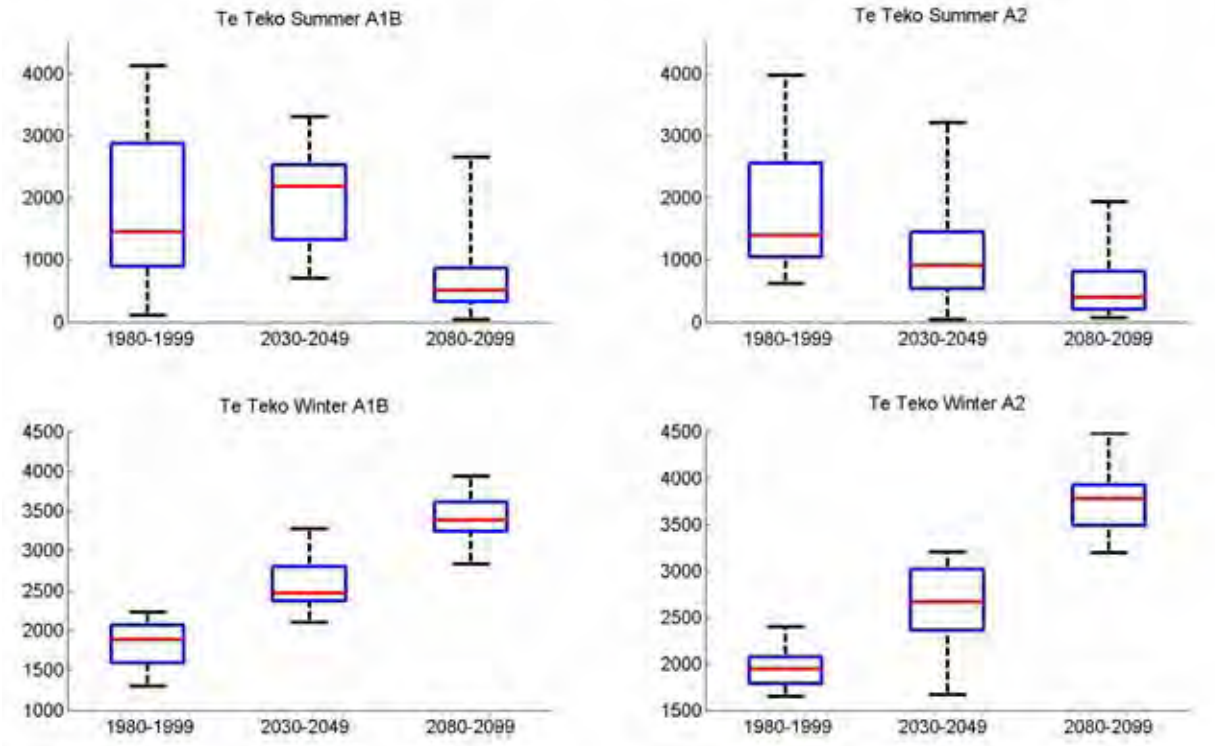

Figure D8: Boxplot of seasonal pasture biomass production in kg per hectare for Te Teko. Boxplots as per Figure D5.

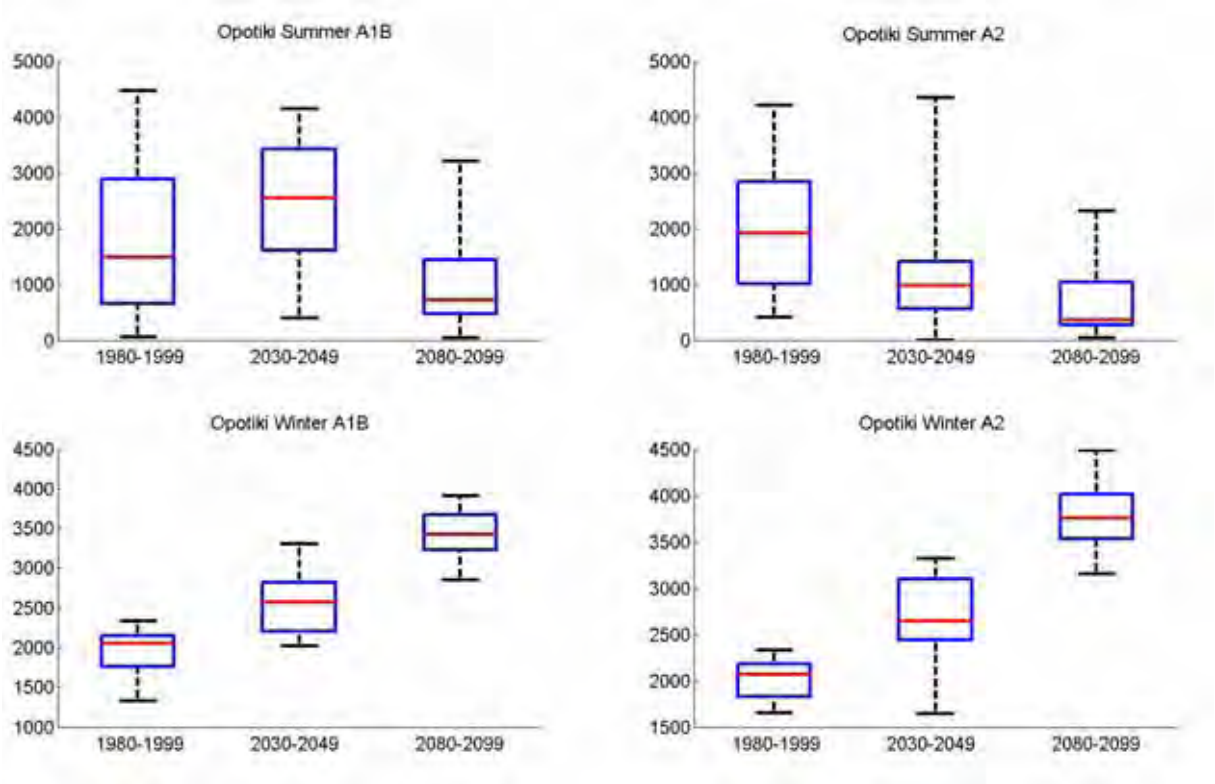

Figure D9: Boxplot of seasonal pasture biomass production in kg per hectare for Opotiki. Boxplots as per Figure D5.